

THE DISTRIBUTION OF TRANSITION METALS
IN BASIC ROCKS AS DETERMINED BY
ACTIVATION ANALYSIS

THESIS

presented for the degree of

Doctor of Philosophy

in the

University of Glasgow

by

I. M. Dale, B. Sc.

Chemistry Department

January, 1972.

ProQuest Number: 11011987

All rights reserved

INFORMATION TO ALL USERS

The quality of this reproduction is dependent upon the quality of the copy submitted.

In the unlikely event that the author did not send a complete manuscript and there are missing pages, these will be noted. Also, if material had to be removed, a note will indicate the deletion.



ProQuest 11011987

Published by ProQuest LLC (2018). Copyright of the Dissertation is held by the Author.

All rights reserved.

This work is protected against unauthorized copying under Title 17, United States Code
Microform Edition © ProQuest LLC.

ProQuest LLC.
789 East Eisenhower Parkway
P.O. Box 1346
Ann Arbor, MI 48106 – 1346

Summary of thesis entitled
"The Distribution of Transition Metals in
Basic Rocks as Determined by Activation
Analysis", presented by Ian M. Dale, for
the Degree of Ph.D. and based upon research
carried out in the Chemistry Department,
University of Glasgow.

January, 1972.

The Distribution of Transition Metals in Basic
Rocks as Determined by Activation Analysis

The research carried out may conveniently be summarised in two sections.

In the first section, accurate analyses have been obtained for the scandium, titanium, chromium, manganese, iron, cobalt and nickel content of basic volcanic rocks from a wide variety of geographical locations. (Reunion Island, British Solomon Islands, Juan Fernandez Islands, Hawaii, Red Sea Islands, Iceland and Greenland). Neutron activation analysis has been shown to be an excellent method for the determination of scandium, chromium, manganese, iron, cobalt and nickel in small samples of rock material. The results obtained for a number of international standard rocks are in very good agreement with reported analyses and indicate that activation analysis should be considered one of the most accurate and sensitive techniques available for the analyses of geological samples.

The second section has dealt with the transition metal concentrations in the minerals of basic volcanic rocks. Results were obtained for systems which have hitherto not been investigated. It has been shown that the non-spherical distribution of the d - electrons surrounding the

transition metal ion exerts a major influence on the partitioning of the ion between olivine and clinopyroxene phenocrysts and the groundmass of basic volcanic rocks.

It has been demonstrated, for the first time, that a linear relationship exists between $\ln k$, where k , the partition coefficient, is defined as:-

$$\frac{[M]_{\text{crystal}}}{[M]_{\text{groundmass}}}$$

M being a transition metal ion, and the octahedral site preference energy (O.S.P.E.) of the ion, defined as the tetrahedral crystal field stabilisation energy minus the octahedral crystal field stabilisation energy for the partitioning of the divalent transition metal ions, Mn^{2+} , Fe^{2+} , Co^{2+} and Ni^{2+} between olivine and groundmass and clinopyroxene and groundmass of a range of basic volcanic rocks.

Zoning of the phenocrysts does not seem to effect the linearity of the plot of $\ln k$ Vs O.S.P.E.

No systematic variation of the slope of the line $\ln k$ Vs O.S.P.E. with either alkalic or tholeiitic basalt type is evident. However, these rock samples containing only olivine phenocrysts tend to have lower values for the partition coefficients.

Crystal field effects have also been shown to be significant in the partitioning of the trivalent transition metal ions, Sc^{3+} and Cr^{3+} , between clinopyroxene phenocrysts and the groundmass of a range of basic volcanic rocks.

These results are consistent with and can be explained by the assumption that these transition metal ions occupy tetrahedral and octahedral sites in the magma while only octahedral or near octahedral sites are available in the olivine and pyroxene structures.

ACKNOWLEDGEMENTS

I am pleased to record my sincere thanks to Dr. P. Henderson for suggesting this line of research and for his constant guidance and advice throughout this work and to Dr. A. Walton for many valuable discussions.

Much of the experimental work was carried out in the Chemistry Department, Glasgow University, and thanks are extended to Professor J. M. Robertson as the Director of the Chemical Laboratories and Head of the Department for use of these facilities.

I gratefully acknowledge receipt of a Natural Environment Research Council Research Studentship from October 1967 to September 1970.

The generosity of the following for donating rock specimens is acknowledged with thanks:

Prof. H. I. Drever (St. Andrews); Prof. I. G. Gass (The Open University); Prof. G. A. Macdonald (Hawaii); Dr. P. E. Baker (Oxford); Dr. J. D. Bell (Oxford); Dr. H. Sigurdsson (Durham); Dr. W. J. Wadsworth (Manchester).

Thanks are extended to the following for permission to use various items of equipment:

Prof. H. W. Wilson (Scottish Research Reactor Centre, East Kilbride) for irradiation and counting facilities; Prof. G. Forbes (Department of Forensic Medicine, Glasgow University) for counting equipment; Prof. T. C. Phemister (Department of Geology & Mineralogy, University of Aberdeen) for use of electron microprobe; Prof. T. N. George (Department of Geology, Glasgow University) for use of D.C. Arc Spectrograph and X-ray fluorescence equipment.

Thanks are due to Miss M. Smith for typing this thesis.

Finally, I wish to express my thanks to my wife, Helen, for her encouragement and understanding while this work was being carried out.

CONTENTS

	Page
Acknowledgements	i
Table of Contents	iii
List of Tables	vii
List of Figures	X
<u>CHAPTER 1</u>	
Introduction	1
<u>CHAPTER 2</u>	
Crystal Field Theory and Its Implication for Geochemistry	
I. Introduction	16
II. Shape and Symmetry of d Orbitals	18
III. Transition Elements	20
IV. Crystal Field Splitting in Octahedral Co-ordination	22
V. Crystal Field Splitting in Tetrahedral Co-ordination	28
VI. Jahn-Teller Effect	33
VII. Evaluation of Δ	34
VIII. Sites available in Silicate Minerals	
(a) Olivine	40
(b) Pyroxene	46
(c) Silicate Melt Structure	49
IX. Trace Element Partitioning	54
<u>CHAPTER 3</u>	
Experimental Methods - Activation Analysis	
I. Introduction	58
II. Principles of Activation Analysis	61
III. Interactions of Neutrons with Nuclei	65

IV.	Methods of Neutron Activation Analysis	70
V.	Detection of Radioactivity	73
	(a) Geiger-Muller Detectors	73
	(b) Solid-State Detectors	74
	(c) Scintillation Detectors	77
VI.	Multichannel Analysers	81
VII.	Procedure	83
	(a) Sample Preparation	85
	(b) Standard Preparation	87
	(c) Non-destructive Analysis	94
	(d) Destructive Neutron Activation Analysis	102
VIII.	Accuracy and Precision	106

CHAPTER 4

Alternative Methods for Trace Element Analysis		
(a)	D. C. Arc Emission Spectrography	120
(b)	Atomic Absorption Spectroscopy	122
(c)	X-Ray Fluorescence	123
(d)	Electron Microprobe Analysis	125
(e)	Chemical Methods	127

Experimental

D. C. Arc Spectroscopy	130
Atomic Absorption Spectroscopy	131
X-Ray Fluorescence	132
Electron Microprobe Analysis	135
Chemical Methods	
(i) Titanium	136
(ii) Ferrous Iron	138

CHAPTER 5

Results and Discussions	141
1. Analysis of the Rock Samples	
(i) Major Element Chemistry	142
(a) SiO_2 Vs Total Alkalies	142
(b) SiO_2 Vs K_2O ; Na_2O ; CaO	144
(c) Na_2O Vs TiO_2 ; P_2O_5	144

(ii)	Transition Metal Chemistry	147
	(a) Scandium	147
	(b) Titanium	147
	(c) Chromium	162
	(d) Manganese	163
	(e) Iron (Ferrous)	163
	(f) Iron (Ferric)	164
	(g) Cobalt	164
	(h) Nickel	165
	(i) Chromium-Nickel Correlation	165
11.	Transition Metal Content of Components of the Rocks and their Distribution	167
	(i) Olivines	
	(a) Scandium	168
	(b) Titanium	169
	(c) Chromium	169
	(d) Manganese	170
	(e) Iron (Ferrous)	171
	(f) Cobalt	171
	(g) Nickel	171
	(ii) Clinopyroxenes	
	(a) Scandium	172
	(b) Titanium	173
	(c) Chromium	173
	(d) Manganese	174
	(e) Iron (Ferrous)	174
	(f) Cobalt	175
	(g) Nickel	175
	(iii) Groundmass	176
	(iv) Electron Microprobe Results	177
	(v) Partition of the Elements between the Minerals and Groundmass	182
	(a) Distribution of divalent ions	
	Reunion Island Samples	185
	British Solomon Islands Samples	188
	Juan Fernandez Islands Samples	188
	Hawaiian Samples	188
	Iceland Samples	195

(a)	Distribution of divalent ions (c'td)	
	Red Sea Islands Samples	199
	Greenland Samples	199
	Published Data	208
	Correlations of Partition Coefficients with Magma Types	212
(b)	Distribution of trivalent ions	212
(c)	Distribution of Titanium	215
	III. Conclusions	216

APPENDIX 1

Covell's Method for Gamma-Ray Photopeak Area Determination	221
---	-----

APPENDIX 2

Description of Sample Preparation	224
-----------------------------------	-----

APPENDIX 3

Electron Microprobe Analysis	227
------------------------------	-----

APPENDIX 4

Description of Rock Samples Investigated	232
--	-----

Bibliography	245
--------------	-----

TABLES

CHAPTER 1

Page

Table 1.	Goldschmidt's Geochemical Classification of the Elements	6
----------	--	---

CHAPTER 2

Table 1.	Electronic Configuration of First Row Transition Metal Ions	21
Table 2.	Electronic Configurations and Crystal Field Stabilisation Energies in Octahedral Co-ordination	27
Table 3.	Electronic Configurations and Crystal Field Stabilisation Energies in Tetrahedral Co-ordination	32
Table 4.	Octahedral and Tetrahedral Crystal Field Stabilisation Energies, data from Dunitz and Orgel (1957)	35
Table 5.	Octahedral and Tetrahedral Crystal Field Stabilisation Energies, data from McClure (1957)	36
Table 6.	Octahedral Crystal Field Stabilisation Energies, from Thermodynamic Data	39
Table 7.	Ionic Radii of Transition Metal Ions	43
Table 8.	Stabilisation Energies of Transition Metal Ions in Six Co-ordinate Sites of Various Symmetries	45
Table 9.	Available Sites in the Bernal Liquid and a Solid Close Packing	50
Table 10.	Filled Sites in Silicates of Various Compositions	51

CHAPTER 3

Table 1.	Range of Concentrations of Transition Metals in Olivine, Clinopyroxene and Basaltic Rocks	59
Table 2.	Nuclear Data for Elements Investigated	84

	Page
Table 3. Gamma-Ray Photopeaks Measured	86
Table 4. Concentrations of Scandium in Rock Standards	110
Table 5. " " " Chromium" " "	111
Table 6. " " " Manganese" " "	112
Table 7. " " " Iron " " "	113
Table 8. " " " Cobalt " " "	114
Table 9. " " " Scandium in French Rock Standards	116
Table 10. " " " Chromium in French Rock Standards	117
Table 11. " " " Manganese in French Rock Standards	118
Table 12. " " " Cobalt in French Rock Standards	119

CHAPTER 4

Table 1. Quantities of Rock Sample required for Analysis using Chemical Methods	128
Table 2. Nickel Concentrations found by Atomic Absorption and X-Ray Fluorescence	133
Table 3. Cobalt and Chromium Concentrations found by Neutron Activation Analysis and X-Ray Fluorescence	134

APPENDIX 4

Table 1. Analytical Methods for Radioactive Material	
--	--

CHAPTER 5

		Page
Table 1.	Analytical Results, Reunion Island Samples	148
Table 1A.	Partition Coefficients, Reunion Island Samples	149
Table 2.	Analytical Results, British Solomon Islands Sample	150
Table 2A.	Partition Coefficients, British Solomon Islands Sample	151
Table 3.	Analytical Results, Juan Fernandez Samples	152
Table 3A.	Partition Coefficients, Juan Fernandez Samples	153
Table 4.	Analytical Results, Hawaiian Samples	154
Table 4A.	Partition Coefficients, Hawaiian Samples	155
Table 5.	Analytical Results, Icelandic Samples	156
Table 5A.	Partition Coefficients, Icelandic Samples	157
Table 6.	Analytical Results, Red Sea Islands Samples	158
Table 6A.	Partition Coefficients, Red Sea Islands Samples	159
Table 7.	Analytical Results, Greenland Samples	160
Table 7A.	Partition Coefficients, Greenland Samples	161
Table 8.	Microprobe Analysis of Minerals from Rock Sample C129	178
Table 9.	Microprobe Analysis of Olivines from Rock Sample 446	179
Table 10.	Microprobe Analysis of Olivines from Rock Sample Z64	180

APPENDIX 3

Table 1.	Counts obtained for Iron in C129 Olivine and Augite using Electron Microprobe	231
----------	--	-----

APPENDIX 4

Table 1.	Analytical Results for Rocks Investigated	234) 235)
----------	---	----------------

FIGURES

CHAPTER 2

		Page
Fig. 1.	Boundary Surfaces of Atomic Orbitals	19
Fig. 2.	Orientation of Ligands in Octahedral Co-Ordination	24
Fig. 3.	Relative Energy Levels of d Orbitals of a Transition Metal Ion in Octahedral Co-ordination	25
Fig. 4.	Arrangement of Ligands in Tetrahedral Co-ordination	29
Fig. 5.	Relative Energy Levels of d Orbitals of a Transition Metal Ion in Tetrahedral and Octahedral Co-ordination	30
Fig. 6.	Lattice Energies for Transition Metal Compounds	37
Fig. 7.	Olivine Crystal Structure	41
Fig. 8.	Crystal Field Stabilisation Energies in Distorted Sites	44
Fig. 9.	Idealised Structure of Diopside	48

CHAPTER 3

Fig. 1.	Activity Vs Irradiation Time	68
Fig. 2.	Resolution Vs X-Ray Energy	78
Fig. 3.	Gamma-Ray Spectrum, Short Lived Activities, NaI (Tl) Detector	95
Fig. 4.	Gamma-Ray Spectrum, Short Lived Activities, GeLi Detector	96
Fig. 5.	Gamma-Ray Spectrum, Long Lived Activities, NaI (Tl) Detector	100
Fig. 6.	Gamma-Ray Spectrum, Long Lived Activities, GeLi Detector	101
Fig. 7.	Activity Vs Time for ^{65}Ni	105

CHAPTER 5

		Page
Fig. 1.	SiO_2 Vs ($\text{Na}_2\text{O} + \text{K}_2\text{O}$)	143
Fig. 2.	SiO_2 Vs CaO ; Na_2O ; K_2O	145
Fig. 3.	Na_2O Vs P_2O_5 ; TiO_2	146
Fig. 4.	Nickel Vs Chromium	166
Fig. 5.	Sample RE331, lnk Vs O.S.P.E.	186
Fig. 6.	" RE512, lnk Vs O.S.P.E.	187
Fig. 7.	" NG367, lnk Vs O.S.P.E.	189
Fig. 8.	" 17840, lnk Vs O.S.P.E.	190
Fig. 9.	" 17901, lnk Vs O.S.P.E.	191
Fig. 10.	" C71, lnk Vs O.S.P.E.	192
Fig. 11.	" C129, lnk Vs O.S.P.E.	193
Fig. 12.	" C209, lnk Vs O.S.P.E.	194
Fig. 13.	" 394, lnk Vs O.S.P.E.	196
Fig. 14.	" 446, lnk Vs O.S.P.E.	197
Fig. 15.	" 448, lnk Vs O.S.P.E.	198
Fig. 16.	" Z39A, lnk Vs O.S.P.E.	200
Fig. 17.	" Z40, lnk Vs O.S.P.E.	201
Fig. 18.	" Z64, lnk Vs O.S.P.E.	202
Fig. 19.	" L5, lnk Vs O.S.P.E.	203
Fig. 20.	" L7, lnk Vs O.S.P.E.	204
Fig. 21.	" 120, lnk Vs O.S.P.E.	205
Fig. 22.	" B5, lnk Vs O.S.P.E.	206
Fig. 23.	" M21-26, lnk Vs O.S.P.E.	209
Fig. 24.	" M-12, lnk Vs O.S.P.E.	210
Fig. 25.	Composite Graph, lnk Vs O.S.P.E.	213

APPENDIX 1

Fig. 1.	Idealised Gamma-Ray Peak	222
---------	--------------------------	-----

CHAPTER 1
INTRODUCTION

The three main tasks of geochemistry as formulated by Goldschmidt (1954) are:-

- i) to establish the terrestrial abundance relationships of the elements
- ii) to account for the terrestrial distribution of elements in the geochemical environment
- and iii) to detect the laws governing the abundance relationships and distribution of the elements

This study was undertaken in order to further elucidate iii) above, in particular to investigate the distribution of certain transition metals between minerals crystallising from a basic magma and to explain the results obtained, paying especial attention to the electronic structures of the elements investigated. At the same time data were obtained for the abundances of transition metals in basic volcanic rocks.

In recent years sensitive and accurate methods of trace metal analysis of rock samples have become available (neutron activation analysis, atomic absorption, electron microprobe, etc.) and accordingly studies of small variations in the concentrations of these metals in geological samples can be more confidently carried out.

Much of the early work dealing with the occurrence, distribution and abundances of most of the elements in geological systems was done by Clarke (1924) and these data were employed extensively in the 1920's and 1930's. This period also saw much work on the sizes of ions and the structures of crystals determined by X-ray diffraction. These two sets of data were collected and collated by Goldschmidt (1937, 1954) and principles were formulated to explain the distribution of elements in geological systems.

More recently, Shaw (1953), Burns & Fyfe (1966), Whittaker (1967), Burns (1970) and others have discussed the factors influencing the distribution of the elements.

Three main distributions of the elements during the evolution of the earth were postulated by Goldschmidt. Firstly a primary fractionation of the elements had occurred in the initial states of the formation of the earth between a metallic core and a silicate crust and mantle containing considerable quantities of sulphides. Secondly, processes of distribution have been taking place in the upper mantle and crust, for example the fractional crystallisation of a body of magma. Thirdly, a redistribution is occurring on the earth's surface through sedimentary and biological processes.

The primary distribution of the elements was formulated after Goldschmidt had investigated element fractionation between the immiscible phases found in meteorites and blast furnaces. Three major categories of elemental distribution behaviour were

described:-

- i) those elements which are preferentially incorporated into a metallic liquid rich in free electrons. In the systems investigated, this liquid is essentially iron. This group of elements was called "siderophile".
- ii) those elements which are concentrated in a sulphide liquid of a semi-metallic nature - referred to as chalcophile.
- iii) those elements which are preferentially incorporated into a silicate melt of an essentially ionic nature - referred to as lithophile.

Two further classifications were later added:-

- iv) elements which accumulate in the gas phase, either as free volatile elements or as gaseous compounds - atmophile.
- v) elements which are concentrated in living organisms - biophile.

Table 1, from Goldschmidt (1954), presents the geochemical classification of the elements, according to the distribution between the various phases.

Goldschmidt related this partition of the elements to their electronic structure and the ease with which cations, metallic phases and covalent bonds are formed. The external conditions of pressure and oxygen content operating on the system will affect the general classification to some extent; thus chromium is found to be a lithophile element on earth, but if oxygen is deficient, as in iron meteorites, chromium is decidedly chalcophile and forms the mineral daubreelite, FeCr_2S_4 .

Whilst this primary classification has generally been accepted. Goldschmidt's secondary classification has, however, given rise to considerable dispute. It deals with the distribution of elements and their incorporation into minerals which crystallise from a liquid or gaseous system. Here Goldschmidt was concerned primarily with the building up of space lattices of particular silicate minerals and the entering of elements, in the form of cations, into the spaces within the negatively charged silicate structure. This theory stressed that

TABLE 1

Goldschmidt's Geochemical Classification of the Elements

<u>Siderophile</u>	<u>Chalcophile</u>	<u>Lithophile</u>	<u>Atmophile</u>
Fe Co Ni	Cu Ag Au	Alkali Metals	H N C O
Ru Rh Pd	Zn Cd Hg	Alkali Earths	Halogens
Re Os Ir Pt Au	Ga In Tl	B Al Sc Y	Inert Gases
Mo Ge Sn C P	Ge Sn Pb	Rare Earths	
Pb As W	As Sb Bi	C Si Ti Zn Hf Th	
	S Se Te	P V Nb Ta	
	Fe Mo Re	O Cr W U	
		Fe Mn	
		Halogens	
		H Tl Ga Ge N	

(ii) If two ions have the same charge but different sizes, the ion with the smaller radius is preferred to the one with the larger radius. This is because the smaller ion has a higher charge density and is more likely to fit into the interstitial spaces of the crystal structure.

These rules are in accord with classical observations.

the behaviour of an element was determined more by its physical size than its chemical properties. On the basis of ionic size and charge, the following rules governing element distribution were formulated:-

- i) if two ions have similar radii and the same charge, they will enter into solid solution in a given mineral in amounts proportional to their abundances. The trace element is "camouflaged" by the major element. The ionic radii should not differ by more than about 15%.
- ii) if two ions have similar radii and the same charge, the smaller ion will be preferentially concentrated in the solid phase; the trace metal is "captured".
- iii) if two ions have similar radii but different charges, the ion with the higher charge will enter into the crystal structure preferentially; the trace metal is "admitted".

These rules are in accord with classical electrostatic theory i.e. the smaller the ion, the greater the electrostatic attraction between it and an oppositely charged ion; the greater the charge, the stronger the attraction.

Although Goldschmidt was able to quote many examples of element distribution which obey the above rules, nonetheless, many authors have expressed serious doubt as to the universal applicability of these rules.

Shaw (1953) criticised the idea of explaining ion enrichment in terms of ionic radii. Goldschmidt's second rule implied that when a solid solution (X, Y)Z crystallised from a liquid then the cations X would be preferentially incorporated relative to Y in the solid if X is smaller than Y. If the solid solution is continuous from XZ to YZ and the solidus has neither maxima nor minima, then the higher melting of the two components will always be enriched in the solid phase. Thus the rule is equivalent to the statement that if two compounds, XZ and YZ, form a continuous solid solution then the compound with the smaller ion has the higher melting point. Examples were given for which this did not hold true, including:-

- a) pyroxene series Ca SiO_3 - $1,540^\circ\text{C}$; Sr SiO_3 - $1,580^\circ\text{C}$
- b) oxide series MgO - $2,800^\circ\text{C}$; NiO $1,990^\circ\text{C}$

Furthermore, if the system's phase diagram has a solidus which passes through a minima or maxima, the component which is enriched in the solid phase must be different on either side of the minima or maxima.

Ramberg (1952) investigated the different distribution of iron and magnesium in different silicate systems, e.g. cordierite, $(\text{Mg, Fe})_2\text{Al}_3(\text{AlSi}_5)_0_{18}$ which commonly contains more magnesium than iron, garnet, $(\text{Ca, Mg, Fe}^{2+})_2(\text{Fe}^{3+}, \text{Al, Cr, Ti})(\text{SiO}_4)_3$ with more iron than magnesium. Also, the distribution of iron and magnesium between co-existing olivine and pyroxene had been investigated by Ramberg and De Vore (1951) and this indicated that iron was enriched relative to magnesium in olivines, magnesium relative to iron in pyroxenes.

These results were explained by making use of the various structures of the silicate minerals and showing that in a qualitative way the electronegativity of the oxygen attached to silicon in the series orthosilicate $(\text{SiO}_4)^{4-} \rightarrow$ pyrosilicate $(\text{Si}_2\text{O}_7)^{6-} \rightarrow$ meta silicate $(\text{SiO}_3)^{2-} \rightarrow$ double chain silicate $(\text{Si}_8\text{O}_{22})^{12-} \rightarrow$ phyllosilicate $(\text{Si}_5\text{O}_{10})^{6-} \rightarrow$ tectosilicate (SiO_2) , increased in a

stepwise manner and that the different metal ions distribute themselves among the different silicate structures according to their positions on the electronegativity scale (values given by Pauling, (1948), were quoted). The distribution of Mg, Fe, Ca, K, Na and Li in silicates was thus explained. This paper (Ramberg,1952) indicated that the structure of the mineral should be taken into account when discussing element distribution.

In spite of these, and other, objections many trace elements do, in fact, follow the rules given by Goldschmidt, although not for the reasons given by him. Whittaker (1967) has discussed these factors, which are:-

- i) As trace elements are present in very low concentrations, the composition of the system will always be on the side of the melting point minima at which the trace element is concentrated in the liquid phase.
- ii) The two general trends for elements of increasing atomic number to become rarer and to increase in ionic radii

(for a given charge) mean that trace elements are generally of a larger radius than the elements for which they substitute.

Whittaker also pointed out that contrary to Shaw's objections (1953) that the melting point of a substance cannot, in general, be predicted from the size of the ions, there are instances where the compound with the smaller ion has the higher melting point e.g. the olivine series (quoted by Goldschmidt) and the alkali halides (of 70 pairs with a common ion, 55 with the smaller ion have the higher melting point and if the exceptional lithium cation is excluded this ratio increases to 53 out of 54.)

Ringwood (1955) and Ahrens (1953) attempted explanations for the distribution of trace metals based on the concept of electronegativity (Pauling, 1948). Many authors, including Burns and Fyfe (1966) and Whittaker (1967) have seriously questioned these conclusions. The application of electronegativity to element fractionation, as given by Ringwood, has been discredited and will not be further discussed.

Nockolds (1966) attempted a unified approach to the problem of element distribution by making use of a term described as "the relative total bonding energy". This term was calculated using covalent bonding energies, ionic resonance bonding and in the case of transition metals, the stabilisation due to crystal field effects. He admitted, however, that certain properties of melts cannot be explained solely by the idea of bond energies, particularly certain melting relationships quoted by Shaw (1953), (e.g. SrO has a lower melting point than CaO, whereas SrAl₂SiO₈ has a higher melting point than CaAl₂SiO₈).

The group of elements which consistently defied explanations in terms of the rules proposed by Goldschmidt, Shaw, Ringwood and others were the transition metals. For example, it is well known that nickel is preferentially incorporated in early forming olivines

(Wager & Mitchell, 1951) and no reasonable explanation, based on the above rules, could be found.

In 1959, Williams showed that the distribution of the transition elements in fractionated igneous rocks could be better explained if use was made of crystal field theory (Bethe, 1929, Orgel, 1952). This aspect of transition metal chemistry, in which the electronic structure of the ions has a strong influence in determining the distribution of these elements, is discussed in Chapter 2.

With the advent of more sophisticated methods of analysis and the development of a technique to determine the site occupancy of ions in minerals (Mossbauer spectroscopy) considerable interest has been expressed in the problems of element distribution, particularly in volcanic rocks. In recent years, papers dealing with the structure and site availability of silicate melts (Burns & Fyfe, 1966; Whittaker, 1967; Boon, 1971; Seward, 1971); the distribution of elements between minerals crystallising from magma (White, 1966; Moore & Evans, 1967; Häkli & Wright, 1967; Onuma et al, 1968;

Gast, 1968), and theoretical aspects of element distribution (McIntyre, 1963; Grover & Orville, 1969; Blander, 1970; Greenland, 1970) have been published.

Of particular interest to geochemists are the transition metals and their fractionation between minerals. These metal ions, although showing similarities in ionic radii and electronegativity, exhibit startling variations in their distribution between minerals. The first important study of trace metal content of minerals was carried out by Wager & Mitchell, (1951), who analysed the minerals crystallising from the Skaergaard basic intrusion in East Greenland. Their results, which showed that scandium, vanadium, chromium, manganese, cobalt and nickel are concentrated in pyroxenes and manganese, cobalt and nickel are concentrated in olivines, have generally been shown to be correct by other investigators, (White, 1966; Moore & Evans, 1967; Håkli & Wright, 1967). Almost no research had been undertaken to determine the distribution of trace metals between the molten rock and the minerals crystallising from it. Thus a considerable gap existed in our understanding of the geochemistry of transition metal ions.

A number of papers, mostly of a theoretical nature, had indicated that a controlling factor in this distribution was the spatial

arrangement of the electrons of the transition metal and the influence of the co-ordination of the ligands formed by the various silicate structures. (Curtis, 1964; Whittaker, 1967; Burns, 1969). Little work had been carried out to quantify these ideas and accordingly this study was initiated in order to determine what effect the electronic structure of the metal ion had on its distribution. It had been shown that the sites available for transition metal ions in olivines and pyroxene (common minerals present in basic igneous rocks) are primarily distorted octahedral (Hanke, 1965; Warren & Bragg, 1928) whereas in the silicate melt, octahedral and tetrahedral sites are available (Burns & Fyfe, 1964; Whittaker, 1967). Accordingly, it was to be expected that the geometries of the various available sites would influence the non-spherical arrangement of the outer electrons of the transition metal ions and that this in turn would influence the distribution of these metal ions between minerals. It will be shown in Chapter 5 of this work that this theory holds true for the distribution of certain transition metal ions between olivine, clinopyroxene and ground-mass of a range of basic igneous rocks.

CHAPTER 2

Crystal Field Theory and its Implications for Geochemistry

1) Introduction

The crystal field theory is concerned primarily with the energy and spatial distribution of electrons, in the incompletely filled d and f orbitals, surrounding the atomic nucleus. Thus the theory is applied to the transition and rare earth elements and their ions and compounds.

Crystal field theory was first developed by Bethe (1929) using group theory, quantum mechanics and electrostatic theory. It was found particularly useful in explaining the absorption spectra and magnetic properties of transition metal and lanthanide compounds. Orgel (1952) successfully applied this theory to explain variations in the heats of hydration of transition metal ions.

Crystal field theory was applied to a petrological problem some seven years later, when Williams (1959) interpreted the distribution of transition metal ions in the various layers of the Skaergaard fractionated basic layered intrusion in East Greenland.

This delay in applying the theory to geology can be explained to some extent by the lack of suitable analytical methods for the accurate analysis of low concentrations of transition metals in small quantities of minerals. The development, in recent years, of such techniques as neutron activation analysis, electron microprobe and Mössbauer spectrometry has greatly increased both the quantity and quality of analyses which can be carried out on small samples of rocks and minerals.

Since 1959, an increasing number of papers and review articles have been published on crystal field theory and its application to mineralogical and geological systems. (Curtis, 1963; Burns & Fyfe, 1964; Schwarz, 1966; Whittaker, 1967; Burns & Fyfe, 1967; Burns, 1968; Burns, 1969, Henderson and Dale, 1970; Burns, 1970)

Transition metal distribution between coexisting minerals and site populations of these minerals are amenable to interpretation by crystal field theory. It is clear that a fuller understanding of the distribution of these metal ions within crystal

structures must consider the spatial arrangement of the electrons. Erroneous conclusions can be drawn if these arrangements are assumed to be spherical.

Crystal field theory has been discussed by Cotton and Wilkinson (1966), Orgel (1966) and Burns (1970).

11. Shape and Symmetry of d Orbitals

The five d orbitals which occur in each shell with principle quantum, number three or higher (i.e. from scandium, atomic number 21) are designated d_{xy} , d_{yz} , d_{xz} , $d_{x^2-y^2}$ and d_{z^2} , and each orbital, except d_{z^2} , has four orthogonally placed lobes. The boundary surfaces of these orbitals are shown in Fig. 1.

Three of the d orbitals have lobes projecting between the cartesian axes (d_{xy} , d_{yz} and d_{xz}) and are referred to as t_{2g} . The other two orbitals ($d_{x^2-y^2}$ and d_{z^2}) have lobes which are directed along the cartesian axes and are referred to as e_g . As each orbital can accommodate up to two electrons, each of the opposite spin, a total of ten electrons can be accommodated in each set of d orbitals. In order to minimise inter-electronic repulsion, the electrons may spread out and occupy singly as many of the orbitals as possible

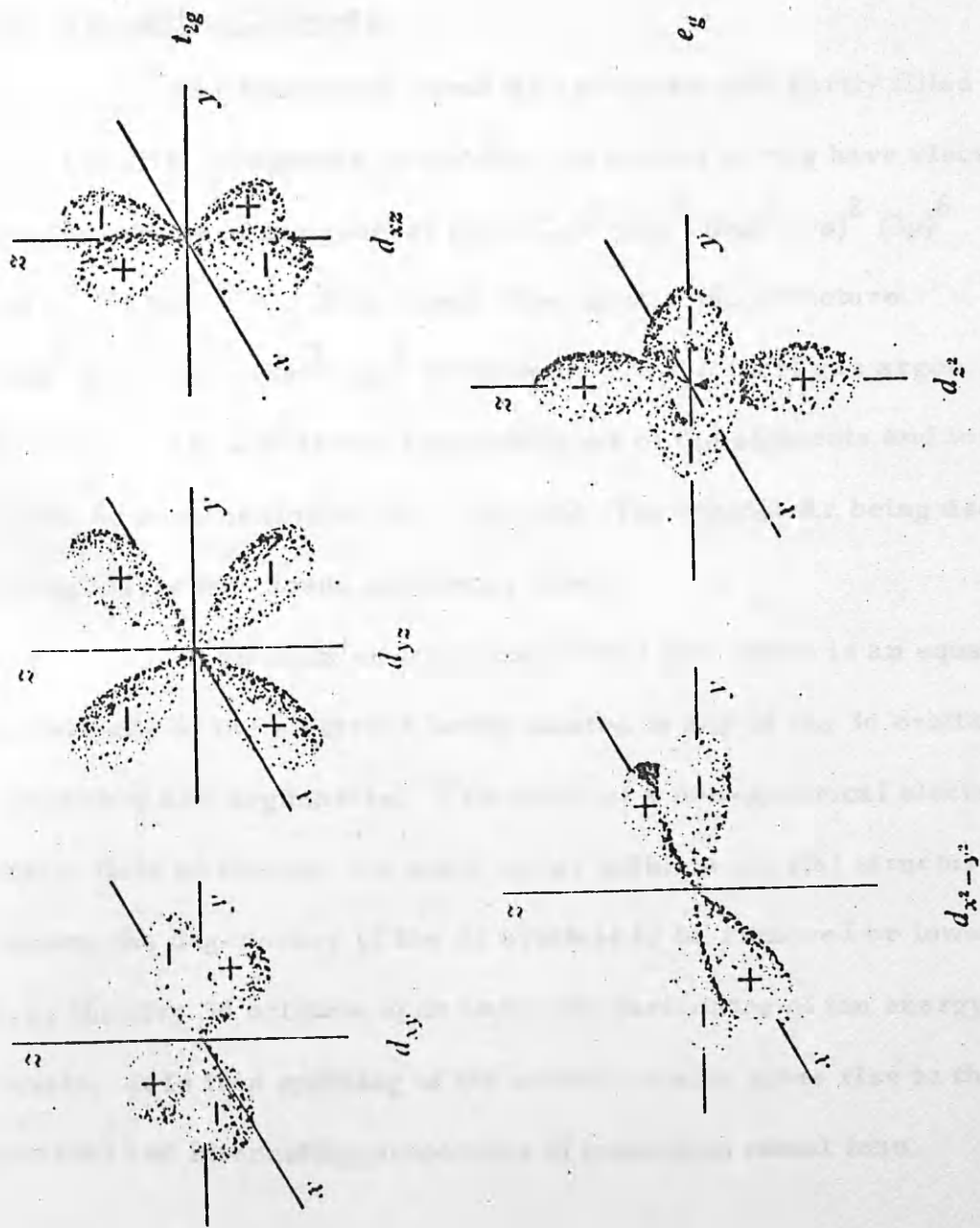


Fig. 1

Boundary Surfaces of Atomic Orbitals

with parallel spin. This principle constitutes Hund's first rule of electronic configuration.

III. Transition Elements

The transition elements are those with partly filled d or f shells. Elements of the first transition series have electronic configurations of the general form $(1s)^2 (2s)^2 (2p)^6 (3s)^2 (3p)^6 (3d)^{10-n} (4s)^1 \text{ or } 2$. The closed shell electronic structure $(1s)^2 (2s)^2 (2p)^6 (3s)^2 (3p)^6$ corresponds to the inert gas argon. In Table 1, the electronic configurations of the elements and ions of the first transition series are given, the symbol Ar being used to represent the closed electronic shells.

In an isolated transition metal ion, there is an equal probability of the electrons being located in any of the 3d orbitals, since they are degenerate. The effect of a non-spherical electrostatic field on the ion, as would occur within a crystal structure, causes the degeneracy of the 3d orbitals to be removed or lowered, i.e. the five 3d orbitals split about the baricentre of the energy levels. It is this splitting of the orbitals which gives rise to the unusual and interesting properties of transition metal ions.

TABLE 1

Electronic Configuration of First Row Transition Metal Ions

<u>Atomic Number</u>	<u>Element</u>	Electronic Configuration		
		<u>Atom</u>	<u>M^{II}</u>	<u>M^{III}</u>
21	Sc	(Ar)3d ¹ 4s ²	(Ar)3d ¹	(Ar)
22	Ti	(Ar)3d ² 4s ²	(Ar)3d ²	(Ar)3d ¹
23	V	(Ar)3d ³ 4s ²	(Ar)3d ³	(Ar)3d ²
24	Cr	(Ar)3d ⁵ 4s ¹	(Ar)3d ⁴	(Ar)3d ³
25	Mn	(Ar)3d ⁵ 4s ²	(Ar)3d ⁵	(Ar)3d ⁴
26	Fe	(Ar)3d ⁶ 4s ²	(Ar)3d ⁶	(Ar)3d ⁵
27	Co	(Ar)3d ⁷ 4s ²	(Ar)3d ⁷	(Ar)3d ⁶
28	Ni	(Ar)3d ⁸ 4s ²	(Ar)3d ⁸	(Ar)3d ⁷
29	Cu	(Ar)3d ¹⁰ 4s ¹	(Ar)3d ⁹	(Ar)3d ⁸

Ar = Argon core, 1s² 2s² 2p⁶ 3s² 3p⁶

The manner and extent to which the five-fold degeneracy is decreased depends on the type, position and symmetry of the ligands surrounding the transition metal ion.

In mineralogical systems, the common co-ordination of transition metal ions within minerals are octahedral and distorted octahedral. In silicate melts, tetrahedral co-ordination sites are available (Whittaker, 1967). The most common ligands are those formed by silicon and oxygen groupings, the oxygen atoms being the negatively charged entities. Crystal field splitting will be discussed with regard to those factors.

IV. Crystal Field Splitting in Octahedral Co-ordination

In octahedral co-ordination, the nucleus of the transition metal ion is placed at the origin of the cartesian axes, with ligands situated on the axes. In this condition, electrons in all five 3d orbitals are repelled by the negatively charged ligands and the baricentre of the degenerate energy levels is raised. The d orbitals are not all influenced in an identical manner by the ligands. Since lobes of the e_g orbitals point towards the ligands,

electrons in these orbitals, i.e. $d_{x^2-y^2}$ and d_{z^2} , are repelled in the t_{2g} orbitals which project between the ligands. This is shown in Fig. 2.

The effect of this is to raise the energy of the e_g orbitals relative to the t_{2g} orbitals as represented in Fig. 3. The difference in energy between the t_{2g} and e_g orbitals is referred to as the crystal field splitting and is commonly designated by Δ_o . The splitting of the energy levels must obey a "centre of gravity" rule and clearly the three t_{2g} will therefore be lowered by $\frac{2}{5} \Delta_o$ below, and the two e_g orbitals raised by $\frac{3}{5} \Delta_o$ above, the baricentre, as seen in Fig. 3. Each electron in a t_{2g} orbital will stabilise the transition metal ion by $\frac{2}{5} \Delta_o$, while each electron in an e_g orbital will reduce the stability by $\frac{3}{5} \Delta_o$. The resultant nett stabilisation energy is termed the crystal field stabilisation energy (C.F.S.E.).

There are thus two opposing tendencies controlling the distribution of d electrons in a transition metal ion. Firstly, the electrons will tend to be distributed in such a way as to minimise electrostatic and exchange interactions between them, so that the

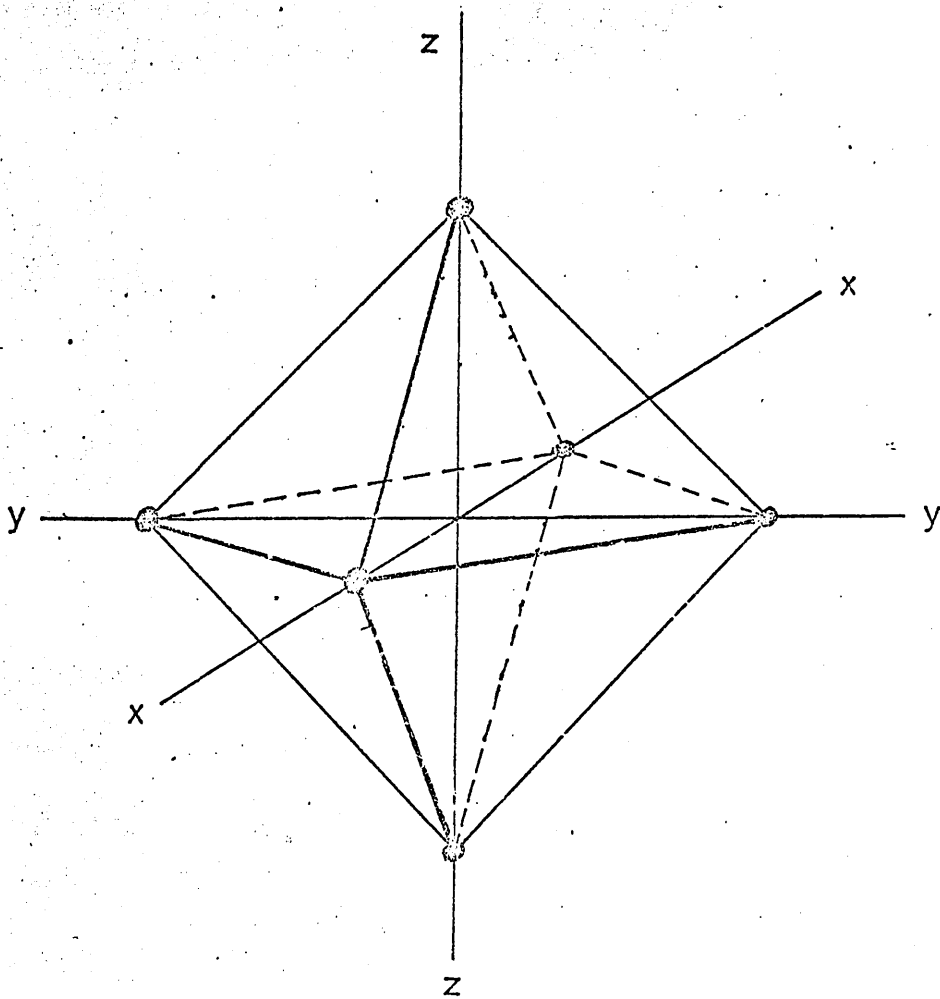


Fig. 2

Orientation of ligands in octahedral co-ordination

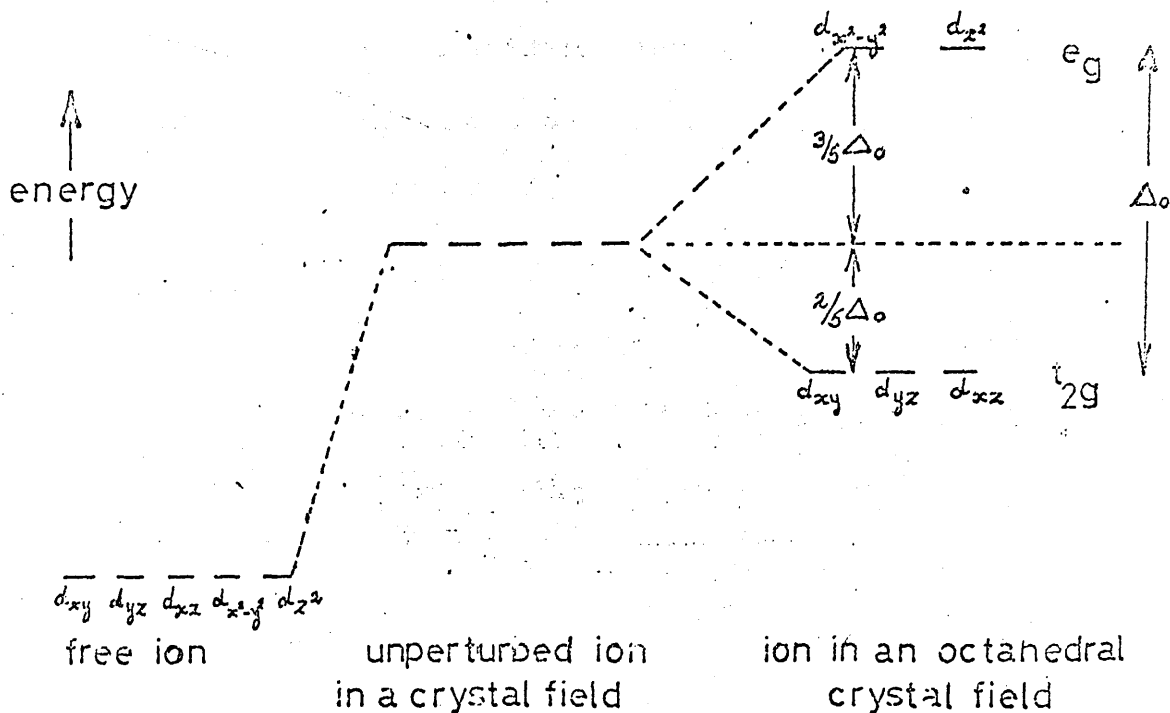


Fig. 3

Relative energy levels of d orbitals of a transition metal ion in octahedral co-ordination

maximum number of orbitals will be occupied with the electrons having parallel spin (Hund's first rule).

Secondly, the effect of crystal field splitting is to cause electrons to favour orbitals with the lowest energy so that for a transition element ion in octahedral co-ordination, the t_{2g} orbitals would be preferred.

These two opposing tendencies lead to high spin (electrons not paired) and low spin (electrons paired) states in certain transition metal ions as a function of the strength of the ligand field. For the first transition series, only ions possessing 4, 5, 6 or 7 electrons in the 3d orbitals can exhibit high or low spin. The electronic configurations of the ions of the first transition series elements in octahedral co-ordination (high spin states only given) are listed in Table 2, together with their crystal field stabilisation energies; from Orgel, (1966).

Clearly greater crystal field stabilisation energy is obtained for the low spin state of the ions, provided this gain in stabilisation energy outweighs the energy of pairing of two electrons in one orbital (of the order of 50 kcal per electron). However,

TABLE 2

Electronic Configurations and Crystal Field Stabilisation

Energies of Transition Metal Ions in Octahedral Co-ordination

and High-Spin

No. of 3d electrons	Ion	Electronic Configuration		Unpaired Electrons	C.F.S.E.
		t_{2g}	e_g		
0	Ca ²⁺ , Sc ³⁺ Ti ⁴⁺			0	0
1	Ti ³⁺	↑		1	2/5 Δ _o
2	Ti ²⁺ , V ³⁺	↑↑		2	4/5 Δ _o
3	V ²⁺ , Cr ³⁺ Mn ⁴⁺	↑↑↑		3	6/5 Δ _o
4	Cr ²⁺ , Mn ³⁺	↑↑↑	↑	4	3/5 Δ _o
5	Mn ²⁺ , Fe ³⁺	↑↑↑	↑↑	5	0
6	Fe ²⁺ , Co ³⁺ Ni ⁴⁺	↑↓↑↑	↑↑	4	2/5 Δ _o
7	Co ²⁺ , Ni ³⁺	↑↓↑↓↑	↑↑	3	4/5 Δ _o
8	Ni ²⁺	↑↓↑↓↑↓	↑↑	2	6/5 Δ _o
9	Cu ²⁺	↑↓↑↓↑↓	↑↓↑	1	3/5 Δ _o
10	Zn ²⁺ , Ga ³⁺ Ge ⁴⁺	↑↓↑↓↑↓	↑↓↑↓	0	0

apart from Co^{3+} and Ni^{3+} , all transition metal ions exist in high spin states in oxide structures on the earth's surface.

In octahedral co-ordination, ions with d^3 , d^8 and low spin d^6 configuration acquire large C.F.S.E. Thus ions such as Cr^{3+} , Ni^{2+} and Co^{3+} would be expected to prefer octahedral co-ordination, while d^0 , d^{10} and high spin d^5 ions (e.g. Sc^{3+} , Zn^{2+} and Mn^{2+} respectively) receive no C.F.S.E. in octahedral co-ordination.

V. Crystal Field Splitting in Tetrahedral Co-ordination

In tetrahedral co-ordination, the transition metal ion may be placed in the centre of a cube with the ligands lying at alternate vertices, as shown in Fig. 4. In such a situation, the electrons in t_2 orbitals are repelled to a greater extent than electrons in the e orbitals and gives rise to crystal field splitting in a similar fashion to octahedral crystal field splitting but with the $d_{x^2-y^2}$ and d_{z^2} orbitals now being lower in energy compared with the d_{xy} and d_{xz} orbitals, Fig. 5. This tetrahedral crystal field splitting parameter is denoted by Δ_t and orbitals of the e group are stabilised by $\frac{3}{5} \Delta_t$ and the t group are destabilised by $\frac{2}{5} \Delta_t$ in order to preserve

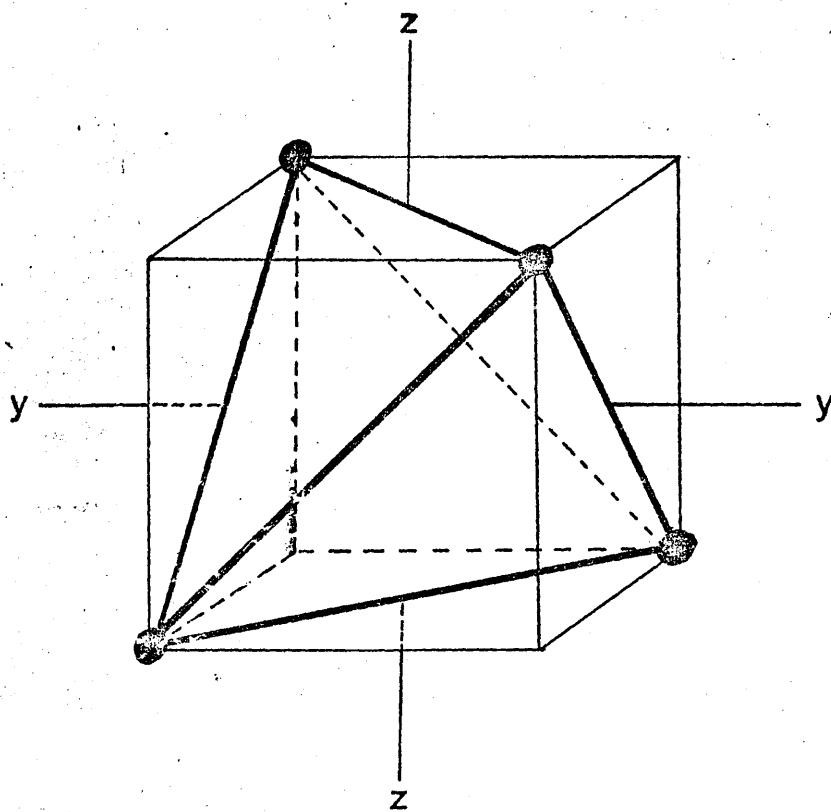


Fig. 4

Arrangement of ligands in tetrahedral co-ordination

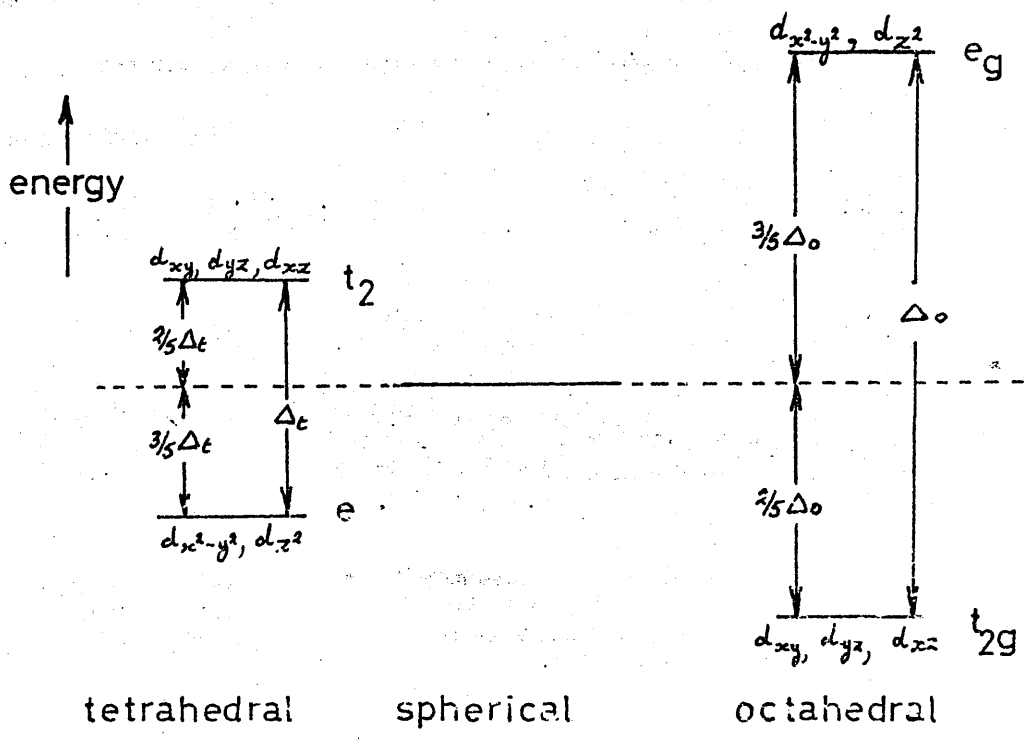


Fig. 5

Relative energy levels of d orbitals of a transition metal ion in tetrahedral and octahedral co-ordinations

the "centre of gravity". For identical cations, ligands and metal-ligand distances, it can be shown that:-

$$\Delta_t = -\frac{4}{9} \Delta_o$$

Table 3, from Orgel, (1966), gives the electronic configurations and crystal field stabilisation energies for the first row transition metal ions in tetrahedral co-ordination and high spin state.

Zn ²⁺				0
Mn ²⁺				0
Cr ²⁺ , Mn ³⁺			↑↑↑	4
Mn ²⁺ , Fe ³⁺			↑↑↑↑	5
Fe ²⁺ , Co ³⁺ , Ni ⁴⁺			↑↑↑↑	4
Co ²⁺ , Ni ³⁺			↑↑↑↑	3
Ni ²⁺			↑↑↑↑	2
Cu ²⁺			↑↑↑↑↑	1
Zn ²⁺ , Co ³⁺			↑↑↑↑↑	0

TABLE 3

Electronic Configurations and Crystal Field Stabilisation

Energies of Transition Metal Ions in Tetrahedral Co-ordination

and High-Spin

No. of 3d electrons	Ion	Electronic Configuration		Unpaired Electrons	C.F.S.E.
		e	t ₂		
0	Ca ²⁺ , Sc ³⁺ Ti ⁴⁺			0	0
1	Ti ³⁺	↑		1	3/5 Δt
2	Ti ²⁺ , V ³⁺	↑↑		2	6/5 Δt
3	V ²⁺ , Cr ³⁺ Mn ⁴⁺	↑↑	↑	3	4/5 Δt
4	Cr ²⁺ , Mn ³⁺	↑↑	↑↑	4	2/5 Δt
5	Mn ²⁺ , Fe ³⁺	↑↑	↑↑↑	5	0
6	Fe ²⁺ , Co ³⁺ , Ni ⁴⁺	↑↓↑	↑↑↑	4	3/5 Δt
7	Co ²⁺ , Ni ³⁺	↑↓↑↓	↑↑↑	3	6/5 Δt
8	Ni ²⁺	↑↓↑↓	↑↓↑↑	2	4/5 Δt
9	Cu ²⁺	↑↓↑↓	↑↓↑↓↑	1	2/5 Δt
10	Zn ²⁺ , Ga ³⁺ , Ge ⁴⁺	↑↓↑↓	↑↓↑↓↑↓	0	0

VI. Jahn-Teller Effect

Jahn & Teller (1937) proved that if the ground state or lowest energy level of a molecule is degenerate, it will distort spontaneously so as to remove the degeneracy and make one energy level more stable compared with the undistorted orbital energy level. Such distortions are predicted for d^4 , d^9 and low-spin d^7 ions in octahedral co-ordination (i.e. Cr^{2+} , Mn^{3+} , Cu^{2+} , Ni^{3+}) and for d^3 , d^4 , d^8 and d^9 ions in tetrahedral co-ordination (e.g. Cr^{3+} , Mn^{3+} , Ni^{2+} and Cu^{2+}). Jahn-Teller effects are generally small in the case of silicates and in this study the distribution of the ions investigated was assumed to be due entirely to simple crystal field effects.

(ii) oxides and metal (ii) sulphates are given in Fig. 5. The curves of George and McClure (1959). These show the characteristic humped curves. The deviations from a smooth variation are

VII. Evaluation of Δ

Two independent methods for the estimation of the crystal field splitting parameter are available.

The first and most commonly used technique involves the measurement of the positions of the absorption bands in the visible and infrared spectra of transition metal compounds. In general, the absorption data has been obtained either from transition metal ions in solution e.g. as determined by Dunitz and Orgel (1957), or in glasses containing transition metal ions e.g. as determined by McClure (1957). Tables 4 and 5 present their data for octahedral and tetrahedral crystal field splitting. The values given by Dunitz and Orgel (1957) have been employed in the present study.

The second method involves the investigation into the thermodynamic properties of transition metal compounds. For example, plots of the lattice energies of metal (III) fluorides, metal (II) oxides and metal (II) sulphides are given in Fig. 6. (Data from George and McClure (1959). These show the characteristic two-humped curves. The deviations from a smooth variation along a row of transition metal ions as a result of the contraction of the ions is because the ions are not spherically symmetrical but display

TABLE 4

Octahedral and Tetrahedral Crystal Field Stabilisation Energies
for Transition Metal Ions, Data from Dunitz & Orgel (1957)

Ion	Octahedral C.F.S.E. k cal mole ⁻¹	Tetrahedral C.F.S.E. k cal mole ⁻¹	Octahedral Site Preference Energy
Ca ²⁺ , Sc ³⁺	0	0	0
Ti ⁴⁺			
Ti ³⁺	20.9	14.0	6.9
V ³⁺	38.3	25.5	12.8
Cr ³⁺	53.7	16.0	37.7
Mn ³⁺	32.4	9.6	22.8
Mn ²⁺ , Fe ³⁺	0	0	0
Fe ²⁺	11.9	7.9	4.0
Co ³⁺	Not	Given	
Co ²⁺	22.2	14.8	7.4
Ni ²⁺	29.2	8.6	20.6
Cu ²⁺	21.6	6.4	15.2

TABLE 5

Octahedral and Tetrahedral Crystal Field Stabilisation Energies
for Transition Metal Ions, Data from McClure (1957)

Ion	Octahedral C.F.S.E. k calmole ⁻¹	Tetrahedral C.F.S.E. k calmole ⁻¹	Octahedral Site Preference Energy
Ca ²⁺ , Sc ³⁺ Ti ⁴⁺	0	0	0
Ti ³⁺	23.1	15.4	7.7
V ³⁺	30.7	28.7	2.0
Cr ³⁺	60.0	13.3	46.7
Cr ²⁺	24.0	7.0	17.0
Mn ³⁺	35.9	10.6	25.3
Mn ²⁺ , Fe ³⁺	0	0	0
Fe ²⁺	11.4	7.5	3.9
Co ³⁺	45.0	26.0	19.0
Co ²⁺	17.1	15.0	2.1
Ni ²⁺	29.3	6.5	22.8
Cu ²⁺	22.2	6.6	15.6

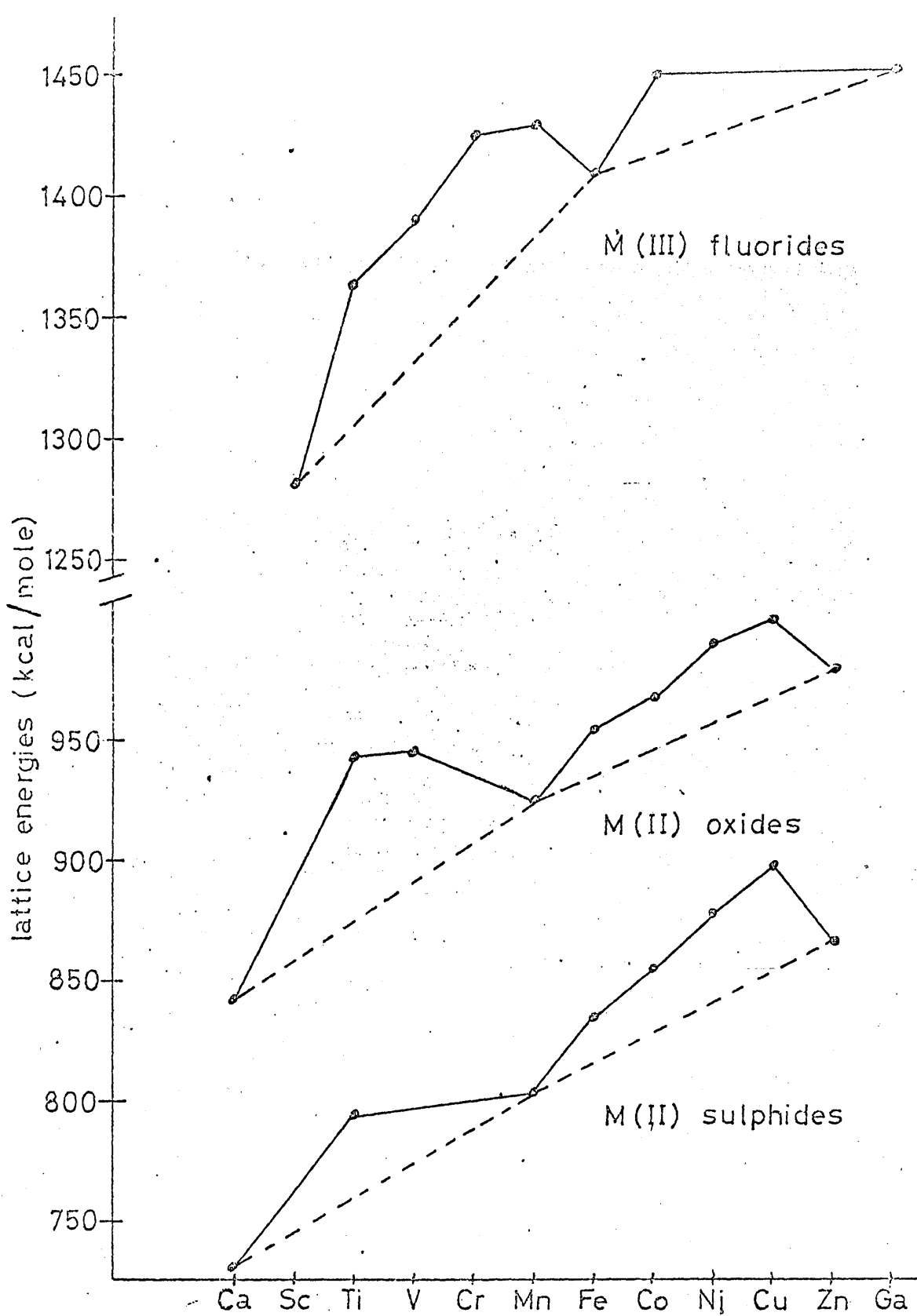


Fig-6

Lattice energies for transition metal compounds.

preferential filling of certain 3d orbitals. Table 6 gives the octahedral crystal field stabilisation energies of transition metal ions (+2 state) estimated from plots of thermodynamic data.

50.8

3

15.6

17.8

31.4

TABLE 6

Octahedral Crystal Field Stabilisation Energies for Transition

Metal (II) Oxide, from Thermodynamic Data

<u>Ions</u>	<u>Crystal Field Stabilisation Energy, kcal/mole</u>
Ca ²⁺	0
Ti ²⁺	45.0
V ²⁺	56.8
Mn ²⁺	0
Fe ²⁺	15.6
Co ²⁺	22.6
Ni ²⁺	31.4

can be regarded as a tetragonally distorted octahedron of the O_h type. The M_2 sites are regarded as a trigonally distorted octahedron compressed along the c -

The average metal to oxygen distances of the M_1 sites

VIII. Sites Available in Silicate Minerals

An appreciation of the dimensions and shapes of the sites available in silicate minerals is important to help to explain the distribution of metal ions between various minerals. For this study, only the structures of olivine and clinopyroxene, together with the possible structure of the silicate melt will be discussed.

a) Olivine

The structure of olivine, $(\text{Fe}, \text{Mg})_2\text{SiO}_4$, consists of independent SiO_4 tetrahedra linked by divalent ions in six-fold co-ordination and fig. 7 shows the olivine crystal structure as determined by Hanke (1965).

There are two non-equivalent six co-ordinate positions in the structure, usually designated by M_1 and M_2 . These two sites are somewhat distorted from pure octahedral symmetry. The M_1 site can be regarded as a tetragonally distorted octahedron elongated along the O_3-O_3 axis. The M_2 site is irregular but may be considered as a trigonally distorted octahedron compressed along the a -axis.

The average metal to oxygen distances of the M_1 site is shorter than that of the M_2 site, the values increasing from forsterite,

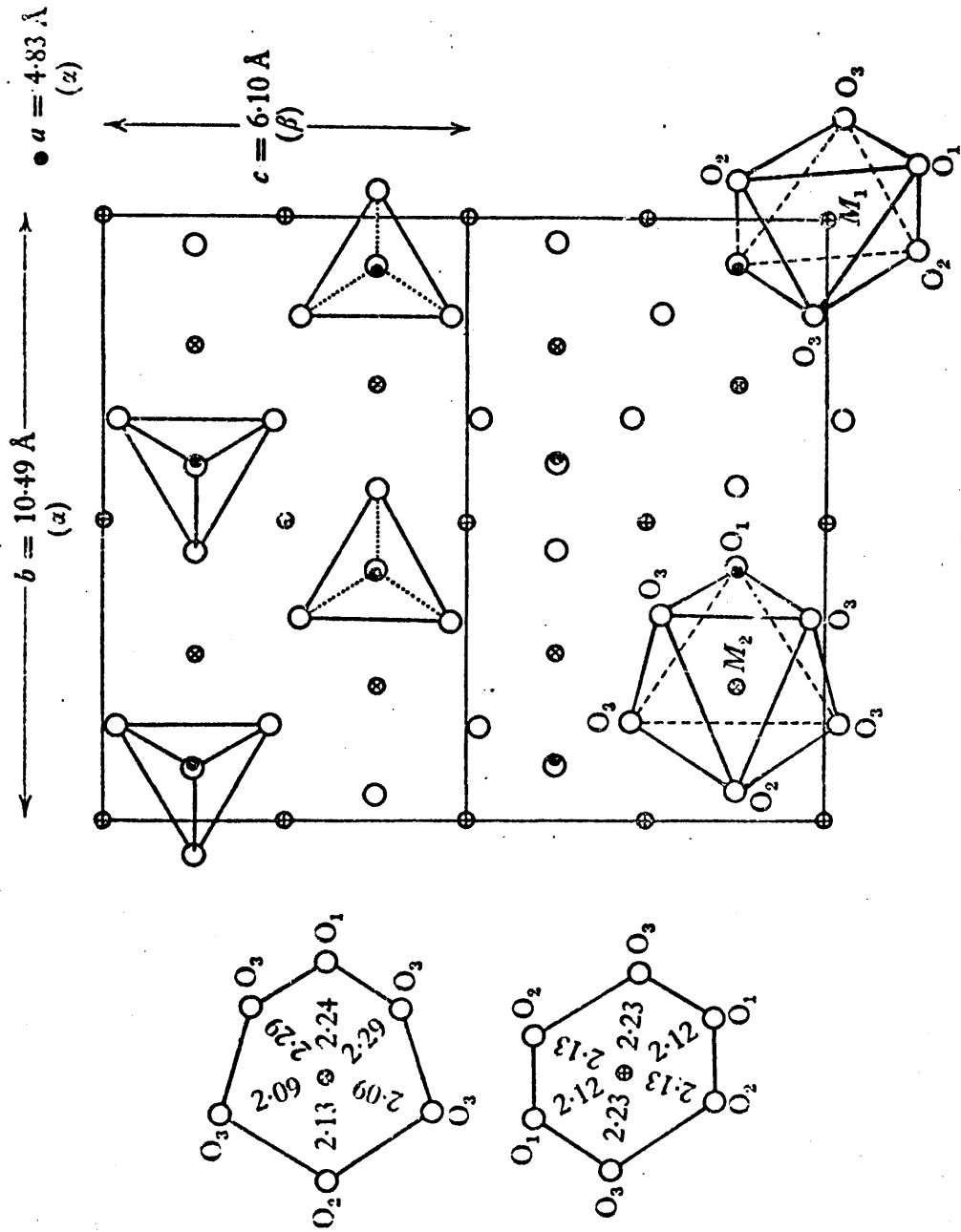


Fig. 7
Olivine Crystal Structure (Hanke, 1965)

Mg₂SiO₄ to fayalite, Fe₂SiO₄, e.g. Fo₉₀, M₁ site 2.10Å,
M₂ site 2.14Å ; Fo₅₃, M₁ 2.14Å, M₂ 2.16Å ; Fo₀, M₁ 2.16Å,
M₂ 2.19Å.

In Table 7 are presented the ionic radii of the first row transition metal ions and for comparison the radii of Mg²⁺, Ca²⁺ and Al³⁺ since as common constituents of many silicate minerals these ions can be replaced by transition metal ions. (Data from Whittaker and Muntus, 1970).

It can be seen from this list that Mn²⁺, Co²⁺ and Ni²⁺ (also Cr²⁺ if this ion could be present) can be accommodated in the olivine structure.

The distortion of the octahedral sites available within the olivine structure causes complete resolution of the 3 d orbitals, as shown in Fig. 8. (From Burns, 1969).

By employing Fig. 8, it is possible to indicate crystal field stabilisation energies in distorted sites - this is given in Table 8.

TABLE 7

Ionic Radii (Å) of Transition Metal Ions,

Data from Whittaker & Muntus (1970)

<u>Element</u>	<u>M²⁺</u>	<u>M³⁺</u>
Sc	-	0.83
Ti	-	0.75
V	-	0.72
Cr	0.81 low spin 0.90 high "	0.70
Mn	0.75 low spin 0.91 high "	0.66 low spin 0.73 high "
Fe	0.69 low spin 0.86 high "	0.63 low spin 0.73 high "
Co	0.73 low spin 0.83 high "	0.61 low spin 0.69 high "
Ni	0.77	0.64 low spin 0.68 high "
Cu	0.81	-

Mg	0.66 (iv) 0.60 (vi)	-
Ca	1.08	-
Al	-	0.47 (iv) 0.61 (vi)

All values for six co-ordinated cations, except for Mg²⁺ and Al³⁺ where four and six co-ordinated values are given.

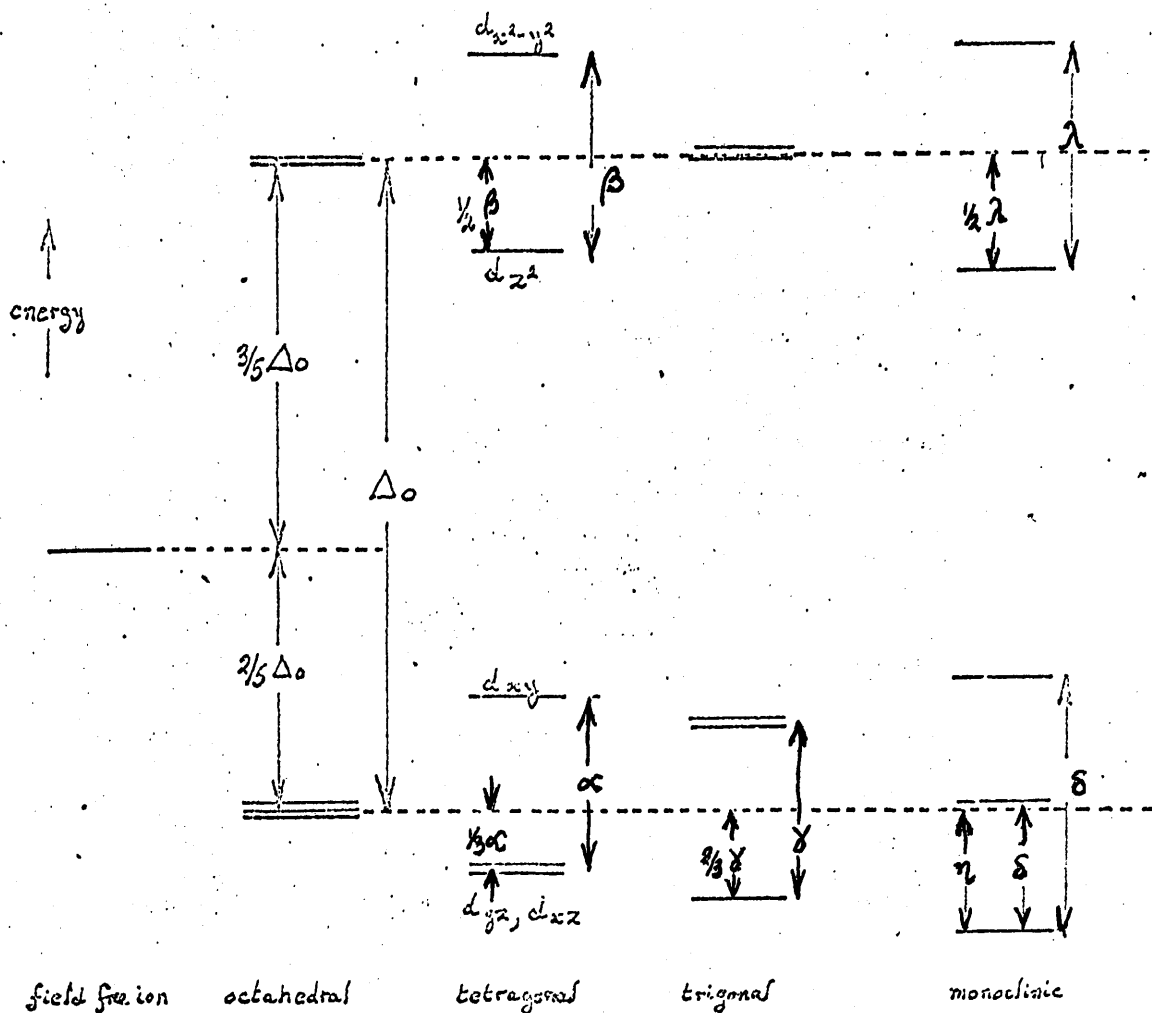


Fig. 8

Crystal field stabilisation energies in distorted sites

Stabilisation Energies of Transition Metal Ions in Six Co-ordinate Sites of Various Symmetries

Ion	Number of d electrons	C. F. S. E. for High Spin States ¹			
		Octahedral	Tetragonal ²	Trigonal ³	Monoclinic
Ca ²⁺ , Sc ³⁺	0	0	0	0	0
Ti ³⁺ ,	1	2/5 Δ_o	2/5 $\Delta_o + \frac{1}{3} \alpha$	2/5 $\Delta_o + \frac{2}{3} \gamma$	2/5 $\Delta_o + \eta$
V ³⁺	2	4/5 Δ_o	4/5 $\Delta_o + \frac{2}{3} \alpha$	4/5 $\Delta_o + \frac{1}{3} \gamma$	4/5 $\Delta_o +$
Cr ³⁺	3	6/5 Δ_o	6/5 Δ_o	6/5 Δ_o	6/5 Δ_o
Cr ²⁺ , Mn ³⁺	4	3/5 Δ_o	3/5 $\Delta_o + \frac{1}{2} \beta$	3/5 Δ_o	3/5 $\Delta_o + \frac{1}{2} \lambda$
Mn ²⁺ , Fe ³⁺	5	0	0	0	0
Fe ²⁺	6	2/5 Δ_o	2/5 $\Delta_o + \frac{1}{3} \alpha$	2/5 $\Delta_o + \frac{2}{3} \gamma$	2/5 $\Delta_o + \eta$
Co ³⁺	6	12/5 Δ_o	12/5 Δ_o	12/5 Δ_o	12/5 Δ_o
Co ²⁺	7	4/5 Δ_o	4/5 $\Delta_o + \frac{2}{3} \alpha$	4/5 $\Delta_o + \frac{1}{3} \gamma$	4/5 $\Delta_o +$
Ni ²⁺	8	6/5 Δ_o	6/5 Δ_o	6/5 Δ_o	6/5 Δ_o
Cu ²⁺	9	3/5 Δ_o	3/5 $\Delta_o + \frac{1}{2} \beta$	3/5 Δ_o	3/5 $\Delta_o + \frac{1}{2} \lambda$
Zn ²⁺	10	0	0	0	0

1 Except Co³⁺

2 Elongate along the tetrad axis (e.g. olivine M₁ site)

3 Compressed along the triad axis (e.g. olivine M₂ site).

The following enrichment pattern has been predicted by Burns (1969) for the M_1 and M_2 sites of olivine:

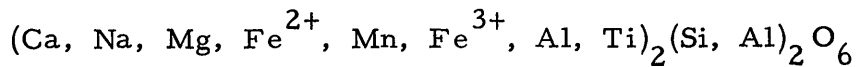
M_1 sites: Ni^{2+} , Co^{2+} , Cu^{2+} and possibly Cr^{2+}

M_2 sites: Fe^{2+} , Mn^{2+}

The results of this work describing the transition metal ion content of olivines will be given in the appropriate section of Chapter 5.

b) Pyroxene

The pyroxenes investigated in this study have been the clinopyroxene augite, having the general chemical formula -



The essential structure of pyroxene is the linkage of SiO_4 tetrahedra by sharing two of the four corner oxygen atoms to form continuous chains of composition $(SiO_3)_n$ with cations (Ca, Mg, Fe, Na, Al) linking the chains. There are two positions of six fold co-ordination, designated M_1 and M_2 . Cations in the M_1 sites are octahedrally co-ordinated by oxygens which are themselves linked to one silicon atom. Cations in the M_2 position are surrounded by four

oxygen ions each linked to one silicon atom and two bridging oxygen atoms which are shared by two silicon atoms. In clinopyroxenes the M_1 sites are more distorted (tetragonal distortion) than similar sites in orthopyroxenes. The M_2 sites are considerably distorted from octahedral symmetry in both types of pyroxenes.

Ca^{2+} ions predominate in the M_2 positions in clinopyroxene.

Fig. 9 shows the clinopyroxene structure as found by Warren & Bragg (1929), as given by Deer, Howie & Zussmann (1966).

In augite deficiencies of Ca^{2+} in M_2 sites of the clinopyroxene structure can occur and substantial amounts of trivalent ions may be present. To balance the charges alkali metal and divalent metal ions can occupy M_2 positions with trivalent ions in M_1 sites. Burns (1969) using similar arguments to those employed in predicting transition metal enrichment patterns for the distorted M_1 and M_2 olivine sites, has suggested that Fe^{2+} , Co^{2+} , Cu^{2+} , Mn^{2+} , and possibly Cr^{2+} will preferentially enter M_2 augite positions.

The analysis of augites for transition metals is described in Section II, ii, in Chapter 5.

(c) Silicate Melt Structure

The possible structures of silicate melts have been discussed by a number of authors, including Barth & Rosenquist (1949), Wasserburg (1957), Burns & Fyfe (1964), Whittaker (1967), Seward (1971) and Boon (1971).

Whittaker (1967) in his study of silicate melt structure suggested that the liquid silicate may approximate to a random close-packing of oxygen ions, similar to the model of liquids proposed by Bernal (1964), with silicon and metal cations occupying available interstitial sites within this packing. The number and co-ordination of the available sites were calculated and these are presented in Table 9. It is evident that the ratio of the number of tetrahedral sites to the number of octahedral and larger sites is much higher in the liquid compared to the solid close-packing (4.4 : 1 as against 2 : 1). In Table 10 are given the number of sites which must be filled in silicates of various compositions. Because of the relatively high ratio of filled octahedral and larger sites to filled tetrahedral sites, the disproportion between the number of unfilled tetrahedral sites and octahedral and larger sites in the liquid and the

TABLE 9

Available Sites, per 24 Oxygen Ions, in the Bernal Liquid
and a Solid Close Packing

	<u>Tetrahedral</u> <u>Type</u>	<u>Octahedral</u> <u>Type</u>	<u>Larger</u> <u>than</u> <u>Octahedral</u> <u>Type</u>	<u>Octahedral</u> <u>and</u> <u>Larger</u>
Bernal Liquid	73	13.6-6.7	3.1-6.7	16.8
Solid Close Packed	48	24	0	24

TABLE 10

Filled Sites, per 24 oxygen ions, in Silicates of Various Compositions

	Tetrahedral Type	Octahedral Type	Larger than Octahedral Type	Octahedral and Larger
Olivine composition	6	12	0	12
Diopside composition	8	4	4	8
Anorthite composition	6-12	6-0	3	9-3
Basic magma (Skaergaard chilled margin composition)	6.9-10	6.2-3.1	2.4	8.6-5.1

solid is even greater than for the total sites, reaching a maximum for olivine composition of 14.3 : 1 in the liquid against 3.5 : 1 in the solid.

Experimental results have been obtained which confirm that these sites are available for transition metal ions in silicate glasses, e.g. Burns & Fyfe (1964) and Seward (1971) who investigated the absorption spectra of transition element doped silicate glasses. However, Boon (1971) in a Mössbauer study of glasses in the system $\text{Na}_2\text{O}-\text{FeO}-\text{SiO}_2$ found that Fe^{2+} occupies only two types of octahedral site, yet Ni^{2+} , with a higher octahedral site preference energy than Fe^{2+} occupies tetrahedral sites in glasses of high Na_2O and SiO_2 content, (Burns & Fyfe, 1964). Absorption spectra of transition metal compounds and their derived liquids were also shown to be similar (Burns, 1970) indicating that ions receive comparable crystal field stabilisation energies in the two phases.

It has already been shown that octahedral and distorted octahedral sites are available for transition metal ions in olivine and clinopyroxene crystals. Thus when a magma crystallises, forming these minerals, there is added stability for the transition metal ions in octahedral sites in the minerals and so it is energetically

more favourable for these ions to be removed from tetrahedral co-ordination in the molten silicate and to enter octahedral sites in the olivine and clinopyroxene crystals. This added stability is referred to as the octahedral site preference energy (O.S.P.E.) and is obtained by subtracting the crystal field stabilisation energy in tetrahedral co-ordination from the crystal field stabilisation energy in octahedral co-ordination. (Tables 4 and 5) Seward, (1971) in his study of element distribution in the synthetic system $\text{CaMgSi}_2\text{O}_6 - \text{Na}_2\text{Si}_2\text{O}_5 - \text{H}_2\text{O}$ showed that the ΔH values for the exchange reaction of Ti^{4+} , V^{3+} , Cr^{3+} , Ni^{2+} and Co^{2+} between co-existing melt and diopside crystals can be directly correlated with the O.S.P.E. of these ions. He also concluded that Ni^{2+} and Co^{2+} are distributed over both tetrahedral and octahedral sites in the melt.

IX. Trace Element Partitioning

A number of papers have been published dealing in a theoretical manner with the partitioning of trace elements between mineral assemblages during crystallisation of a magma (Neumann et al, 1954; McIntire, 1963; Grover & Orville, 1969; Blander, 1970; Greenland, 1970). In this study a simplified approach to element partitioning was found to be perfectly adequate to describe the results obtained. The discussion of trace metal fractionation closely follows that given by Håkli & Wright (1967) in their investigation of the distribution of nickel between olivine, augite and glass of samples of lava from Makaopuhi, Hawaii.

The chemical potential μ of a component distributed between two phases I. and II. is

$$\text{in phase I. } \mu_{\text{I}} = \mu_{\text{I}}^{\circ} + RT \ln a_{\text{I}}$$

$$\text{in phase II. } \mu_{\text{II}} = \mu_{\text{II}}^{\circ} + RT \ln a_{\text{II}}$$

where

a_{I} = activity of the component in phase I.

a_{II} = " " " " " " II.

μ_{I} = chemical potential of the component in phase I.

μ_{II} = chemical potential of the component in phase II.

R = the gas ^{constant} content

T = absolute temperature

At equilibrium the two values of the potential are equal and since μ_I^o and μ_{II}^o are constants, at fixed temperature and pressure, it follows that

$$\frac{a_I}{a_{II}} = \text{constant, } k.$$

If the concentrations of the element in both phases is low, activities can be replaced by concentrations. In general, the partition coefficient, k , is not constant but depends on pressure, temperature and composition of the phases. If pressure and composition are held constant and assuming ΔH to be independent of temperature, pressure and composition, then

$$\ln k = - \frac{\Delta H}{RT} + B$$

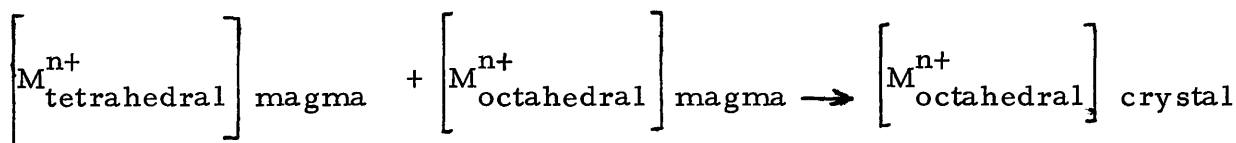
where

ΔH = enthalpy (the difference between the heats of solution of the trace component in phase I. and phase II. respectively)

B = integration constant

This relationship is the integrated form of the Van't Hoff equation. Håkli & Wright (1967) and Håkli (1968) have shown that this equation is applicable to the distribution of nickel between olivine, augite and glass of basic intrusive and extrusive rocks.

In this study, it was considered that the following partition of ions takes place during crystallisation of a silicate melt -



since, as discussed above, tetrahedral and octahedral sites are available in the magma while octahedral and distorted octahedral sites are found in olivine and clinopyroxene crystals.

If it is assumed that entropy changes for transition metal ions of the same oxidation state are similar, then the use of crystal field stabilisation energy terms can be applied when comparing the distribution of transition metals between coexisting minerals and the magma from which these minerals crystallised. Throughout this study, it has been considered that a large part of

the enthalpy term is made up of the octahedral site preference energy and that a major difference in the partition of transition metal ions of the same oxidation state can be directly related to the O.S.P.E. If this reasoning is valid, a direct relationship between $\ln k$ and O.S.P.E. should be obtained, where k , the partition coefficient is given by

$$\frac{[M]_{\text{crystal}}}{[M]_{\text{groundmass}}}$$

Results obtained for the rocks investigated are discussed in section 11. v, of Chapter 5 and it is shown that such a relationship holds for the partition of divalent manganese, iron, cobalt and nickel between olivine and groundmass, and clinopyroxene and groundmass of a range of basaltic rocks. The partitions of the trivalent ions, scandium and chromium, can be explained qualitatively by employing crystal field stabilisation energy terms.

CHAPTER 3

Experimental Methods - Activation Analysis

1. Introduction

In the basaltic rocks investigated, the principal minerals present were olivine and clinopyroxene, together with the ground-mass remaining after these minerals had crystallised. The range of concentrations of the transition metals in these minerals and in basaltic rocks are presented in Table 1. (Data from Wager and Mitchell, 1951; Muir and Tilley, 1964; White, 1966; Håkli and Wright, 1967; Manson, 1967; Prinz, 1967; Onuma et al, 1968.)

Numerous methods of analysis are available for such concentrations in rock samples including D.C. arc emission spectrography, atomic absorption, X-ray fluorescence spectrography, electron microprobe, neutron activation and various chemical methods.

Neutron activation analysis was chosen as the main method of analysis because -

- i) it combined high sensitivity with accuracy, thus reducing the quantity of sample required - particularly important when analysing mineral separates

TABLE 1

Range of Concentrations of Transition Metals in Olivine,
Clinopyroxene and Basaltic Rocks

	<u>Olivine</u>	<u>Clinopyroxene</u>	<u>Basaltic Rocks</u>
Sc (p.p.m.)	5	20-150	0-60
Ti (as % TiO ₂)	0-0.20	0.87-2.72	1.20-1.53
V (p.p.m.)	45-100	30-750	10-600
Cr (p.p.m.)	0-700	700-2500	0-700
Mn (p.p.m.)	1400-2300	800-1400	1100-1300
Fe Fe ₂ O ₃ (%)	0.05-0.43	0.21-3.74	1.50-6.00
Fe FeO (%)	8.4-65.02	5.06-31.54	2.50-15.00
Co (p.p.m.)	20-250	15-60	7-80
Ni (p.p.m.)	10-3200	26-255	3-1000

Data from Wager & Mitchell (1951); Muir & Tilley (1964); White (1966); Häkli & Wright (1967); Manson (1967); Prinz (1967); Onuma et al (1968).

- ii) a number of elements could be analysed simultaneously on the same sample
- and iii) the near proximity of the Scottish Research Reactor Centre (12 miles away) meant that irradiations could easily be carried out.

The other methods of analysis mentioned above were used in those cases where activation analysis was not suitable and also to confirm activation analysis results.

Activation analysis is a technique which involves the production of a radioactive isotope by the bombardment of a target element with incident particles (e.g. neutrons, protons, deuterons, alpha particles, gamma rays, etc.). The characteristic decay of the isotope is then measured, e.g. the characteristic gamma ray energy emitted. Activation analysis is one of the few modern an-

II. Principles of Activation Analysis

This analytical method has been described by various authors including Lenihan and Thomson (1965) and Schultze (1969) for general principles, and by Mapper (1960) and Winchester (1961) for its application to geological samples.

The technique of neutron activation was first employed in 1936 following the demonstration by Fermi et al (1934) that a number of elements when bombarded with neutrons became radioactive, the radioactivity being characteristic of the newly formed nucleus. Hevesy and Levi (1936), using a radium-beryllium neutron source, were able to detect impurities in rare earth samples (dysprosium in yttrium and europium in gadolinium). This method involves the production of a radioactive isotope by the interaction of incident particles (e.g. neutrons, protons, electrons) or rays (photons) on the nucleus of the target element and measurement of the characteristic radioactive decay of the activated nucleus e.g. the characteristic gamma ray energy or the half-life. Activation analysis is one of the few modern analytical techniques which are concerned solely with the nucleus, the other

methods which measure some property of the nucleus are mass spectrometry and nuclear magnetic resonance.

Three main types of artificially induced nuclear reactions are possible:

i) Energy can be given to the nucleus by high energy photons or electrons and this excess energy may be released by the emission of nuclear particles.

ii) Charged atomic particles, such as protons and deuterons, can be accelerated by electrical means and used to bombard the target nucleus. These particles can either increase the energy of the nucleus and give rise to the emission of other nuclear particles as in i), or be incorporated into the nucleus and thereby produce a nucleus with different mass, charge and radioactive status.

iii) Neutrons can be incorporated into the nucleus. As neutrons are uncharged particles this process is more readily accomplished than nuclear reactions involving charged particles which must overcome the coulombic repulsion between the nucleus

and the bombarding particles.

Nuclear reactions i) and ii) have not reached the stage of being widely used primarily because high cost linear accelerators are required either to accelerate the nuclear particles for interaction with the target nucleus or to produce high energy gamma ray quanta in the bremsstrahlung from targets bombarded with electrons. Very efficient cooling systems are required to protect the sample from the heat produced by these reactions.

Neutrons have been the most widely used activating species as they are readily available by:-

i) Nuclear reactors : neutrons being produced in the fission of the nuclear fuel. Fluxes of 10^{11} to more than 10^{14} neutrons $\text{cm}^{-2} \text{sec}^{-1}$ are common.

ii) Radioisotope neutron sources : making use of (α, n) reactions (e.g. americium 241-beryllium, curium 242-beryllium) or (γ, n) reactions (e.g. antimony 124-beryllium). These sources are convenient to handle but the maximum neutron flux obtainable is only of the order of $10^8 \text{ n cm}^{-2} \text{sec}^{-1}$.

iii) Particle accelerators : neutrons produced by bremsstrahlung interacting with a beryllium target ; the bremsstrahlung is obtained by the bombardment of a target of high atomic number (e.g. gold or tungsten) with high energy electrons, usually produced by a Van den Graaf electron accelerator. Neutron fluxes of $10^{10} - 10^{11} \text{ n cm}^{-2} \text{ sec}^{-1}$ can be obtained with a 25 MeV accelerator.

iv) Tritium neutron sources are produced by the interaction of 150 - 400 keV deuterons, obtained from a Cockcroft-Walton generator, with tritium atoms by the ${}^3\text{T}(d, n){}^4\text{He}$ reaction. Fluxes of $10^{10} - 10^{11} \text{ n cm}^{-2} \text{ sec}^{-1}$ can be obtained by this method.

All of the above methods of neutron production are used for activation analysis but nuclear reactor irradiations are preferred because the higher neutron fluxes enable more accurate and sensitive analyses to be made.

III. Interaction of Neutrons with Nuclei

In nuclear reactors, neutrons of thermal energies, as determined by the Boltzmann distribution appropriate to the ambient temperature, are obtained by the use of large quantities of moderators (e.g. graphite or water) which slow down the fission neutrons from the reactor fuel. These thermal neutrons are easily captured by nuclei of most elements, to give an (n, γ) type of nuclear reaction. If the isotope produced by the absorption of a neutron into the nucleus is unstable, the resulting radioactivity can be measured.

The radioactive atoms follow the normal law of radioactive decay:

$$A_t = A_o e^{-\lambda t}$$

where A_t = activity in disintegrations per unit time at time t .

A_o = activity in disintegrations per unit time at time = 0.

λ = radioactive decay constant.

The half-life $t_{\frac{1}{2}}$, is related to λ by:

$$t_{\frac{1}{2}} = \frac{0.693}{\lambda}$$

The factors which determine the amount of radioactivity formed under the influence of neutron bombardment are:-

- i) the weight of element present, W
 - ii) the fractional abundance of the isotope undergoing the (n, γ) reaction, θ
 - iii) the activation cross-section for the nuclide concerned, σ .
 - iv) the neutron flux, ϕ .
 - v) the half-life with which the radioactive species decays, $t_{\frac{1}{2}}$.
- and vi) the length of time of irradiation, t_i .

If N^* is the number of radioactive atoms formed after a time t_i secs., the ratio $\frac{dN^*}{dt}$, at which the number of radioactive atoms increase is given by:

$$\frac{dN^*}{dt} = \phi \sigma N - \lambda N^* \quad \text{--- (i)}$$

where N is the number of atoms of the isotope being activated present in the sample and is given by:

$$N = (6.025 \times 10^{23}) \theta \cdot \frac{W}{M}$$

where M is the mass number of the isotope being activated.

$\phi\sigma N$ represents the rate of formation of radioactive atoms, and λN^* their rate of decay.

Integration of equation (i) gives the number, N^* , of radioactive atoms present after time t_i .

Since N^* is very small compared with N , N can be assumed to remain constant.

Integration gives,

$$\phi\sigma N e^{-\lambda t_i} = \phi\sigma N - \lambda N^*$$

The activity, A_t , in disintegrations per second, due to the atoms N^* produced after t_i , is given by:

$$A_t = \lambda N^* = \phi\sigma N(1 - e^{-0.693t_i/t_{1/2}})$$

or

$$= 6.025 \times 10^{23} \phi \sigma \theta \left(\frac{W}{M}\right) (1 - e^{-0.693t_i/t_{1/2}})$$

When t_i becomes long compared with $t_{1/2}$, then $(1 - e^{-0.693t_i/t_{1/2}})$ approaches unity and the saturation activity, A_{∞} , is obtained, i.e. for $t_i \geq 7t_{1/2}$. Fig. 1 is a plot of activity vs irradiation time.

$$A_{\infty} = 6.025 \times 10^{23} \phi \sigma \theta \left(\frac{W}{M}\right)$$

Activity vs Irradiation time

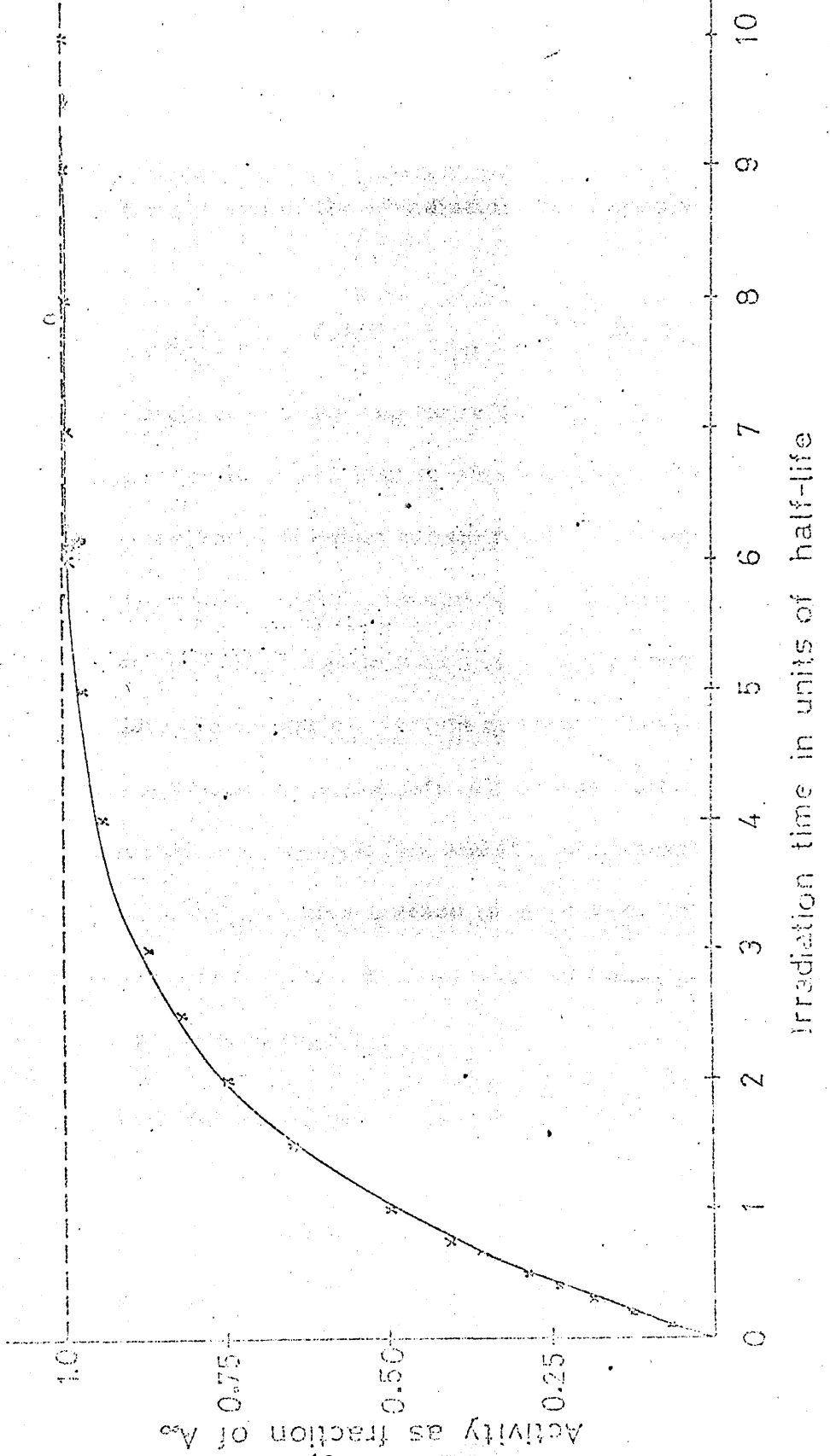


Fig. 1

At the end of the irradiation, the activity of the radioactive isotope will decay with its characteristic half-life, $t_{\frac{1}{2}}$, so that at time t_d after the end of the irradiation, the activity A_d will be given by:-

$$A = 6.025 \times 10^{23} \phi \sigma \theta \left(\frac{W}{M}\right) (1 - e^{-0.693t_i/t_{\frac{1}{2}}}) (1 - e^{-0.693t_d/t_{\frac{1}{2}}})$$

Thus, the highest activity and therefore the highest sensitivity for a given weight of element is obtained if the neutron flux, isotopic abundance and activation cross-section are high.

If the neutron flux, isotopic abundance, activation cross-section, half-life and time of irradiation are accurately known, it is possible to calculate the weight of element present. This method is rarely, if ever, used because of the difficulties associated with the accurate determination of neutron flux and the total disintegration rate. In most cases, a comparative method is employed, in which sample and a standard, containing a known weight of the element to be determined, are processed together.

IV. Methods of Neutron Activation Analysis

There are three main methods of activation analysis:

- i) the destructive method of analysis in which the radioactive isotope to be determined is separated completely from interfering active isotopes.
- ii) the non-destructive method in which the radioactivity induced in the sample is separated according to the energies of the gamma rays emitted by the various isotopes, using a NaI(Tl) or GeLi detector coupled to a multichannel analyser.
- iii) group separation of radioactive isotopes and measurement of the various gamma rays using NaI(Tl) or GeLi detectors.

Each of the above methods has been applied to geological samples, as described by Smales, Mapper and Wood (1957) for destructive analysis; Gordon et al (1968), Dale, Henderson and Walton (1970) for non-destructive analysis; Morrison et al (1969), Laul et al (1970) for group separation.

Destructive neutron activation analysis has been described by Mapper (1960). For the analysis of trace quantities of an element, a fixed amount of inactive carrier is added after irradiation. After chemical separation of the element of interest, the chemical yield is determined and in this way quantitative separation is not required.

This technique can be used for a large number of elements of interest in rock analysis but rarely more than three elements are determined simultaneously.

Simple Geiger-Muller end window beta counters and a scalar can be perfectly adequate equipment for this method. The total cost for equipment can be as low as a few hundred pounds.

Non-destructive neutron activation analysis allows for the simultaneous determination, in suitable circumstances, of a number of elements, e.g. Gordon et al (1968) analysed rock samples for Na, K, Rb, Cs, Ba, La, Ce, Sm, Eu, Tb, Tm, Yb, Lu, Th, Zr, Hf, Ta, Mn, Co, Fe, Sc, Cr, and Sb. This method can only be used if the isotope to be activated has a reasonable natural abundance and the active isotope decays with gamma ray emission

of suitable energy, free from interference from other isotopes produced by the neutron bombardment, a reasonable half-life is also desirable. The equipment for this method of analysis ranges in cost from £3,000 - £20,000.

Group separation methods are employed so that interference from gamma ray emitters of similar energy is eliminated. This method can allow for the simultaneous analysis of a larger number of elements compared to non-destructive analysis but the time required is increased. Morrison et al (1969) analysed rock samples for 45 elements using this method.

ery and one of the other-Muller's accounts he

Prigalnikov, Kennedy & Miller (1964) and

caused.

V. Detection of Radioactivity

Most methods used to detect radioactivity depend on the ionisation produced by the radiation as it passes through matter.

This ionisation can have two effects:-

- i) it can change the conductivity of the material:
as used in Geiger-Muller detectors (change in the conductivity of a gas), or in solid state detectors (change in the conductivity of a solid).
- ii) it can produce flashes of light in a suitable scintillator by the photoelectric process. The scintillator can be either a liquid (certain aromatic organic compounds e.g. 2.5-diphenyl-oxazole dissolved in toluene) or a solid (e.g. sodium iodide crystal containing thallium)

a) Geiger-Muller Detectors

The theory and use of Geiger-Muller detectors has been described by Friedlander, Kennedy & Miller (1964) and will not be further discussed.

b) Solid State Detectors

These detectors can be considered the solid phase counterparts of the gaseous ionisation detectors. The theory of the use of solid state detectors has been described by Girardi and Guzzi (1969).

The type most usually employed is produced from germanium crystals which have been grown in such a way as to incorporate trivalent elements (e.g. B, Ga, In) in the crystal structure. The addition of these elements produce holes in the electron conduction band (positive holes) and fixed negative charge centres (p-type germanium). When an E.H.T. is applied across the crystal, the crystal will conduct electricity by movement of these holes.

A readily ionisable metal such as lithium is now diffused interstitially through one surface of the germanium crystal. The crystal region in which lithium is present now behaves as an n-type germanium crystal (i.e. having extra free electrons in the lattice) as the number of free electrons from the lithium atoms will far exceed the number of free holes from the trivalent doping element.

At the interface, a depletion layer is formed in which the electrons from the lithium compensate for the holes produced by the trivalent element. The only type of conduction possible is that due to the thermal motion of the electrons. This conduction mode (intrinsic conduction) is important at room temperatures, but at lower temperatures (e.g. liquid nitrogen temperature) is virtually absent.

An electric potential is applied to the faces of the crystal to increase the region of intrinsic conduction by the drift of lithium ions. The maximum depth of the depletion layer at present obtainable is of the order of 15 mm.

When a gamma ray strikes the intrinsic conduction region, the ionisation produced by the absorption of the ray generates electron hole pairs which are rapidly collected at the electrodes, giving rise to a voltage pulse proportional to the number of ion pairs formed and therefore to the energy of the gamma ray. This voltage pulse is amplified, shaped by electronic equipment to a form suitable for a multichannel analyser.

Energy Resolution of a Germanium Detector

If a gamma ray of energy E keV is completely absorbed in a germanium detector then the mean square variation in the number of ion pairs produced per keV (σ^2) is given by:-

$$\sigma^2 = \frac{F.E.}{\epsilon}$$

where ϵ is the average energy required for the production of one ion pair

and F is the proportionality constant (Fano Factor)

The energy resolution of the detector, ΔE , is normally referred to the full width half maximum (F.W.H.M.) of the gamma ray photopeak, and is given by:-

$$\Delta E = 2.355 \epsilon \sigma$$

$$\text{thus } (\Delta E)^2 = (2.355 \epsilon \sigma)^2$$

$$\text{and } \Delta E = 2.355 (\epsilon . F . E.)^{\frac{1}{2}}$$

An accurate value of ϵ is given by Antmann (1966) as 2.93eV/ion pair and F by Bilger (1966) as 0.129.

$$\text{Thus } \Delta E = 45.9(E)^{\frac{1}{2}} \text{ keV}$$

This theoretical detector resolution cannot be achieved because of various noise sources associated with detector leakage and auxiliary electronic currents.

Fig. 2, from Girandi and Guzzi is a plot of resolution Vs gamma ray energy for,

- i) theoretical resolution
 - ii) 2cm^3 planar detector
 - iii) 47cm^3 coaxial detector
- and
- iv) $3'' \times 3''$ NaI(Tl) crystal

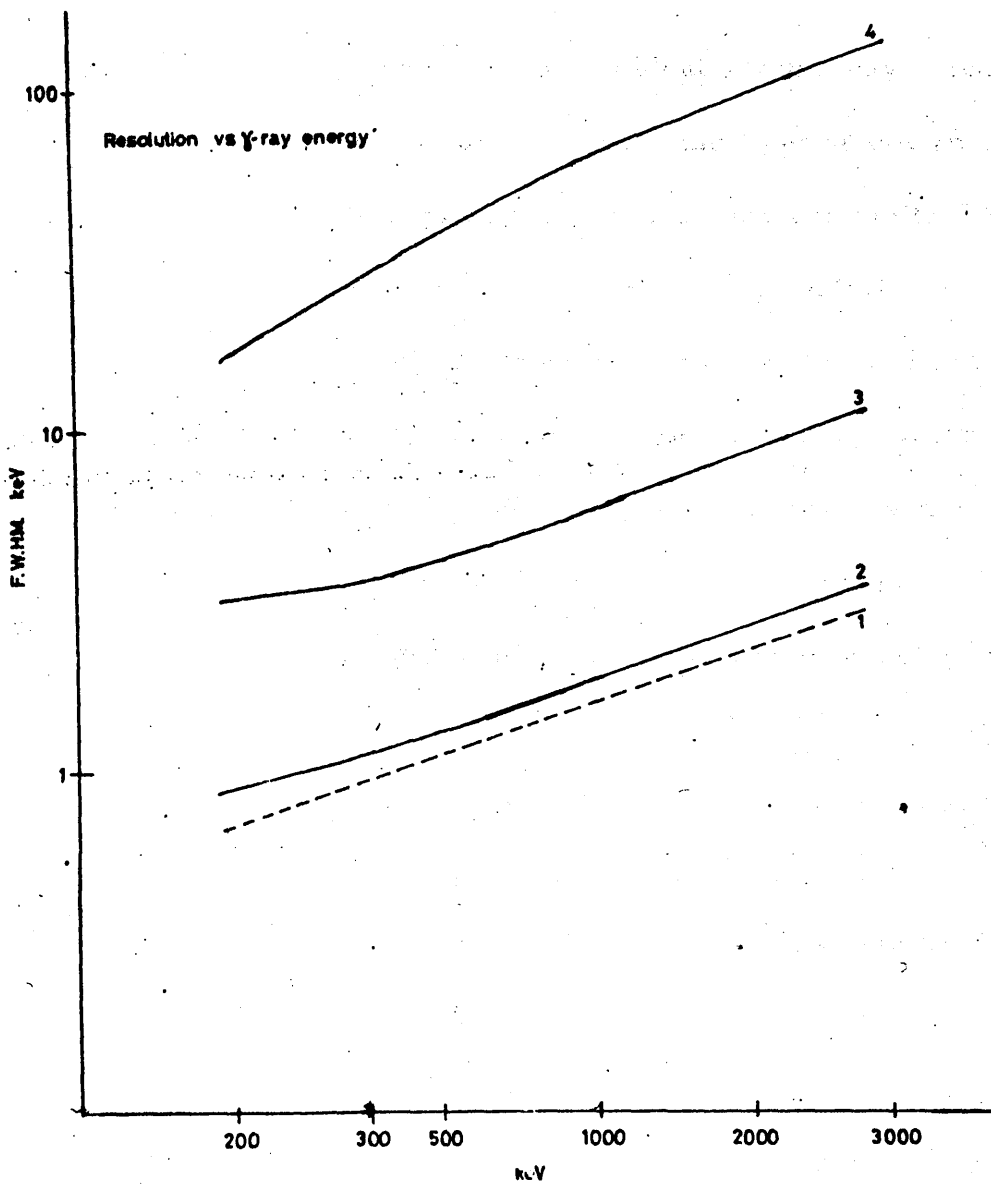
c) Scintillation Detectors

The most common type of scintillation detector for gamma ray spectrometry is a sodium iodide crystal containing 0.1 - 1 % (by weight) thallium. Crouthamel (1960) has described in some detail the interactions of gamma rays with scintillation detectors.

Briefly, the incident ray can have three main effects on the detector:-

- i) Photoelectric
- ii) Compton Scattering
- iii) Pair Production

The photoelectric effect is the one most used in gamma ray spectrometry. The incident ray ejects an electron from the atom, usually from the K or L electron shell, and a flash of light is emitted



- Curve 1: theoretical resolution with Fano factor of 1.5
 Curve 2: experimental resolution of a 2cm³ planar detector (Heath et al, 1966)
 Curve 3: experimental resolution of a 47cm³ coaxial detector (Girardi et al, 1967)
 Curve 4: experimental resolution of a 3x3in NaI(Tl) detector (Girardi et al, 1967)

Fig. 2

as an electron from a higher energy level fills the vacancy in the lower energy level. The total intensity of the light flash is proportional to the energy of the incident gamma ray. The light emitted by the crystal is directed onto the light sensitive photocathode of a photomultiplier tube. Electrons are emitted by the action of the light and are accelerated by a potential of the order of 100 volts to the first electrode where each electron produces several secondary electrons (n). These secondary electrons are further accelerated to the secondary electrode where the electrons are again increased n fold. Thus with a photomultiplier having x electrodes the charge of the original photoelectrons is multiplied n^x times; this can be 10^5 to 10^8 times. The final pulse from the photomultiplier tube is further amplified by suitable electronic equipment and fed into a multichannel analyser. Because of the proportionality of incident gamma ray energy \rightarrow number of photons produced \rightarrow number of photoelectrons produced in the photocathode of the photomultiplier tube \rightarrow final output pulse, the final pulse size is directly related to the energy of the incident gamma ray.

The energy resolution of the sodium iodide (thallium) crystal is much less than a germanium-lithium detector. Typically, the width of the photopeak at half maximum is 56keV for an incident gamma ray of 662keV using a sodium iodide crystal, while the comparable value for a germanium detector is of the order of 2-3keV.

The main advantage of the scintillation detector is its higher efficiency, a germanium detector has normally only 5-10% of the efficiency of a sodium iodide detector.

VI. Multichannel Analysers

A full description of the design and use of multichannel analysers has been given by Chase (1961) and therefore only a brief outline will be given of their construction.

These devices sort the electrical pulses, produced by amplification of the signals from a solid state detector or scintillation detector and photomultiplier tube according to their size, this being proportional to the energy of the incident gamma ray.

The memory of the analyser is divided into channels, each channel covering a particular voltage range. The input pulses are sorted and stored in the appropriate part of the memory. The size of the memory in equipment at present available ranges from 100 to more than 10,000 channels.

For sodium iodide detectors, memories of 400 are usually sufficient, but for the higher resolution of the germanium-lithium detectors a larger memory is required for optimum operation.

The number of counts in each channel can be presented on a cathode ray tube or read out through a pen recorder or printer. In this manner, a gamma ray spectrum is recorded and displayed.

The sample is placed in a plastic container and sent through the pneumatic system to the irradiation chamber. After irradiation, two to three hours were allowed for cooling so as to allow short lived isotopes to decay. e.g. ^{27}Mg , $t_{1/2}$ 0.5 min., gamma rays of 0.84 MeV. ^{28}Al , $t_{1/2}$ 2.3 min., gamma ray of 1.785 MeV. A gamma ray from ^{56}Mn was measured using a scintillation counter.

After the manganese analysis had been completed

VII. Procedure

Neutron activation analysis was used for the determination of scandium, chromium, manganese, iron, cobalt and nickel concentration. The relevant nuclear data for these elements is given in table 2. (Data from Heath (1969)).

Three separate irradiations were required. The first of three minutes at a thermal neutron flux of $10^{12} \text{ n cm}^{-2} \text{ sec}^{-1}$ in the Scottish Research Reactor, East Kilbride, for manganese analysis. Samples and standards were placed in a plastic irradiation container and sent through the pneumatic system into the reactor for irradiation.

After irradiation, two to three hours were allowed to elapse before counting so as to allow short lived interfering isotopes to decay, e.g. ^{27}Mg , $t_{\frac{1}{2}}$ 9.5 min., gamma rays of 0.844 and 1.014 MeV; ^{28}Al , $t_{\frac{1}{2}}$ 2.3 min., gamma ray of 1.788 MeV. The 0.874 MeV gamma ray from ^{56}Mn was measured using a suitable gamma ray detector.

After the manganese analysis had been completed the second of the irradiations was performed on the same specimen.

TABLE 2

Nuclear Data for Elements Investigated

Target Isotope	Isotopic Abundance (%)	Product Nuclide	Thermal Neutron Absorption Cross Section (Barns)	Half-Life of Product Nuclide	-Ray Photopeak (MeV)
^{45}Sc	100	^{46}Sc	25 ± 2	83.8d	0.889; 1.121 2.01 (sum peak)
^{50}Cr	4.31	^{51}Cr	16 ± 0.5	27.8d	0.320
^{55}Mn	100	^{56}Mn	13.3 ± 0.1	2.58 hr	0.847
^{58}Fe	0.33	^{59}Fe	1.23 ± 0.05	45.1d	1.099; 1.292
^{59}Co	100	^{60}Co	36.9 ± 2.91	5.26	1.173; 1.332 2.505 (sum peak)
^{64}Ni	1.08	^{65}Ni	1.52 ± 0.24	2.52 hr	1.116; 1.624

This consisted of an irradiation of 96 hours at a thermal neutron flux of $2 \times 10^{12} \text{ n cm}^{-2} \text{ sec}^{-1}$ in the DIDO Reactor, A.E.R.E. Harwell, for the scandium, chromium, iron and cobalt analysis. An aluminium can (internal diameter 2.3 cm., depth 6.6 cm.) was used as a container for the samples and standards. After irradiation, the samples and standards were left for three to four weeks to allow interfering isotopes to decay, e.g. ^{24}Na , $t_{\frac{1}{2}}$ 15.0 hrs, gamma rays of 1.369 and 1.732 MeV.

The gamma ray photopeaks used for the above analyses were those advised by Gordon et al (1968) and given in table 3.

The samples were finally irradiated for forty minutes at a thermal neutron flux of $2 \times 10^{12} \text{ n cm}^{-2} \text{ sec}^{-1}$ in the Scottish Research Reactor, East Kilbride, and the nickel analysis carried out using the method described by Smales, Mapper & Wood (1958), which involved the destruction of the sample.

a) Sample Preparation

The following procedure was adopted for all samples:-

50 - 100 mgs. of the rock or mineral powder were heat sealed in 3 cm. lengths of polythene tubing (3 mm. internal diameter, 0.7 mm. wall thickness). For the nickel analysis, the samples were weighed before irradiation. These ampoules were then wrapped in

TABLE 3

Gamma-Ray Photopeaks Measured

Energies of Gamma-Rays Detected (MeV)

<u>Isotope</u>	<u>NaI(Tl) detector</u>	<u>Ge(Li) detector</u>
^{45}Sc	2.009	0.889 : 1.120
^{51}Cr	0.320	0.320
^{56}Mn	0.847	0.847
^{59}Fe	-	1.100 : 1.291
^{60}Co	2.505	1.173 : 1.332

aluminium foil and packed, with suitable metal standards, in a container for irradiation.

For the manganese, scandium, chromium, iron and cobalt analyses, the irradiated rock powders were weighed into clean 2.5 ml. polythene ampoules (internal diameter 1.3 cm., depth 2.8 cm.) for counting.

b) Standard Preparation

Several methods for the preparation of standards for non-destructive neutron activation analysis have been described in the literature (methods i) to iii) briefly described below). None of these techniques proved to be completely successful and so another method iv) was devised which produced results with lower standard deviations.

Method i) Microgram quantities of the pure element or oxide were accurately weighed out on a micro-balance and the standard used for counting without further manipulation.

Method ii) Milligram quantities of the metal were irradiated, then dissolved in a suitable mineral acid (usually nitric or hydrochloric), evaporated to dryness, taken up in water and made to volume in a volumetric flask. Small aliquots, usually 1 ml., of this

solution were introduced into polythene containers, similar to those used for the counting of the rock samples, and evaporated to dryness in an oven at 85 - 90°C.

Method iii) Suitable volumes of solutions of the element (as in ii) above) were sealed in quartz tubes and irradiated. The liquid was then either counted directly or diluted further and aliquots taken and processed as in ii).

Method iv) Small volumes, usually 10 μ l, of solutions of the element were introduced onto filter paper or glass fibre circles using a microsyringe. The impregnated circles were then irradiated and counted without further treatment. This method had the advantage that smaller amounts of radioactivity were handled.

Difficulties associated with methods i), ii) and iii) were discovered:-

Method i) 100 - 200 μ g of the metal standard had to be accurately weighed out. It was difficult to obtain a high degree of accuracy using the available balances.

After introducing the standards into the polythene vials after irradiation differences were noted between the geometry of the rock powder and the metal standard. In particular, when metal oxide powders were used, e.g. Mn_3O_4 and Sc_2O_3 , electrostatic effects on the inside surfaces of the polythene containers caused the powders to adhere to the walls of the vials.

Methods ii) and iii)

These methods were found to give reliable results (method ii) for manganese, chromium and cobalt: method iii) for scandium, when sodium iodide detectors were used.

When a germanium-lithium detector became available, discrepancies were noted between the values obtained with the different counting systems for the same samples. Typically, the germanium-lithium detector gave results which were 20-30 % higher than those with the sodium iodide detector.

The structure and detecting properties of the germanium-lithium system are somewhat different to that of the sodium iodide detector with the result that differences in geometry between sample and standard affected the germanium-lithium detector to a far greater extent. Closer examination of the polythene ampoules containing the standards revealed that the solutions of the metals tended to evaporate in such a way as to produce a ring of metal salt on the bottom of the vial.

Method iv)

This procedure gave reliable and reproducible results with the different detector systems.

Spectroscopically pure metal (chromium, manganese, iron and cobalt) or metal oxide (scandium oxide, Sc_2O_3) were used for the preparation of the standards. Suitable quantities, for example 500 mg manganese, of the metal or oxide, were accurately weighed out and dissolved

by heating in the minimum quantity of "Analar" quality nitric or hydrochloric acid. The solutions were then transferred to a volumetric flask (usually 50 or 100 ml) and made up to the mark with distilled water. A previously calibrated $10\mu\text{l}$ syringe was used to transfer the solutions onto 1 cm. diameter glass fibre filter discs (Whatman No. GF/A). The discs were then held under a heat lamp with a pair of tweezers and the liquid evaporated off. The circles were then wrapped in pure aluminium foil. Glass fibre discs were found to be more absorbent than filter paper and accordingly were used for standard preparation. The aluminium foil which was used to wrap the discs was counted after the irradiation. No transference of the standard onto the foil was detected.

Each metal standard was prepared in triplicate for each irradiation and the weights of metal on the glass fibre circles were:-

Scandium $2\mu\text{g}$; Chromium $250\mu\text{g}$; Manganese $60\mu\text{g}$;
Iron 2 mg ; Cobalt $100\mu\text{g}$.

As a control, pure glass fibre discs were irradiated along with the standards. No interferences were detected.

With practice, the quantities of metal introduced onto the glass fibre circles were reproducible to better than $\pm 1\%$, as determined by the gamma ray photopeak area.

Standard Preparation for Nickel Analysis

Approximately 20 mg. samples of "specpure" nickel foil were accurately weighed out and heat sealed in polythene ampoules. These standards were prepared in duplicate for each determination.

After irradiation, the metal was dissolved in the minimum quantity of dilute nitric acid, the solution transferred to a 250 ml. volumetric flask and made up to the mark with distilled water.

1 ml. aliquots of this solution were used as the nickel standards (in triplicate for each sample of foil irradiated) and the radiochemical separations were carried out on these samples together with a suitable weight of inactive nickel carrier, usually 10 mg. nickel.

c) Non-Destructive Analysis

Manganese, scandium, chromium, iron and cobalt were determined in the rock and mineral samples by non-destructive neutron activation analysis.

With an irradiation of one to three minutes in a thermal neutron flux, the main activity present in a sample of rock powder after a cooling period of two to three hours is due to ^{56}Mn , with a half-life of 2.58 hr., and gamma rays of 0.847 and 1.811 MeV, and ^{24}Na , with a half-life of 15 hr., and gamma rays of 1.369 and 1.732 MeV.

A 3" x 3" flat-topped sodium iodide (thallium) detector coupled to a 400 channel Technical Measurement Corporation analyser was generally used for manganese analysis and the 0.847 MeV gamma ray was measured. Fig. 3 shows the gamma ray spectrum of RE 331 wholerock, three hours after an irradiation of one minute at a thermal neutron flux of $3 \times 10^{12} \text{ n cm}^{-2} \text{ sec}^{-1}$, using the NaI(Tl) detector. For comparison, Fig. 4 shows the spectrum obtained using a 40 cc. active volume GeLi detector coupled to a PDP 8e computer through a

120.4mg RE 331 whole rock: counted 3hrs.
after irradiation of 1min at 3×10^{12} n cm⁻² sec⁻¹
NaI(Tl) detector.

⁵⁶Mn
0.847 MeV

²⁴Na
1.368 MeV

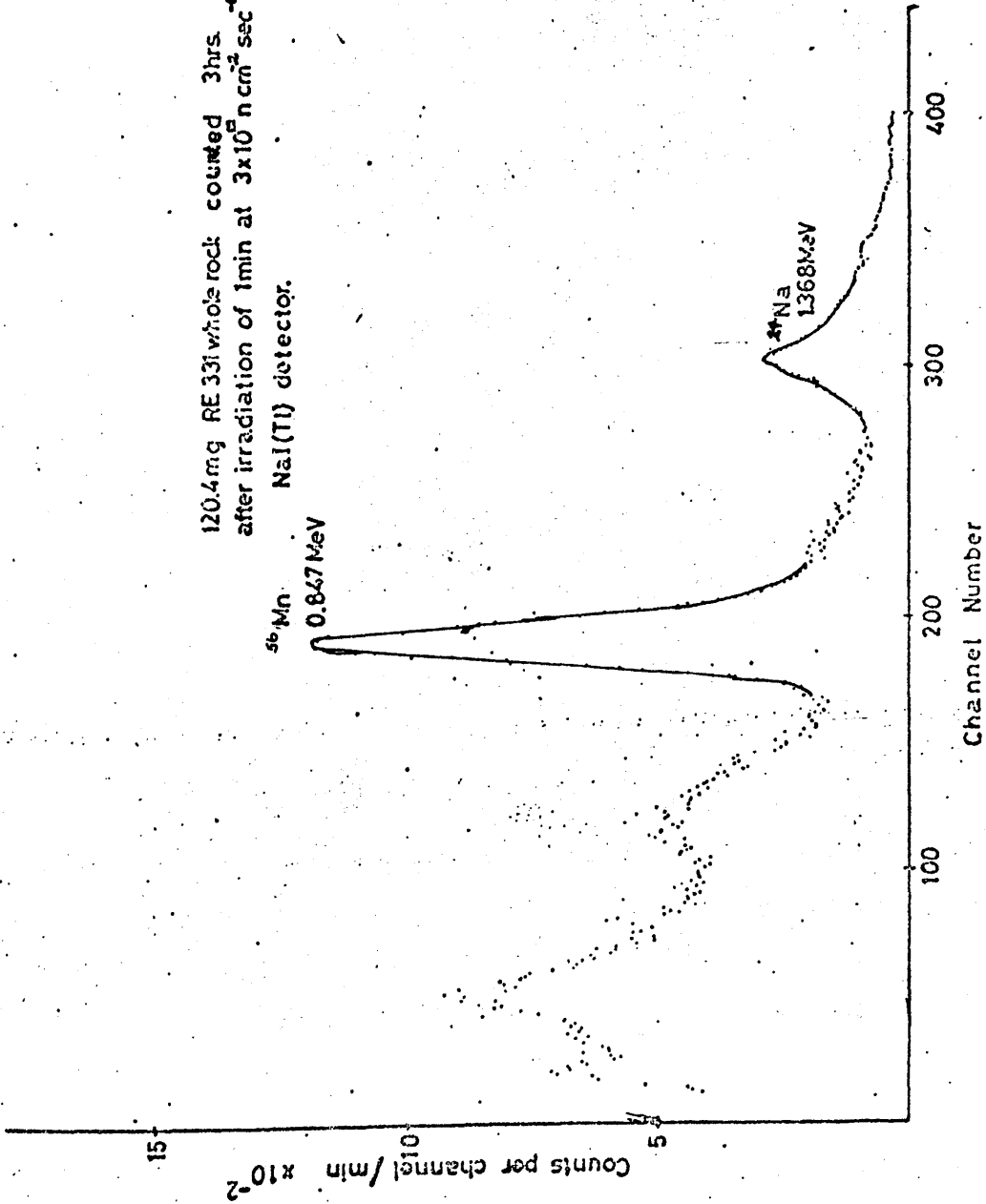


Fig. 3

120.4 mg RE 331 wholerock counted 3hrs after irradiation of
1min at $3 \times 10^{12} \text{ n cm}^{-2} \text{ sec}^{-1}$ GeLi detector

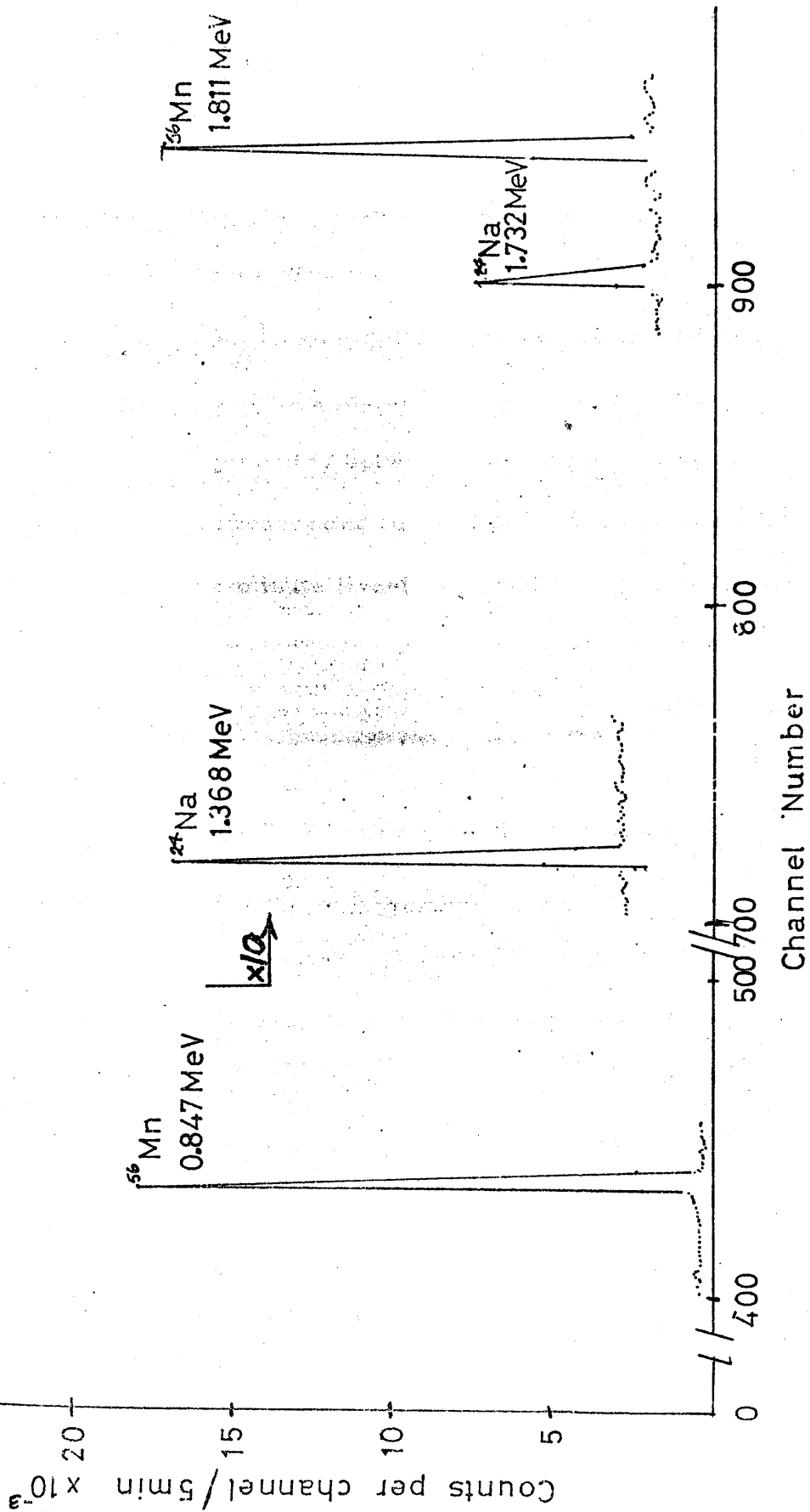


Fig. 4

Northern-Scientific 8192 A.D.C.

The samples and standards were positioned 10 cm. from the surface of the detector. This arrangement -

- i) cuts down the dead-time of the instrument
- ii) produced a better gamma ray photopeak
- iii) lessened the effect of any slight differences in geometry between the sample (a layer of rock powder) and the standard (a glass fibre disc).

A one minute live-time count for the NaI(Tl) detector gave an integrated count under the photopeak of greater than 10,000. The area under the photopeak was determined by Covell's method (1959) see Appendix 1.

With an irradiation of 96 hours in a thermal neutron flux, many radioactive isotopes are produced in a sample of rock or mineral powder and some twenty-six gamma ray emitting species can be detected using a high resolution germanium-lithium detector. (Gordon et al, 1968).

The most prominent gamma ray peaks after a cooling period of two to three weeks in irradiated samples of basaltic rock and

minerals obtained from basaltic rocks are:-

^{51}Cr , $t_{\frac{1}{2}}$ 27.8 days, gamma ray of 0.320 MeV

^{46}Sc , $t_{\frac{1}{2}}$ 83.9 days, gamma rays of 0.889, 1.120 and 2.009 (sum) MeV

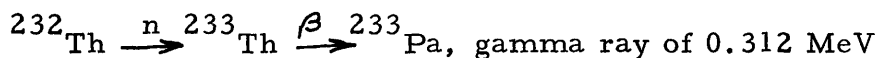
^{59}Fe , $t_{\frac{1}{2}}$ 45.0 days, gamma rays of 1.100 and 1.291 MeV

^{60}Co , $t_{\frac{1}{2}}$ 5.26 years, gamma rays of 1.173, 1.332 and 2.505 (sum) MeV

With rocks having appreciable concentrations of thorium,

(mostly acidic rocks) chromium abundances cannot be determined

because of the strong 0.312 MeV gamma ray from ^{233}Pa formed by:



$t_{\frac{1}{2}}$ 22 mins. $t_{\frac{1}{2}}$ 27.0 days

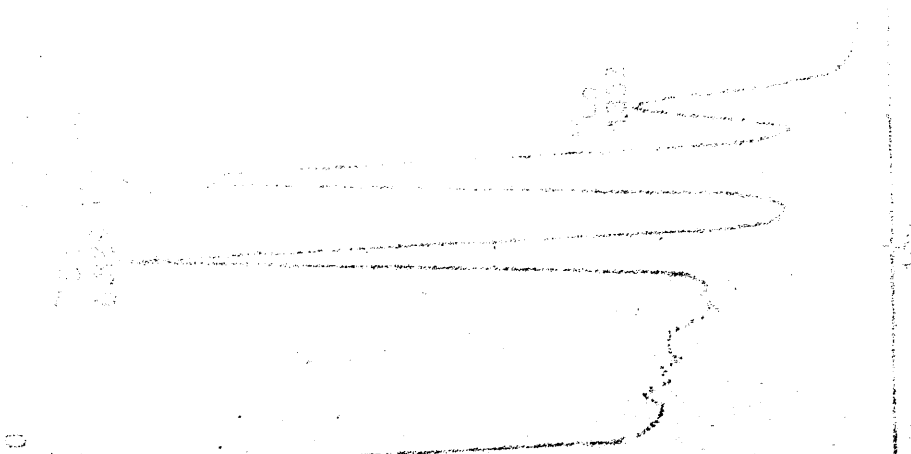
This interference was not a problem in the rocks investigated.

Gordon et al (1968) have pointed out that determining the abundances from the sum peaks of ^{46}Sc (2.009 MeV) and ^{60}Co (2.505 MeV) are probably more accurate than using the lower energy peaks due to Compton edge effects.

A $4\frac{1}{2}'' \times 4\frac{1}{2}''$ sodium iodide (thallium activated) crystal coupled to a 400 channel Intertechnique analyser was used for the scandium and cobalt determinations. Using this system, the samples and standards were positioned 15 cm. from the surface of the detector and counted for one to five minutes live-time.

Chromium was determined using this system as well as by the germanium-lithium detector. With the sodium iodide detector a one minute live-time count was required.

Fig. 5 shows the gamma ray spectrum of 76.6 mgs. of 17901 wholerock, 15 days after an irradiation of 96 hours at a thermal neutron flux of $2 \times 10^{12} \text{ n cm}^{-2} \text{ sec}^{-1}$ obtained using a $4\frac{1}{2}'' \times 4\frac{1}{2}''$ NaI(Tl) detector coupled to a 400 channel Intertechnique analyser. Fig. 6 shows the spectrum obtained using the 40 cc. active volume GeLi detector coupled to a PDP 8e computer through a Northern-Scientific 8192 A.D.C.



76.6mg 17901 whole rock counted 15days
after irradiation NaI(Tl) detector

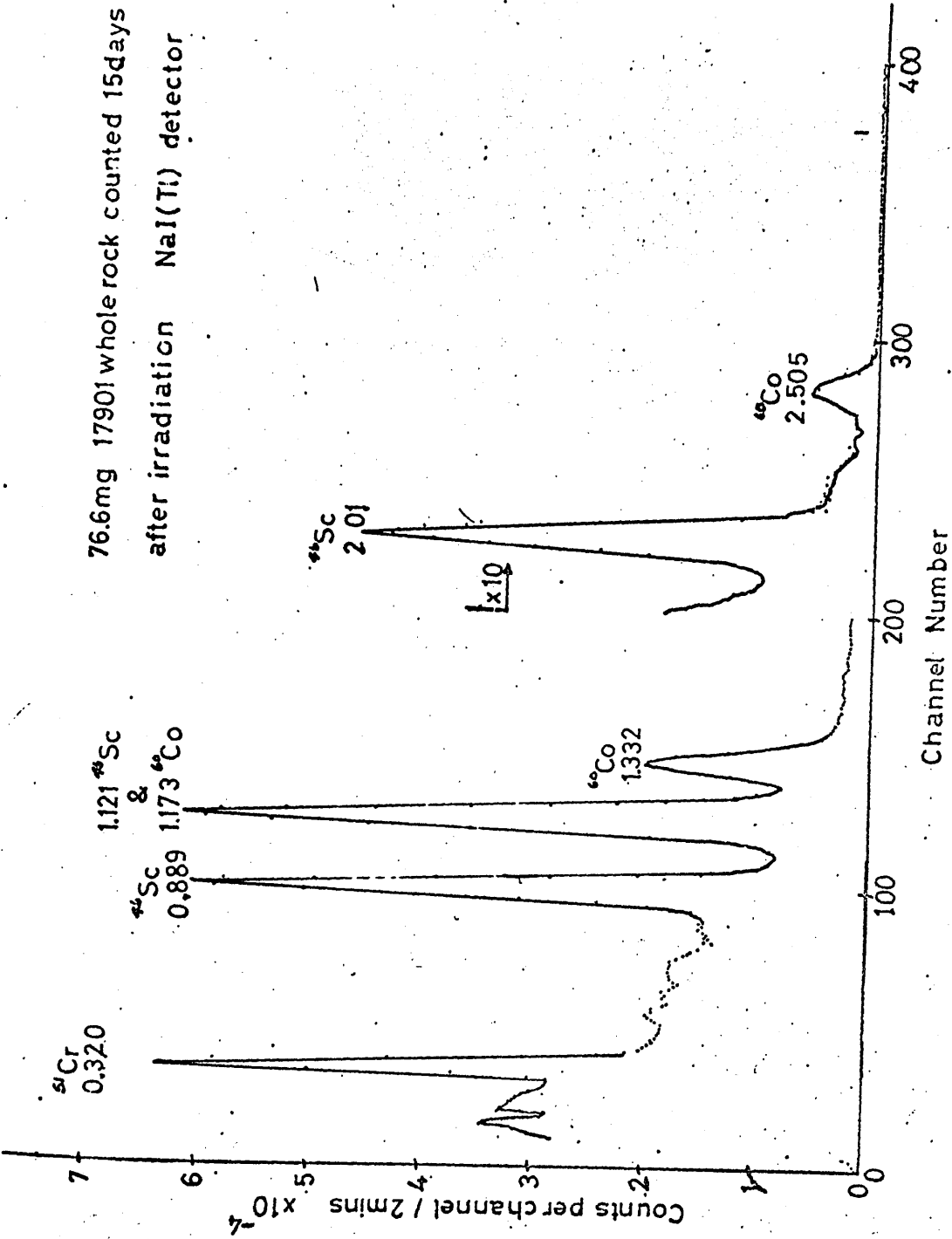


Fig. 5

76.6 mg 17901 wholerock counted
15 days after irradiation
GeLi detector

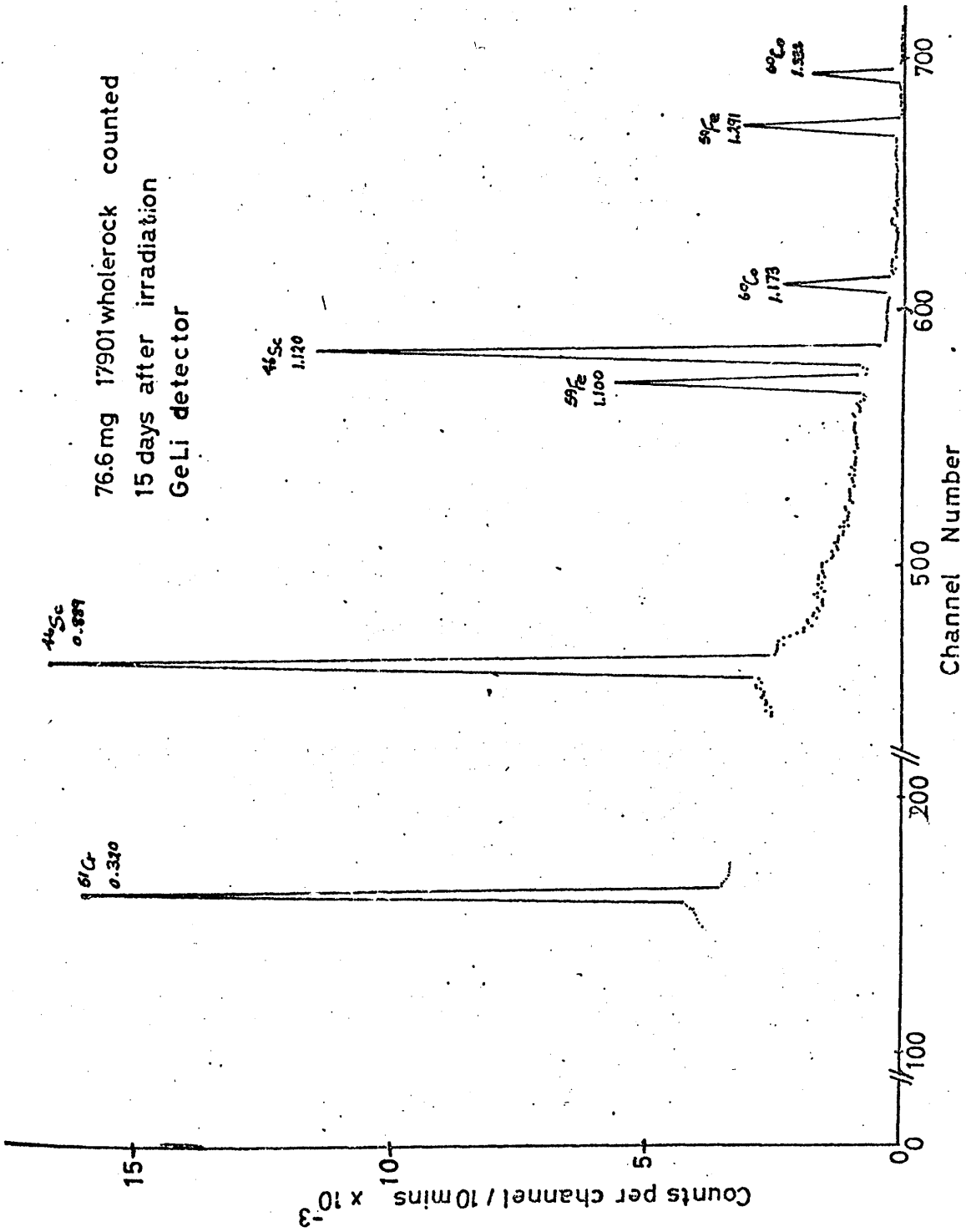


Fig. 6

d) Destructive Neutron Activation Analysis

Nickel was the only element determined by this method using the procedure described by Smales, Mapper and Wood (1958).

This method involved the addition of an inactive carrier of nickel (usually 10 mg) to the solution of the rock material. This facilitated the chemical manipulations and enabled the chemical yield of the separation to be calculated.

Radiochemically pure nickel was obtained using a series of precipitations steps after the addition of milligramme quantities of various metal ions, including copper (removed using thionalide and thiocyanate precipitations), bismuth (removed as the hydroxide) and a mixture of ferric iron, manganese, calcium, strontium and barium (precipitated as hydroxides and carbonates).

Dimethylglyoxime was used throughout as the precipitant for nickel.

The low natural abundance of the target nuclide, ^{64}Ni (1.08%) and small thermal neutron capture cross-section (1.52 barns) precluded the use of any non-destructive method. It is interesting to note that manganese-56 with a half-life similar to nickel-65 (^{56}Mn , 2.58 hr, ^{65}Ni , 2.52 hr.) has an isotopic abundance

for its target nuclide of 100% and cross-section of 13.3 barns; thus the radioactivity induced in a sample of manganese is approximately 10^3 that induced in a similar weight of nickel irradiated for the same period of time.

Some problems were noted when using the method as described by Smales et al. In particular, the final precipitate of nickel dimethylglyoxime was liable to contamination from iron which produced a dark red or black precipitate. It was found to be important to ensure that -

- i) the solution with bromine, nitric acid and ferric iron, manganese, calcium, strontium and barium was boiled for at least 10 minutes, to ensure oxidation of any ferrous iron that may be present.
- and ii) after precipitation of the scavenging compounds with ammonium hydroxide and ammonium carbonate the solution was boiled for a further 10 minutes, to ensure complete precipitation and coagulation.

When centrifuging the nickel dimethylglyoxime precipitate in the final step, it was found to be beneficial to add a few drops of

a 0.1% aqueous solution (v/v) of Nonidet P40 (a nonionic surfactant).

The beta particles from the ^{65}Ni were counted using a Nuclear Chicago gas flow proportional counter with automatic sample changer. Standards and samples were counted for 1 - 5 mins. Fig. 7 is a graph of activity vs time and indicates the radiochemical purity of the final precipitates; $t_{\frac{1}{2}}$ from the graph is 2.50 hr.

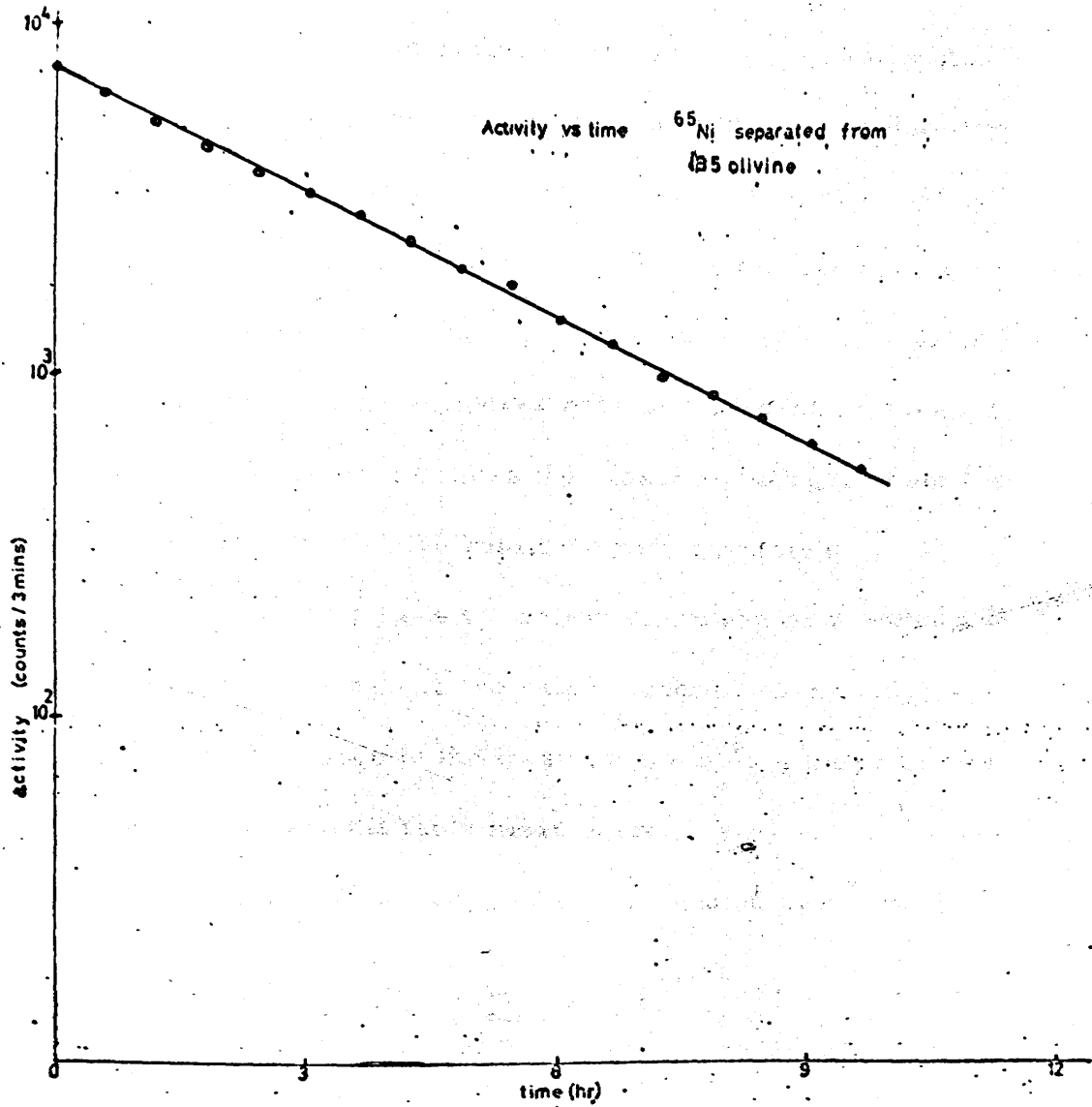


Fig. 7

VIII. Accuracy & Precision

Some understanding of the terms accuracy and precision and the realisation of the errors inherent in an analytical procedure is necessary in order to evaluate the usefulness of any method of analysis. These terms have been discussed in some detail by Strouts, Wilson & Parry-Jones (1962) and Ecksehlager (1969).

The term accuracy defines the closeness of agreement between an experimental value and the "true" value. This true value cannot be known and is employed only as a theoretical concept.

Precision defines the closeness of agreement between experimental values of the replicate determinations.

Mean defines the arithmetic mean or average and is usually denoted by \bar{x} , where x is the value found for each analysis.

Variance is the mean of $(x - \bar{x})^2$, a measure of the dispersion of observations around their mean value.

Mathematically variance, denoted by σ^2 , is given by:

$$\sigma^2 = \frac{\sum (x - \bar{x})^2}{n - 1}$$

where n is the number of results obtained.

The standard deviation, σ , is given by:

$$\sigma = \sqrt{\frac{\sum (x - \bar{x})^2}{n - 1}}$$

This gives an estimate of the error associated with the mean value found from a number of determinations.

Often the relative standard deviation, v , is employed -

$$v = \frac{\sigma}{x} \times 100\%$$

As much of the present study is concerned with taking the ratio of two values (e.g. concentrations of metals in olivine and ground-mass) each of which is subject to an error, it is important to determine the error associated with taking a quotient.

The standard deviation of the final result y , σ_y , obtained by the expression -

$$y = \frac{x_1}{x_2}$$

where x_1 and x_2 are values obtained with standard deviations σ_{x_1} and σ_{x_2} , is given by:

$$\sigma_y = \sqrt{y^2 \left\{ \frac{\sigma_{x_1}^2}{x_1^2} + \frac{\sigma_{x_2}^2}{x_2^2} \right\}}$$

This expression was used throughout to determine the errors associated with the evaluation of distribution coefficients.

In this study, the use of a range of international standard rocks was employed to test the precision of the analytical method used and to give an estimate of the accuracy of the analysis, from the recommended values published in the literature.

Each time a batch of samples was irradiated, quantities of a number of the standard rocks were processed at the same time. In this way, some twelve to fifteen analyses for the elements Sc, Cr, Mn and Co (latterly also Fe, when a high-resolution GeLi detector became available) in each rock were obtained by instrumental neutron activation analysis throughout a period of two years.

The results obtained indicated a relative standard deviation of $\pm 5\%$, with generally good agreement between neutron activation results obtained in this study, activation results obtained by other laboratories and other methods of analysis.

The following rock samples were obtained:

W-1, G-2, GSP-1, AGV-1, PCC-1, DTS-1, BRC-1 from the United States Geological Survey: T-1 from the Tanzanian Geological Survey: SY2, SY3 from the Spectroscopy Society of Canada.

Results for scandium, chromium, manganese, iron and cobalt concentrations in these rocks are given in Tables 4-8, together with the mean of results obtained by neutron activation analysis (Brunfelt & Steinnes, 1966; Alian & Shabana, 1967; Cobb, 1967; Stueber and Goles, 1967; Gordon et al, 1968; Johansen & Steinnes, 1968; Das, quoted by Flanagan, 1969; Sijperda, quoted by Flanagan, 1969; Bender, quoted by Flanagan, 1969; Greenland, quoted by Flanagan, 1969; Morrison et al, 1969; Wytttenbach, 1969; Melsom, 1970), mean of results obtained by other methods (Fleischer, 1969; Flanagan, 1969; Tanzanian Geological Survey, 1963) and the recommended or average results. These values were given by:-

Fleischer (1969)	for W-1
Flanagan (1969)	for G-2, GSP-1, AGV-1, PCC-1, DTS-1 & BCR-1
Tanzanian Geological Survey, (1963)	for T-1
Spectroscopy Society of Canada, (1968)	for SY2 & SY3

Towards the end of this study, samples of the French rock standards, GA, GH, BR, DR-N, UB-N, BX-N, DT-N, were obtained and although only duplicate analyses were carried out, for

TABLE 4

Concentrations (p. p. m.) of Scandium in Rock Standards

Rock	Split and Position Numbers	This work	Other N. A. A. Results (Mean \pm S. D.)	Other Methods (Mean \pm S. D.)	Recommended or Average
W-1		33.7 \pm 1.7	34.8 \pm 1.3	42.0 \pm 5.7	34.0
G-2	92-19	3.6 \pm 0.2	3.3 \pm 0.2	5.3 \pm 1.9	3.9
GSP-1	9-12	5.8 \pm 0.3	5.9 \pm 0.2	10.2 \pm 4.5	9.2
AGV-1	17-17	12.2 \pm 0.6	11.6 \pm 0.4	12.8 \pm 3.2	13.3
PCC-1	35-7	9.2 \pm 0.5	8.3 \pm 0.9	8.3 \pm 1.8	8.7
DTS-1	58-24	3.8 \pm 0.2	3.4 \pm 0.4	4.0 \pm 0.9	3.8
BCR-1	44-8	34.9 \pm 1.7	32.5 \pm 1.5		36.5
T-1		11.0 \pm 0.5			10-20
SY2		6.3 \pm 0.3			10
SY3		5.6 \pm 0.3			10

TABLE 5

Concentrations (p.p.m.) of Chromium in Rock Standards

Rock	Split and Position Numbers	This work	N.A.A. results (Mean \pm S.D.)	Other methods (Mean \pm S.D.)	Recommended or Average
W-1		89 \pm 4	108 \pm 15.5	121 \pm 18	120
PCC-1	35-7	2660 \pm 130	2715 \pm 55	2923 \pm 725	3090
DTS-1	58-24	4210 \pm 210	4200 \pm 10	4019 \pm 736	4230

600 \pm 40
2510 \pm 130
2422 \pm 100

TABLE 6

Concentrations (p.p.m.) of Manganese in Rock Standards

Rock	Split and Position Numbers	This work	N.A.A. results (Mean \pm S.D.)	Other methods (Mean \pm S.D.)	Recommended or Average
W-1		1130 \pm 60	1277 \pm 78	1347 \pm 134	1316
G-2	92-19	253 \pm 12	253 \pm 20	262 \pm 59	265
GSP-1	9-12	307 \pm 15	296 \pm 19	320 \pm 56	326
AGV-1	17-17	773 \pm 38	700 \pm 41	719 \pm 154	728
PCC-1	35-7	895 \pm 44	888 \pm 8	929 \pm 240	889
DTS-1	58-24	988 \pm 49	949 \pm 39	971 \pm 221	963
BCR-1	44-8	1330 \pm 60	1360 \pm 56	1357 \pm 294	1350
T-1		840 \pm 42			850
SY2		2610 \pm 130			2650
SY3		2420 \pm 130			2480

TABLE 7

Concentrations (As Fe_2O_3 %) of Iron in Rock Standards

Rock	Split and Position Numbers	This work	N.A.A. results (Mean \pm S.D.)	Other methods (Mean \pm S.D.)	Recommended or Average
G-2	92-19	2.39 \pm 0.12	2.51 \pm 0.13	2.72 \pm 0.27	2.69
GSP-1	9-12	4.00 \pm 0.20	4.05 \pm 0.08	4.32 \pm 0.23	4.35
AGV-1	17-17	6.61 \pm 0.33	6.67 \pm 0.35	6.81 \pm 0.24	6.79
PCC-1	35-7	7.68 \pm 0.38		8.58 \pm 0.68	8.41
DTS-1	58-24	8.14 \pm 0.41		8.92 \pm 0.64	8.75
T-1		5.82 \pm 0.29		6.01 \pm 0.17	6.02
SY2		6.36 \pm 0.32			7.15
SY3		5.86 \pm 0.29			7.01

TABLE 8

Concentrations (p.p.m.) of Cobalt in Rock Standards

Rock	Split and Position Numbers	This work	N.A.A. Results (Mean \pm S.D.)	Other methods (Mean \pm S.D.)	Recommended or Average
W-1		49.4 \pm 2.5	48.2 \pm 3.9	42.7 \pm 5.8	50
G-2	92-19	5.5 \pm 0.3	4.7 \pm 0.8	6.1 \pm 4.1	4.9
GSP-1	9-12	7.6 \pm 0.4	7.3 \pm 1.2	8.4 \pm 4.8	7.5
AGV-1	17-17	15.3 \pm 0.7	15.4 \pm 1.5	16.8 \pm 4.6	15.5
PCC-1	35-7	121 \pm 6	124 \pm 10	115 \pm 46	112
DTS-1	58-24	145 \pm 7	144 \pm 2.5	134 \pm 27	132
BCR-1	44-8	41.2 \pm 2.1	39.3 \pm 3.2	36.5 \pm 4.9	35.5
T-1		12.8 \pm 0.6			13
SY2		10.8 \pm 0.5			20
SY3		11.6 \pm 0.6			N.D.

N.D. = Not Detected

completeness, the results are given in Tables 9-12.

The recommended or mean values are those given by Roubault, de la Roche and Govindaraju (1968), de la Roche and Govindaraju (1969), de la Roche and Govindaraju (1970).

For samples DR-N, UB-N, BX-N, and DT-N few results have so far been reported in the literature, therefore, the average of the reported analyses may not be very meaningful.

1.8

0.7

4

0.1

TABLE 9

Concentrations (p.p.m.) of Scandium in French Rock Standards

<u>Rock</u>	<u>This work</u>	<u>Reported</u>	
		<u>Recommended or Average</u>	<u>Range</u>
GA	8.8 \pm 0.4	7	4.3-10
GH	0.8 \pm 0.1		<2-7.4
BR	30 \pm 1.5		0.6-30
DR-N	36 \pm 1.8		31-32
UB-N	14.3 \pm 0.7		<31-15
BX-N	79 \pm 4		41-60
DT-N	2.2 \pm 0.1		<2

TABLE 10

Concentrations (p. p. m.) of Chromium in French Standard Rocks

<u>Rock</u>	<u>This work</u>	<u>Reported</u>	
		<u>Recommended or Average</u>	<u>Range</u>
BR	340 \pm 20	420	340-610
UB-N	2120 \pm 110	2200	116-2520
DT-N	290 \pm 15		210-242

TABLE 11

Concentrations (p.p.m.) of Manganese in French Rock Standards

<u>Rock</u>	<u>This work</u>	<u>Reported</u>	
		<u>Recommended or Average</u>	<u>Range</u>
GA	600 \pm 30	665	550-740
GH	360 \pm 20	360	260-360
BR	1350 \pm 70	1600	1450-1650
DR-N	1660 \pm 80		890-2045
UB-N	1100 \pm 60	110	320-1065
BX-N	180 \pm 10		40-395
DT-N	430 \pm 20		<10-350

TABLE 12

Concentrations (p. p. m.) of Cobalt in French Rock Standards

<u>Rock</u>	<u>This work</u>	<u>Reported</u>	
		<u>Recommended or Average</u>	<u>Range</u>
BR	47 \pm 2.5	50	16-90
DR-N	32 \pm 2	35	20-62
UB-N	92 \pm 5	110	101-300
DT-N	14 \pm 1		11

The principles underlying this method have been described by Miller and Margoshes (1965) who took into account the work of Agnew, Moore and Taylor (1961) and Mitchell (1964) on the analysis of geological and related samples.

The method of analysis depends on the excitation of the atoms of the element present in the sample by the passage of an electric current (20-30 amp) in air between the two electrodes normally being constructed from spectrograph

CHAPTER 4

Alternative Methods for Trace Metal Analysis

All the following analytical techniques have been employed for the determination of trace or minor amounts of metals in rocks and minerals. These methods were used in this study to confirm and supplement neutron activation analysis data and to obtain results for those elements which could not be determined by activation e.g. titanium and ferrous iron.

a) D.C. Arc Emission Spectrography

The principles underlying this method have been described by Scribner and Margoshes (1965) who dealt with general techniques; Ahrens and Taylor (1961) and Mitchell (1964) discussed the analysis of geological and related samples.

This method of analysis depends on the excitation of the orbital electrons of the atoms present in the sample by the arcing of an electric current (20-30 amp) in air between the two electrodes, the electrodes normally being constructed from spectrographically pure carbon. In geological work the sample is normally prepared

in the form of a fine powder intimately mixed with "specpure" graphite and placed in a hollow in one of the electrodes.

The temperature in the core of the arc is approximately 4,000^o K and this is sufficient to both vaporise the sample and to excite the orbital electrons to higher energy states. As the electrons return to the lower energy levels light quanta of characteristic energy are emitted. The light is passed through some suitable resolving device, usually a prism, and the resulting line spectrum focussed and recorded on a photographic emulsion. A rotating step sector is normally positioned near the entrance slit of the spectrograph in order to vary the exposure times in a regular manner. In this way, very intense lines can be conveniently measured. The degree of darkening of the photographic plate is proportional to the quantity of that element present. Various methods have been used to relate the intensity of the line to the weight of element present. The most common technique employs the use of an internal standard and was first described by Gerlach (1925), Gerlach & Schweitzer (1929).

The accuracies for trace element analysis have been reported by Wager & Mitchell (1951) as being $\pm 30\%$. However, more recently higher accuracies, of the order of $\pm 4-10\%$ have been claimed by Hirst (1962) and Taylor & Kolbe (1964). For routine analysis, accuracies better than $\pm 30\%$ are difficult to obtain.

The main advantages of this method are convenience, speed and versatility. In geological work 25 - 50 mg. of rock or mineral powder, mixed with graphite, are required for the analysis of the sample in triplicate.

b) Atomic Absorption Spectroscopy

This technique first described by Walsh (1955) and Alkemade & Milatz (1955) is discussed in detail by Ramirez-Munoz (1968) and Slavin (1968).

Basically, this method involves the measurement of the characteristic light energy absorbed by atoms in the ground stage. A solution of the sample to be analysed is converted into atomic vapour by introducing it, usually in the form of an aerosol, into a flame. Walsh (1955) has calculated the ratio of excited to unexcited atoms as a function of the temperature of the flame, and has shown that the vast majority of atoms are present in the ground state (ratios

of unexcited:excited atoms range from 7.24×10^{-3} for the 8521Å Cs line to 5.6×10^{-10} for the 2139Å Zn line at 3,000°K - the temperature of the usual air/acetylene flame is somewhat below this value, normally 2,400°K). Thus atomic absorption is more sensitive than flame photometry - a method which it compliments.

For geological samples, 0.1-0.5 g. are usually required for analysis.

c) X-Ray Fluorescence Spectrography

Discussions of this technique have been given by Liebhafsky, Pfeiffer & Winslow (1964) and Norrish and Chappell (1967).

In this method, orbital electrons are excited by allowing a beam of X-rays to fall on the sample. The characteristic energy given off by the excited electrons as they return to the groundstate is measured. The spectral lines emitted are in the X-ray region (λ , 1 - 3Å) and special crystals are required to resolve the spectrum (lithium fluoride and ammonium dihydrogen phosphate are the most common materials used in the construction of resolving crystals). The X-rays are detected using suitable scintillation counters, or gas-flow proportional counters.

Qualitative analysis by this method is readily carried out by scanning the resolving crystal over the appropriate X-ray region.

Some problems are encountered when quantitative analysis is required. Corrections are applied to reduce the effect of absorption and enhancement when the incident X-rays strike the sample.

Tables are available giving the absorption coefficients for the elements and these and other factors can be applied to the raw data in order to ensure higher accuracy. These corrections can be carried out using computer programming.

Variations in particle size has also been shown to effect the analysis and to overcome this fusion in lithium borate, glass has been recommended. (Norrish & Hutton, 1964).

For geological samples 0.2-5 g. are normally required.

d) Electron Microprobe Analysis

This technique has been discussed by Wittry (1964) and Long (1967).

A beam of focussed electrons are accelerated onto the surface of the sample (in geological work usually prepared as a thin section (0.06 mm. thickness) with a coating of carbon deposited on the surface to ensure an electrical conducting surface) with the result that some of the inner K-shell electrons are ejected from the atom. This vacancy is filled by an electron from a higher energy shell and the energy difference is made up by the emissions of X-radiation characteristic of the excited atom.

The diameter of the electron beam where it strikes the surface of the sample is typically of the order of $1\mu\text{m}$ and for this size and counting the X-rays for 60 seconds, the limit of detectability for a number of elements is approximately 200 p.p.m. In absolute terms this quantity is about 10^{-15} g. thus the electron microprobe is one of the most sensitive analytical instruments.

For quantitative work, corrections are required to obtain the true intensities from the observed intensities. Corrections are applied to take account of -

- i) absorption of X-rays by the specimen
- ii) fluorescence by line radiation

- iii) fluorescence by the continuum
- iv) background caused by the continuum
- v) detector dead time - and occasionally -
- vi) wavelength shift due to valence and co-ordination state of the excited atom

These corrections are discussed by Wittry (1964) and Thiesen (1965).

The characteristic X-rays are resolved by prisms similar to those required for X-ray fluorescence analysis and detected using gas flow proportional counters.

Smith (1966), Hakli & Wright (1967), Sweatman & Long (1969) and Gibb & Zussman (1971) are amongst many authors who have applied the electron microprobe to the analysis of minerals in rock samples.

One of the great advantages of the microprobe for geological work is its ability to detect variations in concentration within a mineral grain.

e) Chemical Methods

The analysis of rocks and minerals using chemical methods has been described in detail by Shapiro and Brannock (1962), Maxwell (1968) and Jeffrey (1970).

Gravimetric, colorimetric and titrimetric are the methods usually employed under this heading. The quantities of rock required for the analysis of the transition metals by various chemical methods, using the procedures described by Maxwell (1968) and Jeffrey (1970) are presented in Table 1. Thus, 0.5 - 2.0 g. of sample are needed to carry out the analysis for the first row transition elements. For determinations on the whole rock, this quantity of material is readily available but for mineral analysis, this weight of sample would require a considerable amount of time-consuming separations.

Chemical methods are employed to determine the concentration of an element in a particular valence state e.g. the concentration of ferrous iron in a mineral.

Two other techniques which have been applied to determining trace metal distributions in minerals are the Mössbauer effect and electron spin resonance. Neither of these

TABLE 1

Quantities of rock sample required for analysis using chemical methods. (Maxwell, 1968; Jeffrey, 1970).

<u>Element</u>	<u>Colorimetric</u>	<u>Gravimetric</u>	<u>Titrimetric</u>
Sc	1.0	5.0	-
Ti	0.05	-	-
V	0.1-0.25	-	0.5-1.0
Cr	0.25-0.50	-	0.5-1.0
Mn	0.20	-	1.0
Fe	0.05	-	0.1-0.2
Co	0.10	-	-
Ni	0.10-0.25	1.0-2.0	-

techniques was used in this study.

The application of Mössbauer spectroscopy to problems of geological interest has been described in a number of papers (Bancroft, Burns & Howie, 1967; Bancroft, Burns & Maddock, 1967).

Low (1968) has reviewed the field of electron spin resonance and its use in geology and mineralogy but as yet, this technique has not been applied to any great extent to geological problems.

Experimental

Sample preparation was carried out as described in Appendix 2.

D.C. Arc Spectroscopy

Analyses were carried out using methods described by Ahrens & Taylor (1961) and Mitchell (1964).

20 mgs. of finely ground (-300 mesh) rock or mineral powder were mixed with 40 mgs. "specpure" graphite powder in a mechanical shaker for five minutes.

This mixture was then placed in a hollow in the pure carbon anode and the sample arced. Duplicate analyses was carried out. The light emitted was analysed using a Hilger Large Quartz Spectrograph and detected using Kodak B10 photographic plates. Iron was used as an internal standard.

The precision and accuracy of this method of analysis were found to be insufficient to detect the variations in trace metal content of the minerals investigated.

Atomic Absorption Spectroscopy

This technique was mostly used to confirm the X-ray fluorescence values found for nickel.

80-100 mgs. of rock powder were accurately weighed out and placed in a teflon crucible.

The sample was dissolved by heating with 40% hydrofluoric acid solution and concentrated nitric acid and evaporated to dryness. The sample was then taken up in 10% (v/v) nitric acid and diluted to 10 ml.

The nickel standard was prepared by dissolving 30 mgs. "specpure" nickel to nitric acid (Analar) and diluting to 1ℓ. Aliquots of this solution were taken so that the final concentration of nickel ranged from $36\mu\text{g.}$ - $120\mu\text{g.}/10\text{ml.}$

A Pye-Unicam Sp-90 Atomic Absorption Spectrophotometer was employed for the determinations and the following operating conditions were used:

Wavelength	232 mm.
Slit Width	0.1 mm.
Air	5 ℓ/min.
Acetylene	0.9 ℓ/min.
Burner height	10 mm.
Scale expansion	X3

Results obtained by atomic absorption and X-ray fluorescence are presented in Table 2.

X-Ray Fluorescence

This technique was used as an independent check on the neutron activation analysis data.

Finely ground (-300 mesh) samples of the rock (2-5 g) were placed in the sample holder so that approximately $\frac{1}{4}$ " thickness of rock powder covered the Mylar film. The X-radiation was directed on to the rock, through the Mylar window. The analysis was carried out using a Philips 1220 semi-automatic X-Ray Fluorescence instrument.

U.S.G.S. standard rocks were used to prepare calibration curves for each element; the ratio of peak to background was plotted against concentration.

Results obtained by neutron activation and X-Ray fluorescence are presented in Table 3.

TABLE 2

Nickel Concentrations found by Atomic Absorption
and X-Ray Fluorescence

<u>Sample</u>	<u>Ni concn. (p. p. m.)</u> <u>Atomic Absorption</u>	<u>Ni concn. (p. p. m.)</u> <u>X-ray Fluorescence</u>
Z39A wholerock	460	430
Z40 "	560	530
Z64 "	735	640
L5 "	1110	1140

TABLE 3

Cobalt and Chromium Concentrations found by Neutron

Activation Analysis (N.A.A.) and X-Ray Fluorescence (X.R.F.)

<u>Sample</u>	<u>Co concn. (p.p.m.)</u>		<u>Cr concn. (p.p.m.)</u>	
	<u>N.A.A.</u>	<u>X.R.F.</u>	<u>N.A.A.</u>	<u>X.R.F.</u>
C71 wholerock	74	74	510	525
C209 "	83	84	980	1125
Z39A "	76	77	380	300
Z40 "	80	98	430	500
120 "	92	62	1230	1325

Electron Microprobe Analysis

This technique was used to obtain full analysis of minerals present in some of the rocks and to check on their homogeneity. A description of the method employed is given in Appendix 3.

Results obtained are given in the appropriate section in Chapter 5.

... solution ... acid ...
... of glacial acetic acid
... aqueous titanium solution
... freshly prepared 20% v/v aqueous thioglycolic

All reagents were of "Analar" quality.

... ("Analar") potassium titanium oxalate was
... weighed out into a conical flask to which was added
... concentrated sulphuric acid:

Chemical Methods

1. Titanium

Titanium was analysed for by measuring the absorption of the titanium - tiron complex at $380\text{ m}\mu$, at pH 3.8 (tiron:- 1,2 dihydroxybenzene - 3,5 disulphonic acid, di-sodium salt) using the method described by Rigg and Wagenbauer (1961).

Reagents

The following reagents were prepared:-

Buffer solution - 136 g sodium acetate trihydrate dissolved in 1ℓ distilled water and 390 ml glacial acetic acid added.

A freshly prepared 5% w/v aqueous tiron solution.

A freshly prepared 20% v/v aqueous thioglycollic acid solution.

All reagents were of "Analar" quality.

Standard

2.216 ("Analar") potassium titanium oxalate were accurately weighed out into a conical flask to which was added 20 g ammonium sulphate and 50 ml concentrated sulphuric acid. This

solution was boiled for 5-10 minutes, cooled and made up to 500 ml with distilled water. This produced a solution equivalent to 1 mg TiO_2 /ml. A 20 ml aliquot was taken and made up to 1ℓ in order to prepare 20 γg TiO_2 /ml standard solution.

Procedure

About 20 mgs rock powder were accurately weighed into a P.T.F.E. crucible, 15 ml 40% hydrofluoric acid and 5 ml concentrated nitric acid were added. The crucible was then placed in a sandbath and the solution evaporated to dryness. This was repeated to affect complete solution of the rock powder. The residue was finally taken up in 5 ml distilled water then transferred to a 50 ml volumetric flask. To this was then added 25 ml buffer solution, 5 ml tiron reagent and 2 ml thioglycollic acid solution. The contents of the flask were well mixed, made up to volume, shaken again and left overnight.

The TiO_2 standards were prepared by taking aliquots of the 20 γg/ml solution so as to give solutions containing 20, 100, 200 and 300 γg TiO_2 /50 ml. These were treated in a similar manner to the rock samples.

The optical density of the solutions were measured in 10 mm cells at 380 *mμ* using a Unicam SP500 spectrophotometer.

11. Ferrous Iron

Ferrous iron was determined using the method described by Wilson (1955, 1960). This method involves the titration of excess ammonium metavanadate with ferrous ammonium sulphate solution.

Reagents

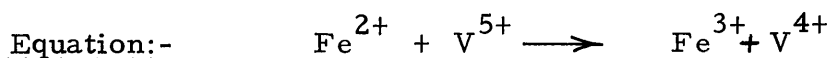
About 13 g. ("Analar") ferrous ammonium sulphate were dissolved in 1ℓ of cold N sulphuric acid. This solution was standardized by titration with 0.05 N ceric sulphate solution using ferroin as indicator.

Diphenylamine indicator - 3% aqueous solution of barium diphenylamine sulphonate.

Procedure

About 50 mg finely powdered rock (-300 mesh) and 30 mg ammonium metavanadate were accurately weighed out into a 50 ml polythene beaker. Three beakers were prepared containing only ammonium metavanadate. To each beaker was added 10 ml of

40% hydrofluoric acid, then covered with "parafilm" and allowed to stand in a fume cupboard until the rock powder had been completely attacked. This normally required 1-2 days. Then 30 ml of a 33% v/v solution of sulphuric acid were added and the contents of the beaker washed with 250 ml saturated boric acid solution into a 800 ml beaker containing 5 d of diphenylamine indicator. The solution was then stirred to dissolve any white precipitates of calcium and magnesium fluorides and titrated with the standardised ferrous ammonium sulphate solution until the purple colour just disappeared.



This reaction is quantitative in strongly acid solution and the ferrous iron in the rock sample is oxidised by the metavanadate to ferric iron. The volume of standardised ferrous ammonium sulphate solution required to titrate the excess ammonium metavanadate is subtracted from the volume expected for the total quantity of metavanadate added to the rock powder in the first step.

CHAPTER 5

Results and Discussion

The results obtained in this study will be presented in three main sections. The first section is intended to set the scene regarding the chemistry of the rocks investigated, to indicate the variations in major and transition metal content and to point to any correlations which exist. The second section presents data on the transition metal content of the components of the rocks analysed (olivine, clinopyroxene and groundmass) and the partition coefficients for these metal ions between the various phases. The results obtained are discussed in the light of crystal field theory. In the third section, the results are summarised and conclusions presented.

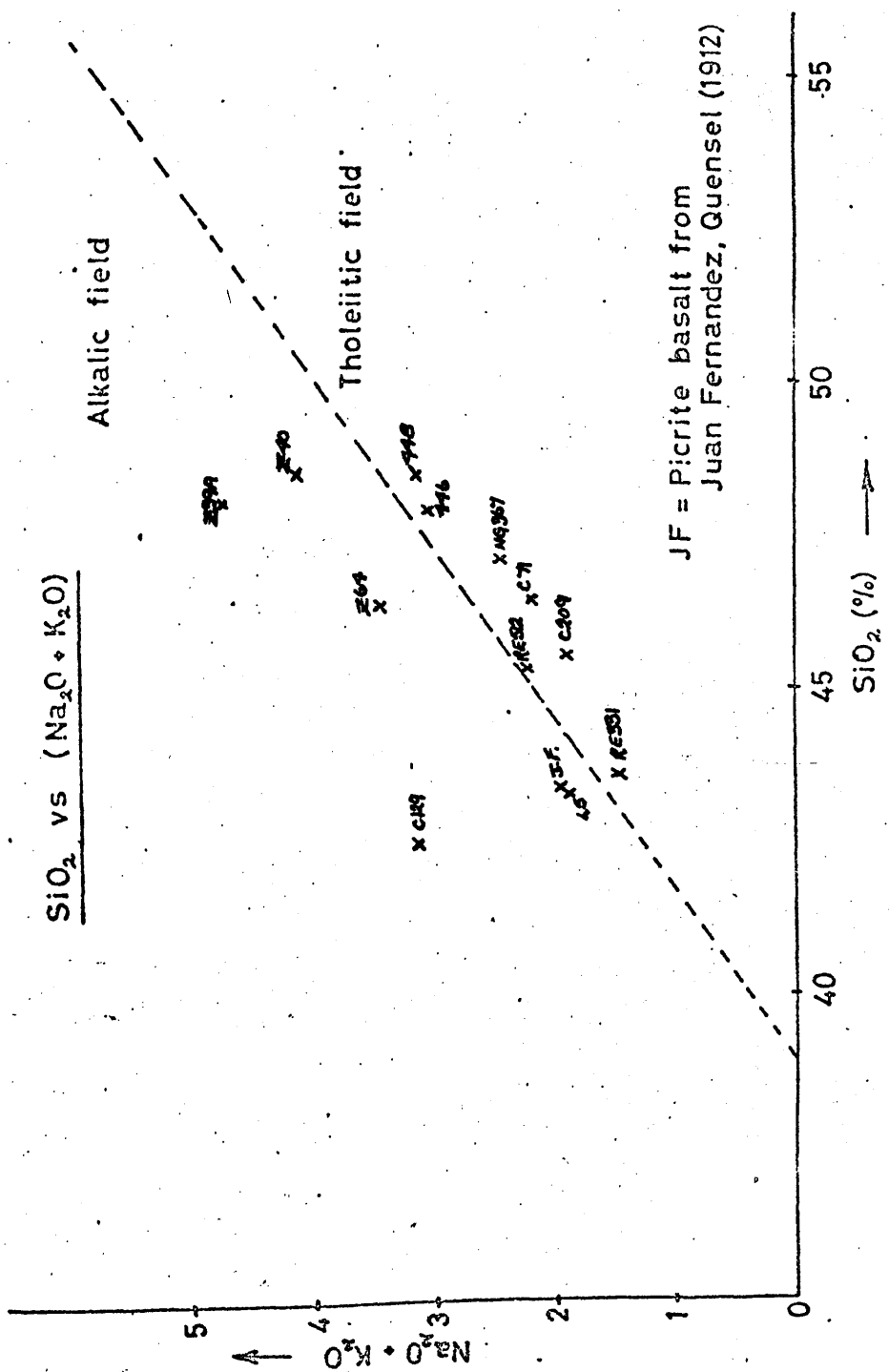
1. Analysis of the Rock Samples

(i) Major Element Chemistry

The analytical data obtained is presented in Table 1, Appendix 4. All of the samples investigated were basaltic rocks and various correlation diagrams were prepared to indicate the similarities which exist between the rocks.

(a) SiO₂ Vs Total Alkalies

As can be seen from Fig. 1 both alkalic-basalts and theoleiitic basalts were obtained: C129; Z39A, Z40, Z64; L5 are alkalic; RE331, RE512; NG367; C71, C209; 446, 448 are theoleiitic. It might have been expected that the different basalts would give rise to different partition coefficients; however, this was not found. No correlation of partition coefficients with alkalic or theoleiitic basalt types was evident.



JF = Picrite basalt from
 Juan Fernandez, Guensel (1912)

Fig.1

(b) SiO₂ Vs K₂O; Na₂O; CaO

These variation diagrams are presented in Fig. 2

Reasonable correlation of K₂O and Na₂O with SiO₂ exists for the rocks investigated; no clear correlation of CaO with SiO₂ was evident.

(c) Na₂O Vs TiO₂; P₂O₅

These variation diagrams are given in Fig. 3

Some correlation is evident in both diagrams, although TiO₂ and P₂O₅ is somewhat enriched in rock sample C129.

SiO₂ vs CaO, Na₂O, K₂O

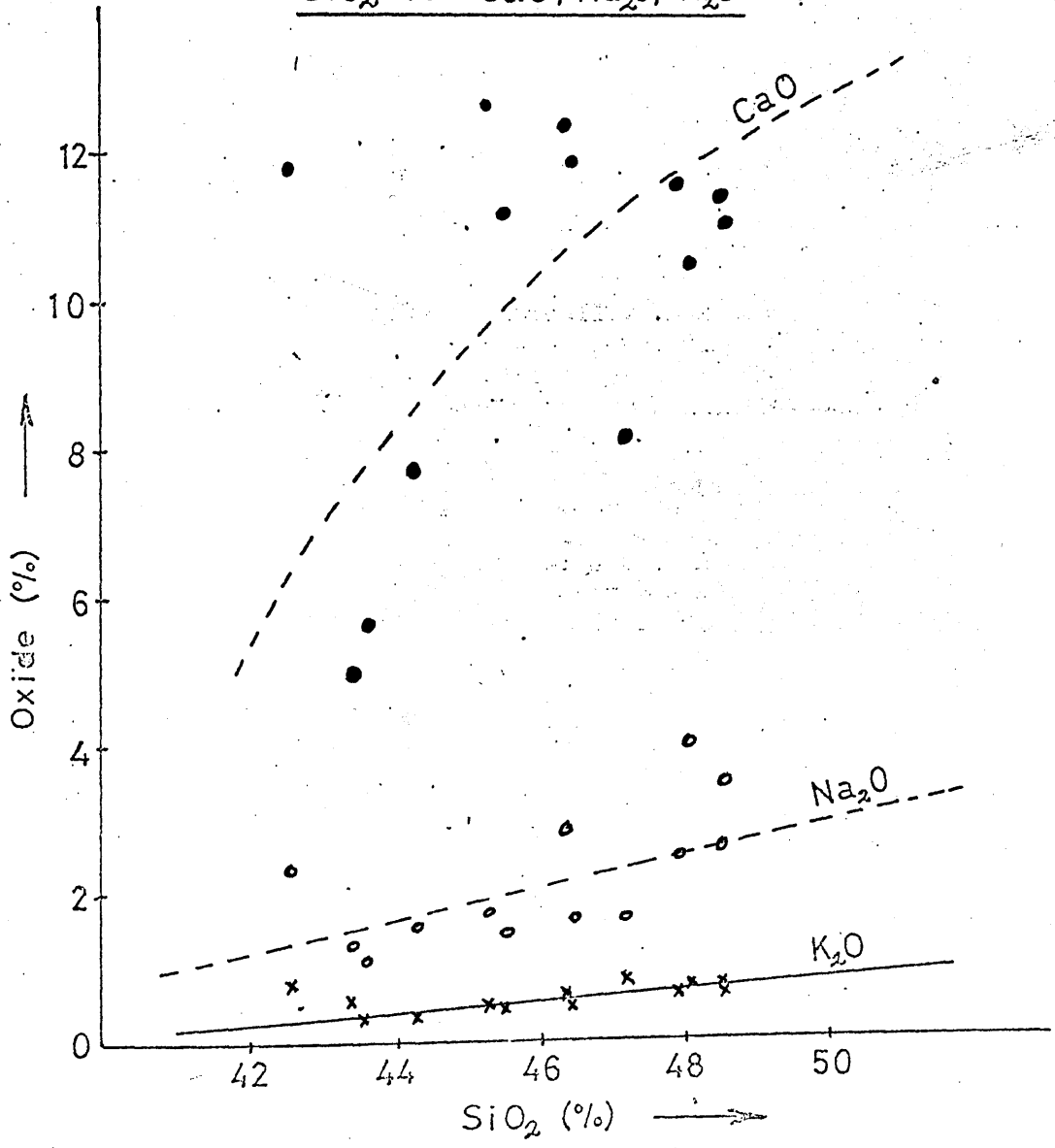


Fig. 2

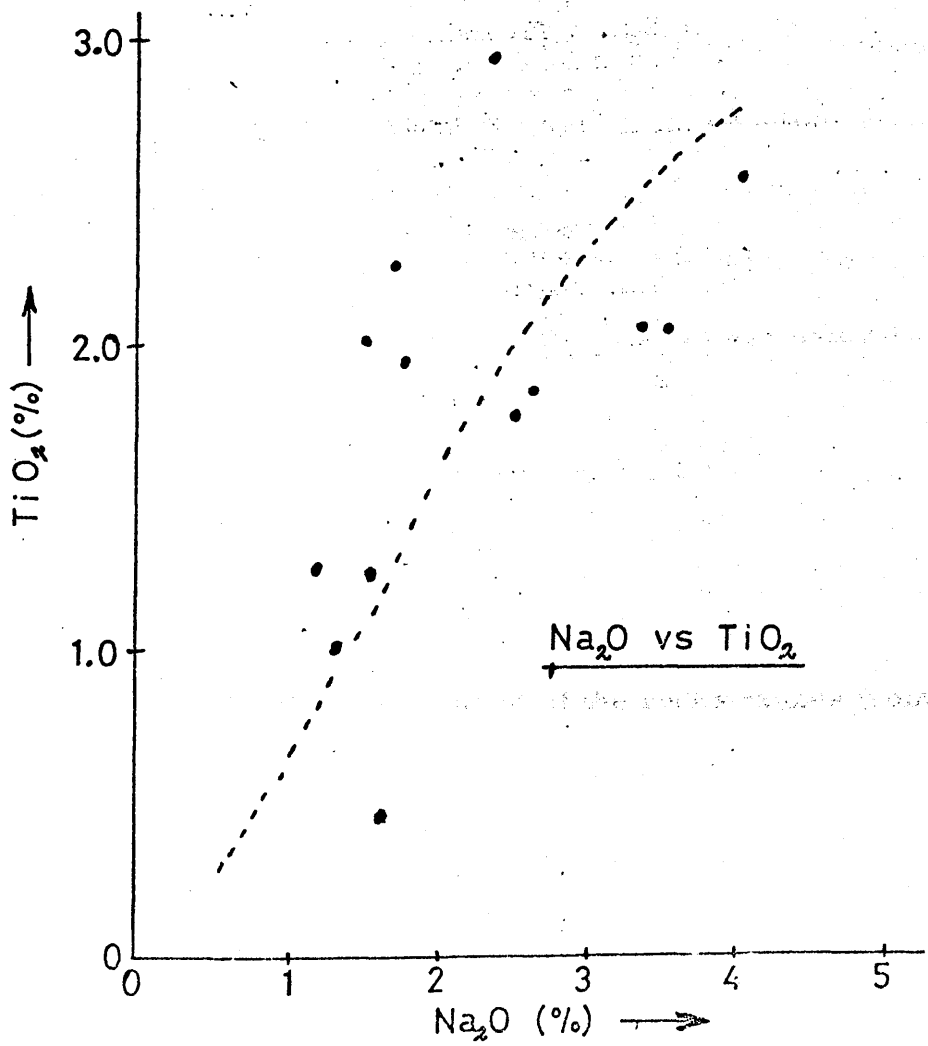
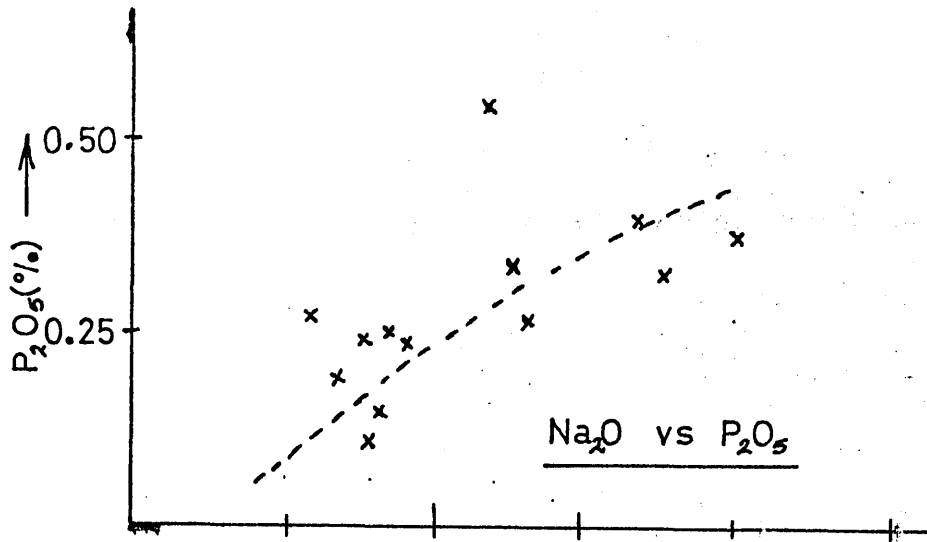


Fig. 3

(ii) Transition Metal Chemistry

The analytical results for the transition metal concentrations in the rocks investigated are given in Tables 1-7.

(a) Scandium

The scandium content of the rocks ranges from 28-55 p.p.m. with a mean of 35 ± 7 p.p.m. Prinz (1967) in his compilation of the trace metal content of rocks of basaltic composition quoted a range of 0-60 p.p.m. with a mean of 27 p.p.m. The results obtained in this work are in general agreement with his findings. No correlation of scandium content with geographical location was evident.

(b) Titanium

The titanium content of the rocks ranges from 0.43-3.13% TiO_2 , with a mean of $1.68 \pm 0.69\%$. Manson (1967) obtained a mean value

(15p. 162)

TABLE 1

Analytical Results, Reunion Island Samples

Specimen	Sc (ppm)	TiO ₂ (%) ²	Cr (ppm)	Mn (ppm)	Fe ²⁺ (%)	Co (ppm)	Ni (ppm)
RE331 olivine	6.0	N.D.	460	1860	11.16 ¹	163	2120
RE331 groundmass	42	2.38 ¹	610	1460	5.19 ¹	(147)	132
RE331 wholerock	-	1.28 ²	1400 ²	1240	7.45 ²	-	1200
RE512 olivine	7.0	N.D.	80	1820	11.16 ¹	250	1690
RE512 pyroxene	103	0.74	2360	930	-	46	310
RE512 groundmass	41	0.78	320	1430	5.05	74	128
RE512 wholerock	-	1.91 ²	210 ²	1550 ²	5.09 ²	-	200 ²

N.D. = Not Detected

1, Upton & Wadsworth (1966)

2, Wadsworth, personal communication (1971)

TABLE 1A

Partition Coefficients, Reunion Island Samples

Specimen	Sc	Ti	Cr	Mn	Fe ²⁺	Co	Ni
RE331 ol/gm	0.14	-	0.75	1.27	2.15	-	16.1
RE512 ol/gm	0.17	-	0.25	1.27	2.21	3.38	13.2
RE512 cpx/gm	2.52	0.95	7.37	0.65	-	0.62	2.42

TABLE 2Analytical Results, British Solomon Islands Sample

Specimen	Sc (ppm)	TiO ₂ (%)	Cr (ppm)	Mn (ppm)	Fe ²⁺ (%)	Co (ppm)	Ni (ppm)
NG367 olivine	7.0	N.D.	960	1840	9.54*	160	1910
NG367 pyroxene	116	0.48*	3390	1030	3.30*	44	220
NG367 groundmass	42	0.60*	720	1050	3.18*	36	103
NG367 wholerock	-	0.43*	-	-	5.28*	-	603*

N.D. = Not Detected

* Stanton & Bell (1969)

TABLE 2A

Partition Coefficients, British Solomon Islands Sample

Specimen	Sc	Ti	Cr	Mn	Fe ²⁺	Co	Ni
NG367 ol/gm	0.17	-	1.33	1.75	3.00	4.44	18.5
NG367 cpx/gm	2.76	0.80	4.72	0.98	1.04	1.22	2.13

TABLE 3Analytical Results, Juan Fernandez Samples

Specimen	Sc (ppm)	TiO ₂ (%) ²	Cr (ppm)	Mn (ppm)	Fe ²⁺ (%)	Co (ppm)	Ni (ppm)
17840 olivine	4.3	N.D.	630	2120	10.95	187	2030
17840 groundmass	30	1.37	440	1630	7.23	91	330
17840 wholerock	28	1.66	700	1200	7.45	87	840
17901 olivine	4.6	N.D.	810	2190	9.71	181	1970
17901 groundmass	27	2.72	490	1950	6.87	96	410
17901 wholerock	30	2.47	960	1400	6.72	93	770

N.D. = not detected

TABLE 3APartition Coefficients, Juan Fernandez Samples

Specimen	Sc	Ti	Cr	Mn	Fe ²⁺	Co	Ni
17840 ol/gm	0.14	-	1.43	1.30	1.51	2.51	6.15
17901 ol/gm	0.17	-	1.65	1.12	1.41	1.89	4.80
	10	2.38	1000	1110	11.20		
	33	3.54	340	1600	10.23		
	43	3.13	610	1130	8.73		
	5.5	N.D.	720	1720	10.32		
	100	1.05	4000	940	3.73		
	31	2.03	350	1700	5.93		
	35	2.25	980	1210	5.74		

from Katsura (1964)

TABLE 4

Analytical Results, Hawaiian Samples

Specimen	Sc (ppm)	TiO ₂ (%) ²	Cr (ppm)	Mn (ppm)	Fe ²⁺ (%)	Co (ppm)	Ni (ppm)
C71 olivine	6.7	N.D.	400	1900	11.25	244	1760
C71 pyroxene	82	1.04	3890	1070	4.04	47	290
C71 groundmass	31	3.15	810	1460	6.51	52	150
C71 wholerock	47	2.62	510	1070	6.35	72	500
C129 olivine	4.9	N.D.	850	1720	17.92	220	1440
C129 pyroxene	76	2.38	(930)	1110	4.56	41	260
C129 groundmass	32	3.54	340	1660	10.25	60	135
C129 wholerock	43	3.13	610	1130	8.73 ¹	80	450
C209 olivine	5.5	N.D.	720	1720	10.32	216	2950
C209 pyroxene	100	1.05	4000	940	3.73	42	380
C209 groundmass	31	2.03	350	1700	5.93	49	210
C209 wholerock	35	2.25	980	1210	6.74 ²	83	840

N.D. = Not Detected

1, Macdonald & Katsura (1964)

2, Macdonald (1968)

TABLE 4A

Partition Coefficients, Hawaiian Samples

Specimen	Sc	Ti	Cr	Mn	Fe ²⁺	Co	Ni
C71 ol/gm	0.22	-	0.49	1.30	1.73	4.69	11.73
C71 cpx/gm	2.64	0.33	4.40	0.73	0.62	0.90	1.93
C129 ol/gm	0.15	-	2.50	1.04	1.75	3.67	10.67
C129 cpx/gm	2.37	0.67	2.74	0.67	0.45	0.68	1.93
C209 ol/gm	0.18	-	2.06	1.01	1.74	4.41	14.05
C209 cpx/gm	3.23	0.52	11.43	0.55	0.63	0.86	1.81

TABLE 5

Analytical Results, Icelandic Samples

Specimen	Sc (ppm)	TiO ₂ (%) ²	Cr (ppm)	Mn (ppm)	Fe ²⁺ (%)	Co (ppm)	Ni (ppm)
394 olivine	7.7	N.D.	97	1610	11.18	224	1550
394 pyroxene	84	0.63	2770	1250	3.22	41	210
394 groundmass	46	0.97	250	800	(1.04)	38	140
394 wholerock	55	0.79	670	980	3.10	90	300
446 olivine	6.0	N.D.	500	1610	11.53	202	2400
446 pyroxene	89	1.90	8280	1100	3.51	47	370
446 groundmass	43	2.02	580	1340	5.98	49	190
446 wholerock	40	1.24	770	1290	6.49	106	370
448 olivine	6.0	N.D.	750	1790	11.80	180	2200
448 pyroxene	124	2.75	3940	1650	3.57	45	400
448 groundmass	39	2.36	460	1260	4.23	47	240
448 wholerock	45	1.68	1180	1540	5.30	77	520

N.D. = Not Detected

TABLE 5A

Partition Coefficients, Icelandic Samples

Specimen	Sc	Ti	Cr	Mn	Fe ²⁺	Co	Ni
394 ol/gm	0.17	-	0.39	2.01	(10.75)	5.89	11.07
394 cpx/gm	1.83	0.65	11.08	1.56	(3.09)	1.08	1.50
446 ol/gm	0.14	-	0.86	1.20	1.93	4.12	12.63
446 cpx/gm	2.07	0.94	14.27	0.82	0.59	0.96	1.95
448 ol/gm	0.15	-	1.63	1.42	2.79	3.83	9.17
448 cpx/gm	3.18	1.17	8.56	1.31	0.84	0.96	1.67

TABLE 6Analytical Results, Red Sea Islands Samples

Specimen	Sc (ppm)	TiO ₂ (%)	Cr (ppm)	Mn (ppm)	Fe ²⁺ (%)	Co (ppm)	Ni (ppm)
Z39A olivine	6.2	N.D.	160	1620	13.79	188	1600
Z39A pyroxene	117	1.20	2860	1080	4.00	41	390
Z39A groundmass	34	0.90	250	1350	5.64	47	136
Z39A wholerock	39	2.64	380	1340	7.97	76	450
Z40 olivine	7.1	N.D.	240	1690	11.18	161	1700
Z40 pyroxene	99	1.34	3760	1020	4.04	46	280
Z40 groundmass	41	1.16	600	1320	4.90	44	197
Z40 wholerock	35	2.15	660	1150	6.93	80	530
Z64 olivine	6.3	N.D.	480	1520	11.07	180	1990
Z64 pyroxene	106	1.44	3710	1500	4.01	64	420
Z64 groundmass	34	1.92	400	1160	6.53	52	210
Z64 wholerock	29	2.15	430	1150	7.91	90	640

N.D. = Not Detected

TABLE 6A

Partition Coefficients, Red Sea Islands Samples

Specimen	Sc	Ti	Cr	Mn	Fe ²⁺	Co	Ni
Z39A ol/gm	0.18	-	0.64	1.20	2.45	4.00	11.76
Z39A cpx/gm	3.44	1.33	11.44	0.80	0.71	0.87	2.86
Z40 ol/gm	0.17	-	0.40	1.28	2.28	3.66	8.63
Z40 cpx/gm	2.41	1.15	6.27	0.77	0.82	1.04	1.42
Z64 ol/gm	0.18	-	1.20	1.31	1.70	3.46	9.48
Z64 cpx/gm	3.12	0.75	9.28	1.29	0.61	1.23	2.00

TABLE 7

Analytical Results, Greenland Samples

Specimen	Sc (ppm)	TiO ₂ (%)	Cr (ppm)	Mn (ppm)	Fe ²⁺ (%)	Co (ppm)	Ni (ppm)
L5 olivine	4.9	N.D.	2490	1770	9.63	162	1900
L5 groundmass	36	1.57	1190	1290	5.64	48	710
L5 wholerock	30	1.52	1470	1140	4.67	83	1140
L7 olivine	5.5	N.D.	1320	1360	8.60	163	1360
L7 groundmass	41	1.58	640	1160	4.71	48	270
L7 wholerock	33	1.28	1370	1560	6.82	108	1220
B5 olivine	7.4	N.D.	890	1660	9.13	121	2510
B5 groundmass	55	1.39	830	1250	5.24	44	284
B5 wholerock	31	1.09	2590	1400	6.79	102	1520
120 olivine	8.3	N.D.	790	1570	8.08	154	3890
120 groundmass	51	1.78	520	1260	3.64	45	307
120 wholerock	35	1.45	1230	1200	6.87	92	1070

N.D. = Not Detected

TABLE 7A

Partition Coefficients, Greenland Samples

Specimen	Sc	Ti	Cr	Mn	Fe ²⁺	Co	Ni
L5 ol/gm	0.14	-	2.10	1.37	1.71	3.38	2.68
L7 ol/gm	0.13	-	2.06	1.17	1.83	3.40	5.04
B5 ol/gm	0.13	-	1.07	1.33	1.74	2.75	8.84
120 ol/gm	0.16	-	1.52	1.25	2.22	3.42	12.67

chromium. The rocks from Ukkusuaq Eja have particularly high concentrations of chromium (e.g., 2990 p.p.m.)

of $1.9^{\pm} 1.03\%$ TiO_2 in his determination of the range in chemistry of basaltic rocks. Reasonable agreement with his compilation is seen. The rock sample from the British Solomon Islands (NG367) has a particularly low concentration of TiO_2 (0.43%).

(c) Chromium

The chromium content of the rocks ranges from 210-2540 p.p.m. and this wide range in analysis is reflected in the mean of $875^{\pm} 550$ p.p.m. These values are much higher than the analyses quoted by Prinz (1967) - a range of 0-550 p.p.m. and a mean of 162 p.p.m. chromium. The rocks from Ubekendt Ejland, West Greenland have particularly high concentrations of chromium (1230, 1370, 1470 and 2590 p.p.m.)

(d) Manganese

The manganese content ranges from 980-1560 p.p.m., with a mean of $1170^{\pm}160$ p.p.m. ; Manson (1967) in his compilation of analyses of basaltic rocks obtained a mean of $1320^{\pm}770$ p.p.m. manganese. The results obtained in this work are in general agreement with his data. No clear correlation of manganese content with geographical location was evident.

(e) Iron (Ferrous)

The ferrous iron content ranges from 3.10-8.73% Fe^{2+} , with a mean of $6.28^{\pm}1.06\%$. Manson (1967) reported a mean of $6.22^{\pm}1.48\text{Fe}^{2+}$ for rocks of basaltic composition. Low values for ferrous iron were obtained for one sample of Icelandic rock (394, 3.10% Fe^{2+}) and one sample of West Greenland rock (L5, 4.67% Fe^{2+}).

(f) Iron (Ferric)

The ferric iron content ranges from 1.07-3.42% Fe³⁺ with a mean of 1.96[±]0.66% Fe³⁺. These values are in agreement with Manson (1967) who reported a mean of 2.10[±]0.94% Fe³⁺ for basaltic rocks.

(g) Cobalt

The cobalt content of the rocks does not vary to any great extent, having a range of 72-108 p.p.m. and a mean of 82[±]10 p.p.m. These values are somewhat at variance with the results quoted by Prinz (1967) i.e. a range of 7-80 p.p.m. and a mean of 40 p.p.m. cobalt. Again no definite correlation of cobalt concentration with locality was observed; this is in agreement with Carr & Turekian (1961) who found no evidence for regional variation of cobalt content of basaltic rocks.

(h) Nickel

The nickel content of the rocks varied very widely from 200-1520 p.p.m. with a mean of 670 ± 360 p.p.m. These results are again at variance with Prinz (1967) who reported a range of 3-350 p.p.m. and a mean of 90 p.p.m. nickel. Particularly high concentrations of nickel were found in one of the Reunion samples (RE331; 1200 p.p.m.) and in all four of the West Greenland samples (1070-1520 p.p.m.)

(i) Chromium - Nickel Correlation

Turekian (1963) and Gast (1968) pointed out that some correlation does exist between the chromium and nickel content of basaltic rocks. Although the results obtained in this study are somewhat higher than the chromium and nickel concentrations reported by these authors, some correlation of chromium to nickel is evident in Fig. 4.

11. Transition Metal Content of Components of the Rocks and
their Distribution

The results obtained for the transition metal content of the olivines, clinopyroxenes and groundmasses of the rocks investigated will be presented in five sections as follows:-

- i) Olivine analysis
- ii) Clinopyroxene analysis
- iii) Groundmass analysis
- iv) Results obtained by electron microprobe
- and v) Distribution of the ions between olivine,
clinopyroxene and groundmass

The analyses are given in Tables

Results quoted from the literature are from the following:-

Wager & Mitchell (1951)	Skaergaard Intrusion, East Greenland
Cornwall & Rose (1957)	Keweenaw ⁱⁿ Lavas, Michigan, U.S.A.
Muir & Tilley (1964)	Rift zone of the Mid-Atlantic ridge
Hakli & Wright (1967)	Makaopuhi, Hawaii
Onuma et al (1968)	North Kyushu, Japan

Rodgers & Brothers (1969) Ultramafic nodules, Auckland, N. Zealand
 Agrell et al (1970) Lunar sample collected on Apollo 11 expedition
 Brown et al (1970) " " " " " " "
 Simkin & Smith (1970) Various lavas, Hawaii
 Gunn (1971) Kilauea Iki, Hawaii

Results are given together with the mean and standard deviation

i) Olivines

a) Scandium

The scandium content of the olivines investigated ranges from 4.3-8.3 p.p.m. with a mean of 5.7 ± 1.1 p.p.m. Few results have been quoted in the literature, however, Wager & Mitchell found a value less than 10 p.p.m. scandium and Cornwall & Rose reported 10 p.p.m. scandium. These low values for the scandium content of olivines are due to the difficulty of incorporating a trivalent ion in the olivine structure. The data obtained indicate a fairly constant level of scandium in olivines.

b) Titanium

Titanium was not detected in any of the olivines; the limit of detection of the method employed was estimated as 0.02% TiO_2 . Rodgers & Brothers obtained values of 0.02-0.10% TiO_2 and Muir & Tilley reported values of 0.08-0.16% TiO_2 . These results suggest that titanium may be present in very small amounts in the olivine structure, either substituting for the iron and magnesium ions or present in place of silicon.

c) Chromium

The presence of very small chrome-spinel crystals in many of the olivine phenocrysts meant that no reliable data for the chromium content of this mineral could be obtained. The wide range of results, 80-2,490 p.p.m., with a mean of $660^{\pm}540$ p.p.m., indicates the problem associated with chromium. It is probably unlikely that chromium can exist as the divalent ion in rocks from earth since it is easily oxidised to the trivalent state; thus chromium cannot be incorporated into the olivine structure for the same reason

as scandium.

Recent results for the chromium content of olivines obtained from the moon's surface suggest that chromium may well be present in the divalent state in lunar rocks; Agrell et al found 400-1,800 p.p.m. chromium and Brown et al 1,400-1,800 p.p.m. As these results were obtained by electron microprobe, it would appear likely that these values reflect the chromium content of the olivines and are not influenced by the presence of chrome-spinels.

d) Manganese

The values found for manganese content of the olivines range from 1,360-2,190 p.p.m., with a mean of 1650[±]200 p.p.m. Simkin & Smith quote values of 1,200-2,800 p.p.m. and Muir & Tilley, 1,100 p.p.m. Divalent manganese can easily be incorporated into the olivine structure, substituting for magnesium and iron.

e) Iron (Ferrous)

The olivines investigated were generally early formed magnesium rich crystals containing 8.08-17.92% Fe^{2+} . Iron content of olivines from similar rocks are given by Muir & Tilley, 6.56% Fe^{2+} and Häkli & Wright, 16.39-23.64% Fe^{2+} .

f) Cobalt

In the olivines analysed, the cobalt concentrations range from 121-250 p.p.m., with a mean of 177^{+32} p.p.m. These values compare well with results quoted by Wager & Mitchell, 150 p.p.m.; Muir & Tilley, 220-250 p.p.m.; Gunn, 190 p.p.m. Divalent cobalt can be accommodated easily in the olivine lattice.

g) Nickel

Nickel contents for the olivines investigated range from 1,360-3,890 p.p.m., with a mean of $1,840^{+590}$ p.p.m. Good agreement exists between these results and data quoted in the

literature e.g. Wager & Mitchell, 2,000 p.p.m.; Muir & Tilley, 2,500-3,200 p.p.m.; Häkli & Wright, 840-1,555 p.p.m.; Gunn, 2,350-2,950 p.p.m. Divalent nickel is thus easily incorporated into the olivine structure.

ii) Clinopyroxenes

a) Scandium

The scandium content of the clinopyroxenes analysed range from 76-124 p.p.m., with a mean of 90^{+15} p.p.m. This range of results is in accord with reported analyses e.g. Wager & Mitchell, 30-150 p.p.m.; Cornwall & Rose, 100-200 p.p.m.; Muir & Tilley, 80-120 p.p.m.; Onuma et al, 50 p.p.m. In contrast to olivine, trivalent scandium can be incorporated into the pyroxene structure.

b) Titanium

The clinopyroxenes investigated contain 0.48-2.75%TiO₂, with a mean of 1.23[±]0.69%TiO₂; accordingly some of the pyroxenes containing higher concentrations of titanium may almost be described as titanaugites, as these generally contain 3-6%TiO₂. (Deer, Howie & Zussman, 1966). Comparable results were quoted by Wager & Mitchell, 0.21-3.74%; Muir & Tilley, 1.17-2.72%; Håkli & Wright, 1.2-1.37%; Onuma et al, 1.25%. The clinopyroxenes obtained from the Apollo 11 lunar samples tend to contain rather more titanium; Agrell et al reported 0.59-5.91%TiO₂.

c) Chromium

The chromium content of the pyroxenes ranges from 2,360-8,280 p.p.m. with a mean of 3,290[±]1,710 p.p.m. One exceptionally low value of 930 p.p.m. in a Hawaiian sample (C129) was obtained. This result was not used when calculating the mean and standard deviation. These analyses are somewhat higher than values given by Wager & Mitchell, 3,000 p.p.m.; Muir & Tilley, 450-2,500 p.p.m.

Clinopyroxenes from lunar rocks were reported to contain 680-4,100 p.p.m. (Agrell et al, Brown et al), These values confirm that the trivalent chromium ion can be easily incorporated into the pyroxene structure.

d) Manganese

The manganese content of the clinopyroxenes investigated range from 930-1,650 p.p.m., with a mean of $1,020 \pm 220$ p.p.m. Previous results give similar values e.g. Wager & Mitchell, 1,500 p.p.m.; Muir & Tilley, 1,320-1,940 p.p.m.; Onuma et al, 1,400 p.p.m. Lunar clinopyroxenes are reported to contain considerable higher concentrations of manganese, 1,940-8,970 p.p.m. (Brown et al, 1970).

e) Iron (Ferrous)

The ferrous iron content of the pyroxenes ranges from 3.22-4.56% Fe^{2+} , with a mean of $3.40 \pm 0.39\%$ Fe^{2+} . These values are somewhat lower than results obtained by Wager & Mitchell, 6.60% Fe^{2+}

and Muir & Tilley, 3.94-7.37% Fe²⁺, however, the wide range of pyroxene types makes comparison difficult.

f) Cobalt

The cobalt concentrations range from 41-64 p.p.m., with a mean of 40[±]6 p.p.m. These values are in agreement with reported results; Wager & Mitchell, 60 p.p.m.; Muir & Tilley, 45 p.p.m.; Onuma et al, 61 p.p.m.

g) Nickel

Nickel values for the clinopyroxenes analysed range from 210-420 p.p.m., with a mean of 280[±]70 p.p.m. Results obtained by others include 50-200 p.p.m. (Wager & Mitchell); 26-220 p.p.m. (Muir & Tilley); 220-255 p.p.m. (Häkli & Wright).

(iii) Groundmass

There have been almost no analyses reported in the literature on the transition metal content of the groundmasses of volcanic rocks. For this reason, the results obtained in this study cannot be compared with previous work and are therefore given without comment.

	<u>Range</u> <u>(p. p. m.)</u>	<u>Mean</u> <u>(p. p. m.)</u>
Scandium	30-55	36 [†] -7
Titanium (as TiO ₂)	0.60-3.54%	1.69 [†] -79%
Chromium	250-1190	520 [†] -230
Manganese	800-1950	1290 [†] -260
Iron, ferrous (1.04)	3.18-10.25%	5.47 [†] -1.55%
Cobalt	36-96 (147)	51 [†] -16
Nickel	103-710	221 [†] -140

The values in brackets are results which were considered in error; this will be discussed in section (v). These values were not used in calculating the mean and standard deviation.

Häkli & Wright (1967) reported 50-115 p.p.m. nickel in the glass from the Makaopuhi lava lake.

(iv) Electron Microprobe Results

Electron microprobe analyses were kindly carried out by the Staff of the Department of Geology and Mineralogy, University of Aberdeen. The following samples were examined:-

C129	olivine and clinopyroxene
446	olivine
Z64	olivine

using the method described in Appendix 3.

Results are presented in Tables 8-10.

The results for samples C129 and 446 indicate that only one generation of olivine (C129 and 446) and pyroxene (C129 only) crystals are present in each sample of lava.

Data for Z64 shows that one olivine (b) is slightly different and earlier formed compared to the other three, suggesting that two generations of olivine crystals may be present, although the difference in analysis is not very great.

Although the minerals were not examined directly for zoning of the crystals, the constancy of the number of counts for the various elements in different parts of each crystal confirmed that the minerals were homogeneous.

TABLE 8

Microprobe Analysis of Minerals from Rock Sample C129

	Olivines		Clinopyroxenes		
	(a)	(b)	(c)	(d)	(e)
SiO ₂	36.90	37.62	44.86	46.14	46.75
Al ₂ O ₃	0.20	0.03	8.02	8.10	7.91
*FeO	22.82	21.99	7.48	7.50	7.70
MgO	36.31	38.10	12.60	12.39	12.36
CaO	0.46	0.27	22.06	21.61	21.50
MnO	0.36	0.31	0.14	0.13	0.16
Cr ₂ O ₃	nil	0.004	0.25	0.34	0.48
NiO	0.054	0.114	0.054	0.05	0.06
TiO ₂	<u>0.06</u> 97.164	<u>0.042</u> 98.480	<u>2.49</u> 97.954	<u>3.14</u> 99.40	<u>2.12</u> 99.04

* Total iron as FeO

TABLE 9

Microprobe Analysis of Olivines from Rock Sample 446.

	Olivines		
	(a)	(b)	(c)
SiO ₂	39.95	40.25	40.56
Al ₂ O ₃	0.16	0.29	0.19
* FeO	16.29	16.86	16.90
MgO	43.66	42.90	42.79
CaO	nil	nil	nil
MnO	0.22	0.28	0.23
Cr ₂ O ₃	0.014	0.03	0.028
NiO	0.12	0.11	0.11
TiO ₂	0.002	nil	nil
	<u>100.416</u>	<u>100.72</u>	<u>100.81</u>

* Total iron as FeO

TABLE 10

Microprobe Analysis of Olivines from Rock Sample Z64

	Olivines			
	(a)	(b)	(c)	(d)
SiO ₂	39.75	40.11	40.48	40.97
Al ₂ O ₃	0.07	0.08	0.06	0.08
FeO	14.87	11.76	13.94	13.73
MgO	43.24	45.48	44.82	44.38
CaO	0.32	0.31	0.30	0.31
MnO	0.18	0.14	0.16	0.14
Na ₂ O	0.05	0.03	0.01	0.02
K ₂ O	0.01	0.001	nil	0.003
Cr ₂ O ₃	0.02	0.06	0.06	0.02
NiO	0.18	0.26	0.19	0.20
TiO ₂	<u>trace</u>	<u>0.021</u>	<u>0.01</u>	<u>0.02</u>
	98.69	98.252	100.00	99.873

* Total iron as FeO

The results obtained generally confirmed the analyses carried out by neutron activation and chemical methods.

$$\ln k = - \frac{\Delta H}{RT} + B$$

k : partition coefficient, defined as $\frac{[X]_{\text{cryst}}}{[X]_{\text{mag}}}$
 X : transition metal ion

ΔH is the enthalpy

B is an integration constant.

For a series of transition metal ions with the same site preference energy a linear relationship should hold between $\ln k$ and $1/T$.

Site preference energy provided:-

the electronegativities and ionic radii of the ions are identical or very similar

the octahedral site preference energy is predominately to the ΔH term

(v) Partition of the Elements between the Minerals and Groundmass

Further to the discussion in section 1X. of Chapter 2, the following relationship should hold for the partition of transition metal ions between olivine and pyroxene crystals and the groundmass of the lava:-

$$\ln k = - \frac{\Delta H}{RT} + B$$

where k is the partition coefficient, defined as $\frac{[X]_{\text{crystal}}}{[X]_{\text{magma}}}$ and X is a transition metal ion

ΔH is the enthalpy

and B is an integration constant.

For a series of transition metal ions with the same oxidation state a linear relationship should hold between $\ln k$ and the octahedral site preference energy provided:-

- i) the electronegativities and ionic radii of the ions are identical or very similar
- ii) the octahedral site preference energy contributes predominantly to the ΔH term
- and iii) tetrahedral and octahedral sites are available for the transition metal ions in the magma while octahedral or near octahedral sites are available in the olivine and pyroxene crystals

These requirements have been discussed in sections VIIIc and IX of Chapter 2.

In order to test this hypothesis, it was necessary to obtain data for the concentration of various transition metal ions in the minerals of volcanic rocks and the groundmass from which they crystallised. These results, together with the partition coefficients of the ions between olivine and pyroxene crystals and the groundmass have been given. (Analytical data in Tables 1-7, partition coefficients in Tables 1A-7A)

In the derivation of the partition coefficients, it can be assumed that the groundmass is compositionally representative of the contemporary magma. This groundmass approximates very closely in composition to that of the initial melt which produced the crystals as only a small amount of crystallisation had occurred compared to the overall bulk of the magma.

In the discussion of ion distribution this scheme will be followed:-

- a) distribution of the divalent ions (Mn^{2+} , Fe^{2+} , Co^{2+} , Ni^{2+}) between olivine and pyroxene crystals and the groundmass. Each locality from which samples were obtained will be discussed separately.

- b) distribution of the trivalent ions (Sc^{3+} , Cr^{3+})
- c) distribution of titanium

In part d) graphs will be presented on which are plotted $\ln k$ Vs octahedral site preference energy (O.S.P.E.), where k is -

$$\frac{[X]_{\text{crystal}}}{[X]_{\text{groundmass}}}$$

and the octahedral site preference energy values are those given by Dunitz & Orgel (1957), for olivine to groundmass and pyroxene to groundmass distributions. In each graph the error bars for the partition coefficients were obtained using the relationship given in section viii) of Chapter 3.

a) Distribution of Divalent Ions

Reunion Island Samples

Results are presented in Tables 1 and 1A and plots of $\ln k$ Vs O.S.P.E. in figs. 5 and 6.

The results are of the expected order of magnitude except for cobalt in the groundmass of sample RE331 which is anomalously high. The reason for this high value is not known but it is thought that the sample was contaminated prior to the analysis being carried out. The groundmass material had already been separated when it was received for this work.

Figs. 5 and 6 show a linear relationship between $\ln k$ and O.S.P.E. for olivine to groundmass (RE331 and RE512) and clinopyroxene to groundmass (RE512) partition for the ions Mn^{2+} , Fe^{2+} , Co^{2+} , Ni^{2+} .

The k values agree with the few results that have been published on these rock types. Häkli & Wright (1967), in their study of Hawaiian lavas, obtained k values for Ni^{2+} , olivine to groundmass of 13.5-16.8; clinopyroxene to groundmass of 2.22-4.40 and for Fe^{2+} olivine to groundmass of 1.85-2.19.

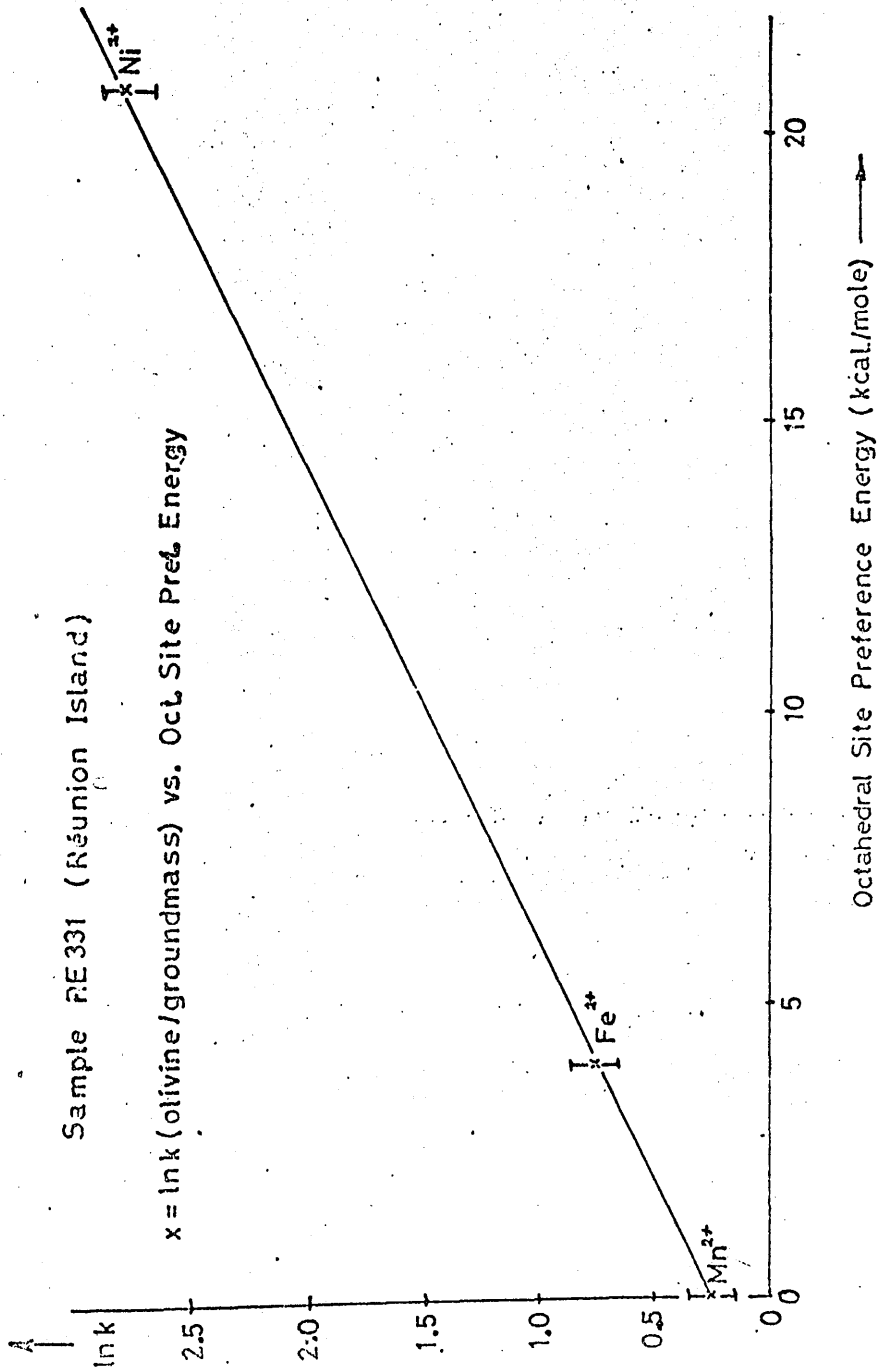


Fig. 5

Sample RE512 (Réunion Island)

x = ln k (olivine/groundmass) vs. Oct. Site Pref. Energy

• = ln k (pyroxene/groundmass) vs Oct.Site Pref. Energy

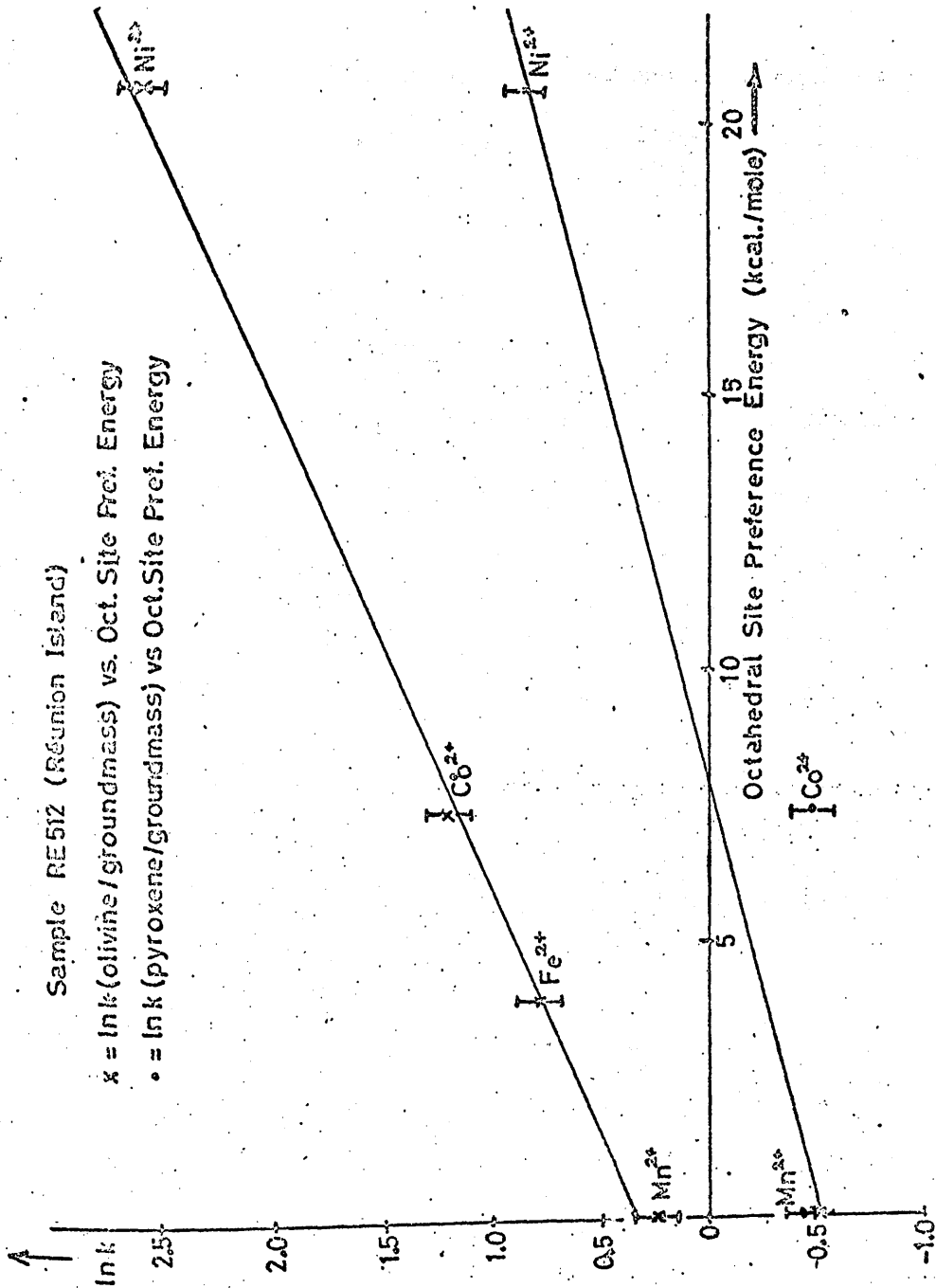


Fig. 6

British Solomon Islands Samples

Results are presented in Tables 2 and 2A and Fig. 7.

A linear relationship is again evident between $\ln k$ and O.S.P.E.

The k values are slightly higher than the Reunion samples.

Juan Fernandez Islands Samples

Results are presented in Tables 3 and 3A and Figs. 8

and 9. The plots again show the linearity between $\ln k$ and O.S.P.E.

although the k values are significantly lower than those of Reunion and British Solomon Islands.

Hawaiian Samples

Results are presented in Tables 4 and 4A and Figs. 10-12.

Again correlation of $\ln k$ with O.S.P.E. is evident. Manganese k

(pyroxene to groundmass) values lie above the least squares line for samples C71 and C129. As Mn^{2+} has zero crystal field stabilisation energy, this relative enrichment of manganese into the pyroxenes is probably due to ionic radii differences.

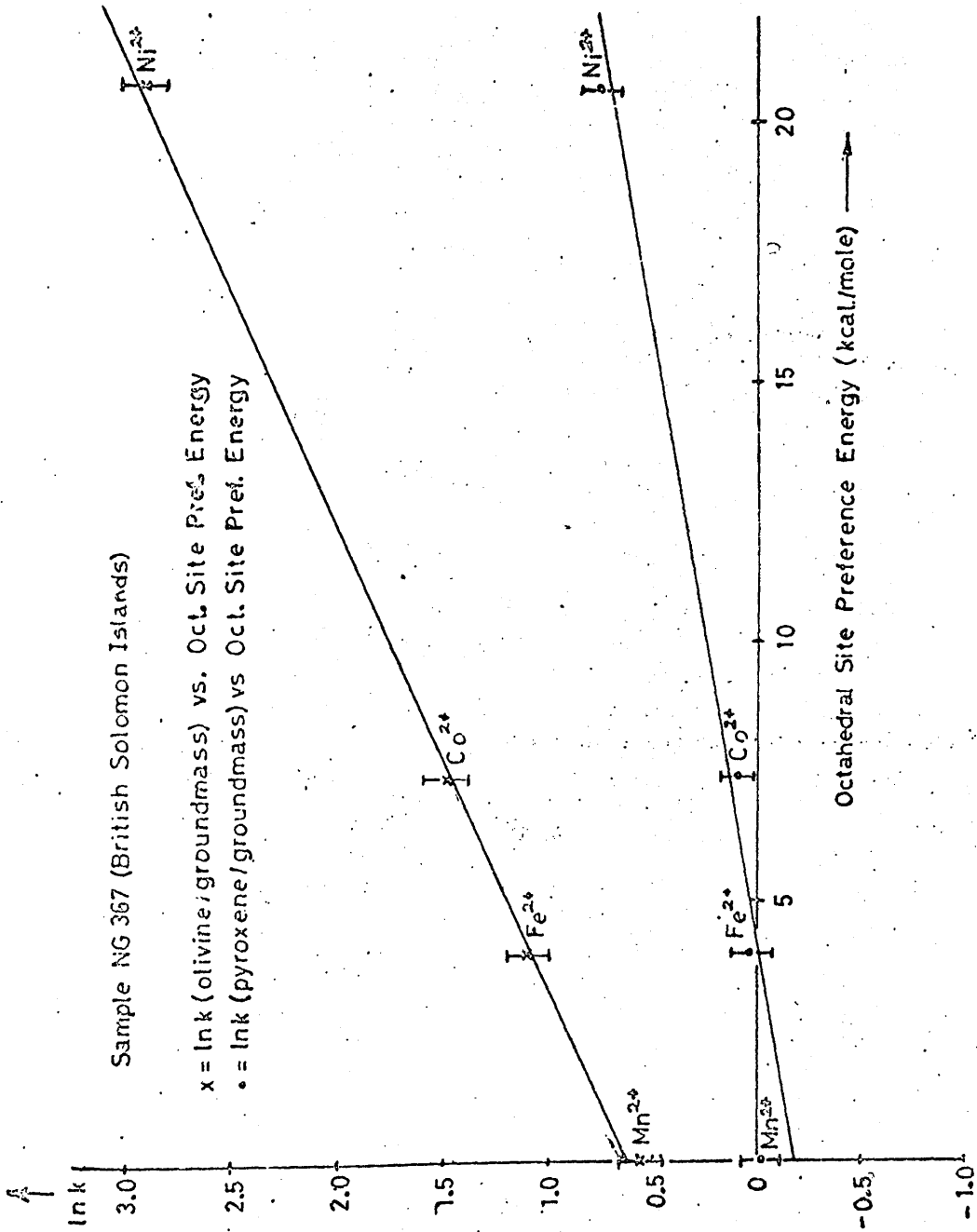


Fig. 7

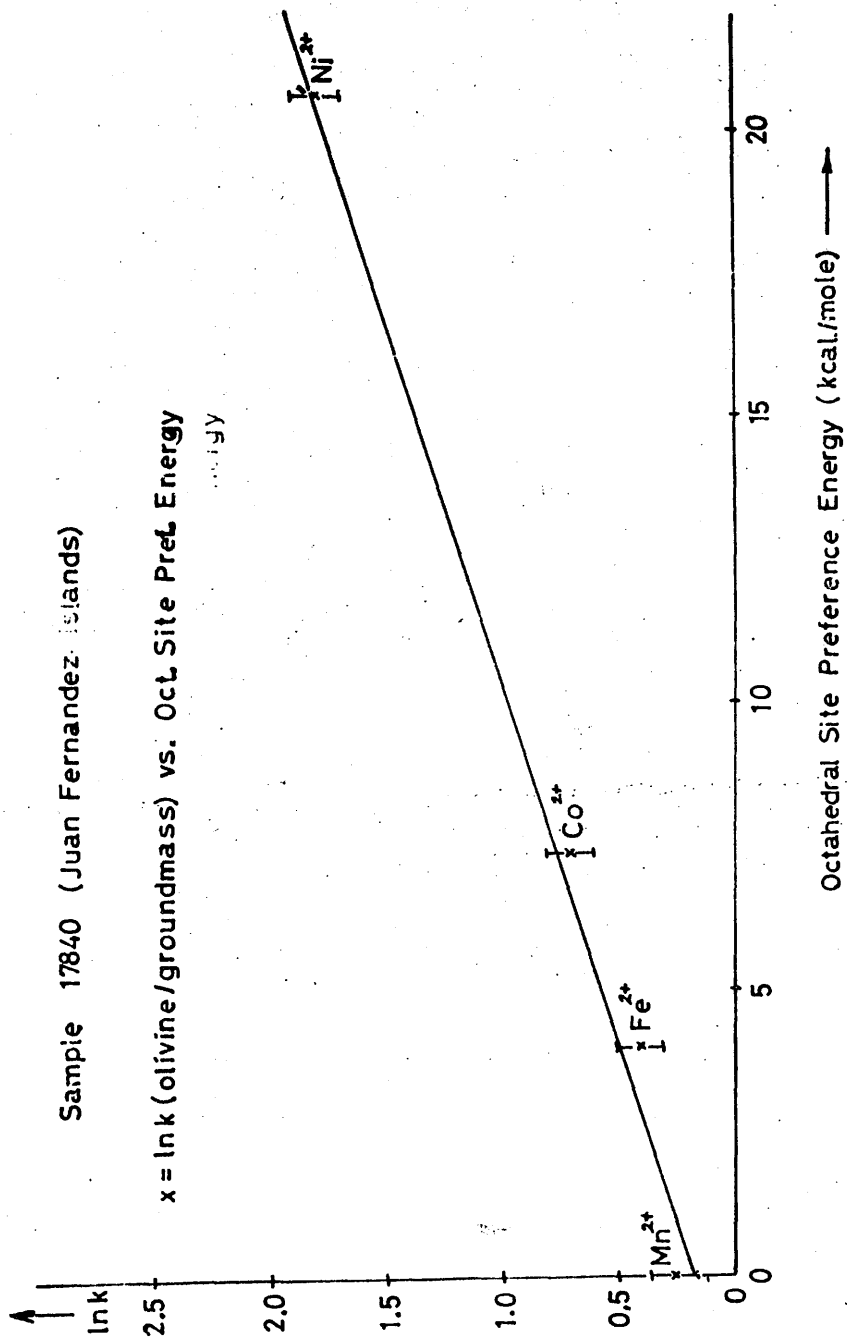


Fig 8.

Sample 17901 (Juan Fernandez Islands)

$x = \ln k$ (olivine/groundmass) vs. Ocl Site Pref. Energy

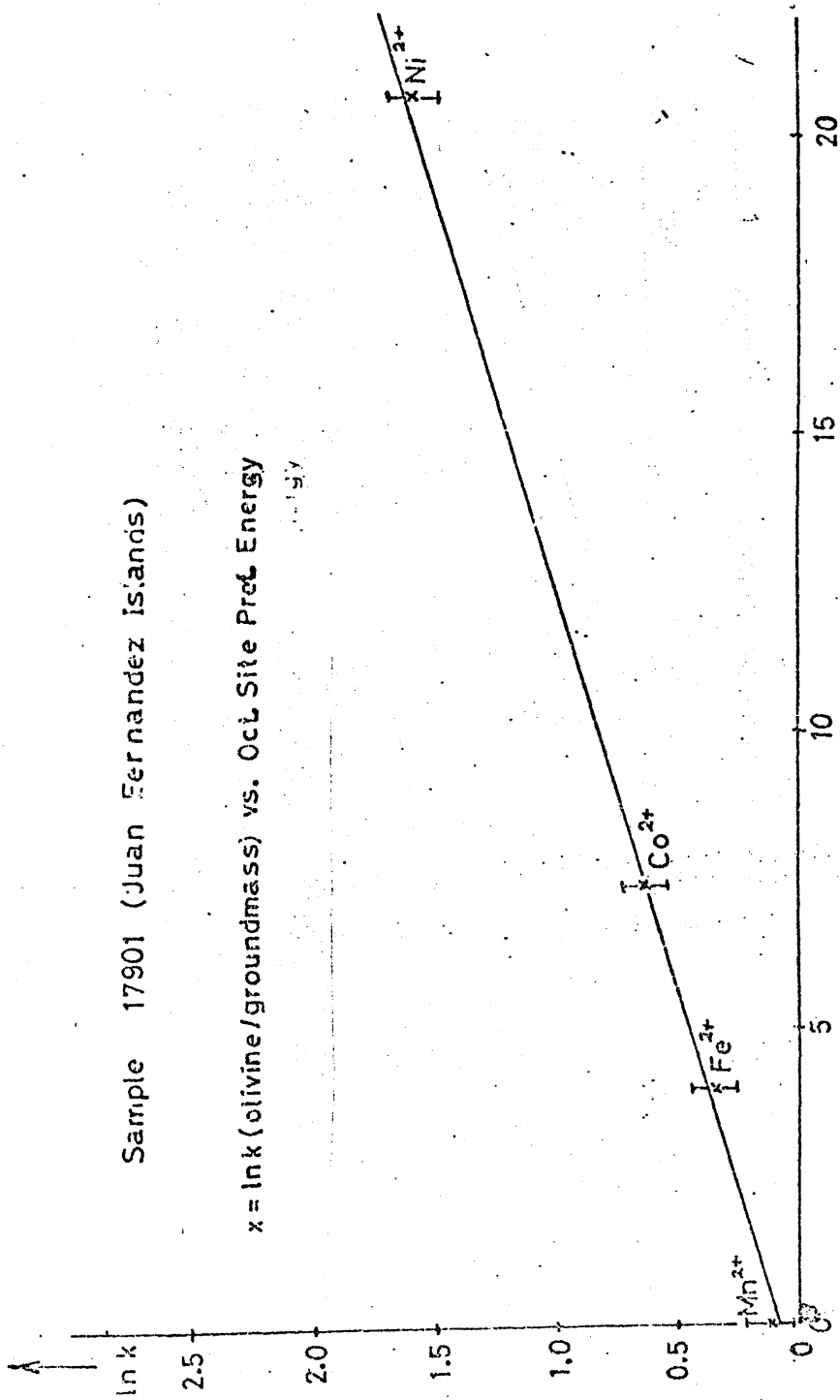


Fig. 9

Sample C₇₁ (Hawaiian Islands)

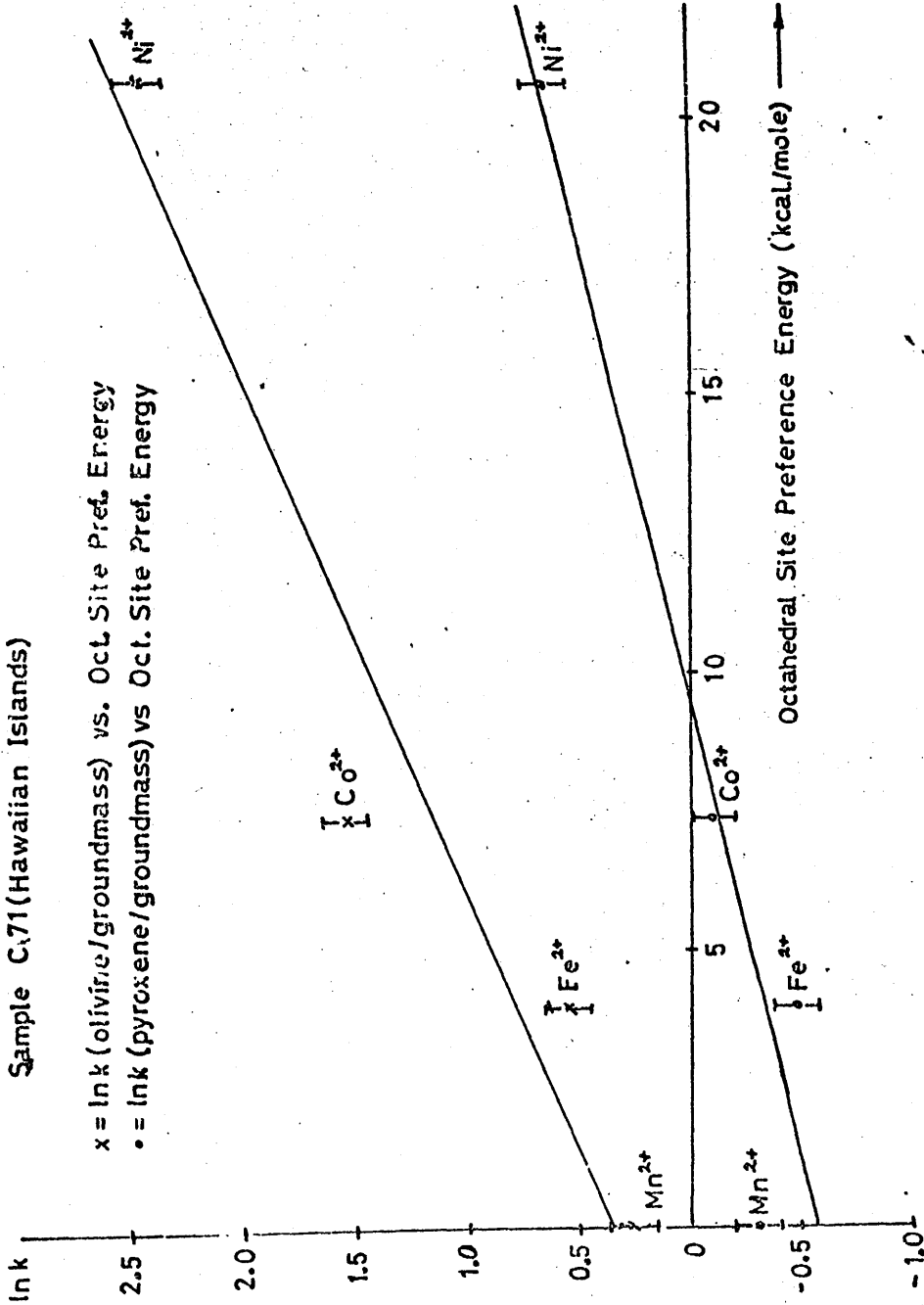


Fig. 10

Sample C 129 (Hawaiian Islands)

$x = \ln k$ (olivine/groundmass) vs. Oct. Site Pref. Energy
 $\bullet = \ln k$ (pyroxene/groundmass) vs. Oct. Site Pref. Energy

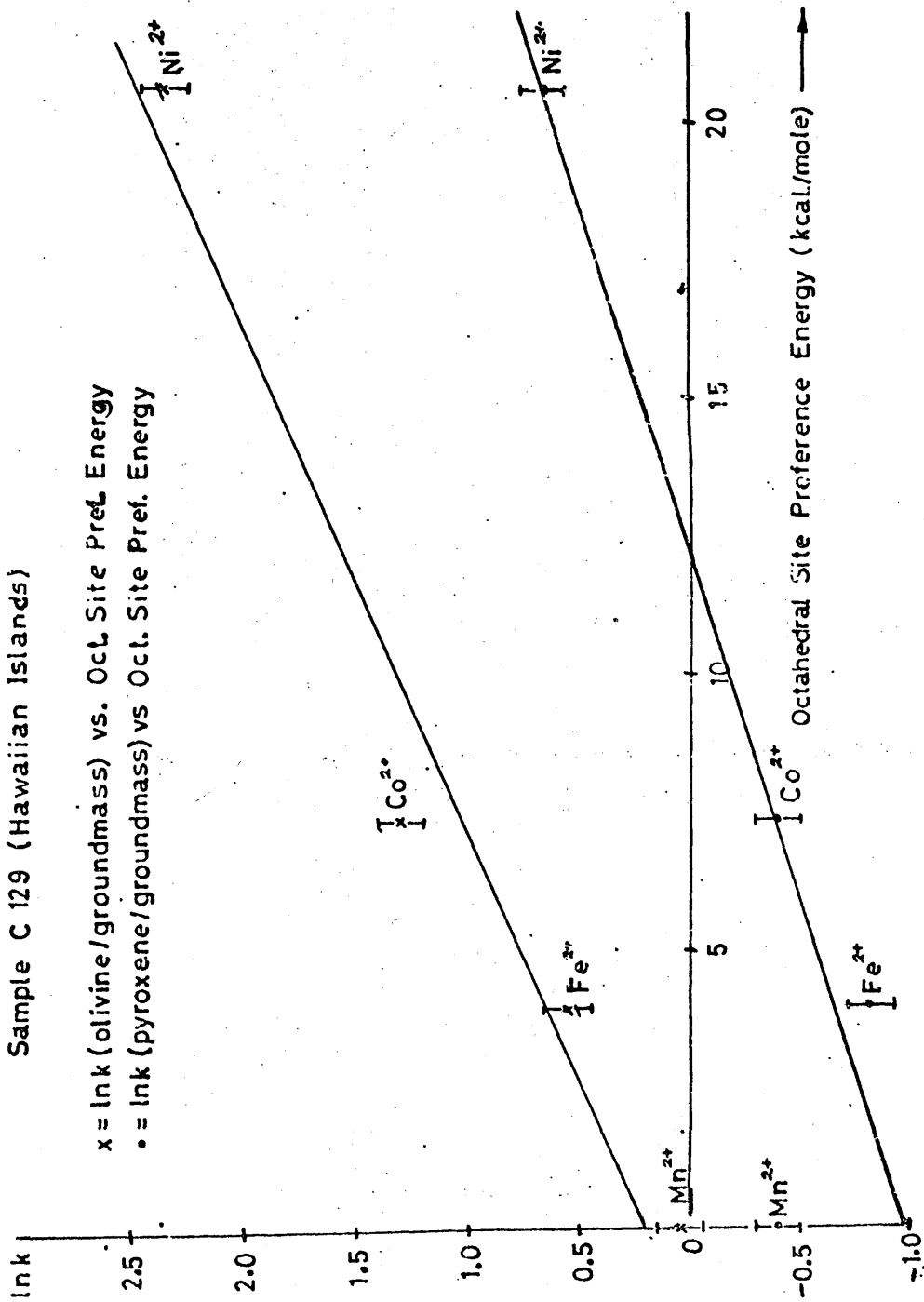


Fig. 11

Sample C 209 (Hawaiian Islands)

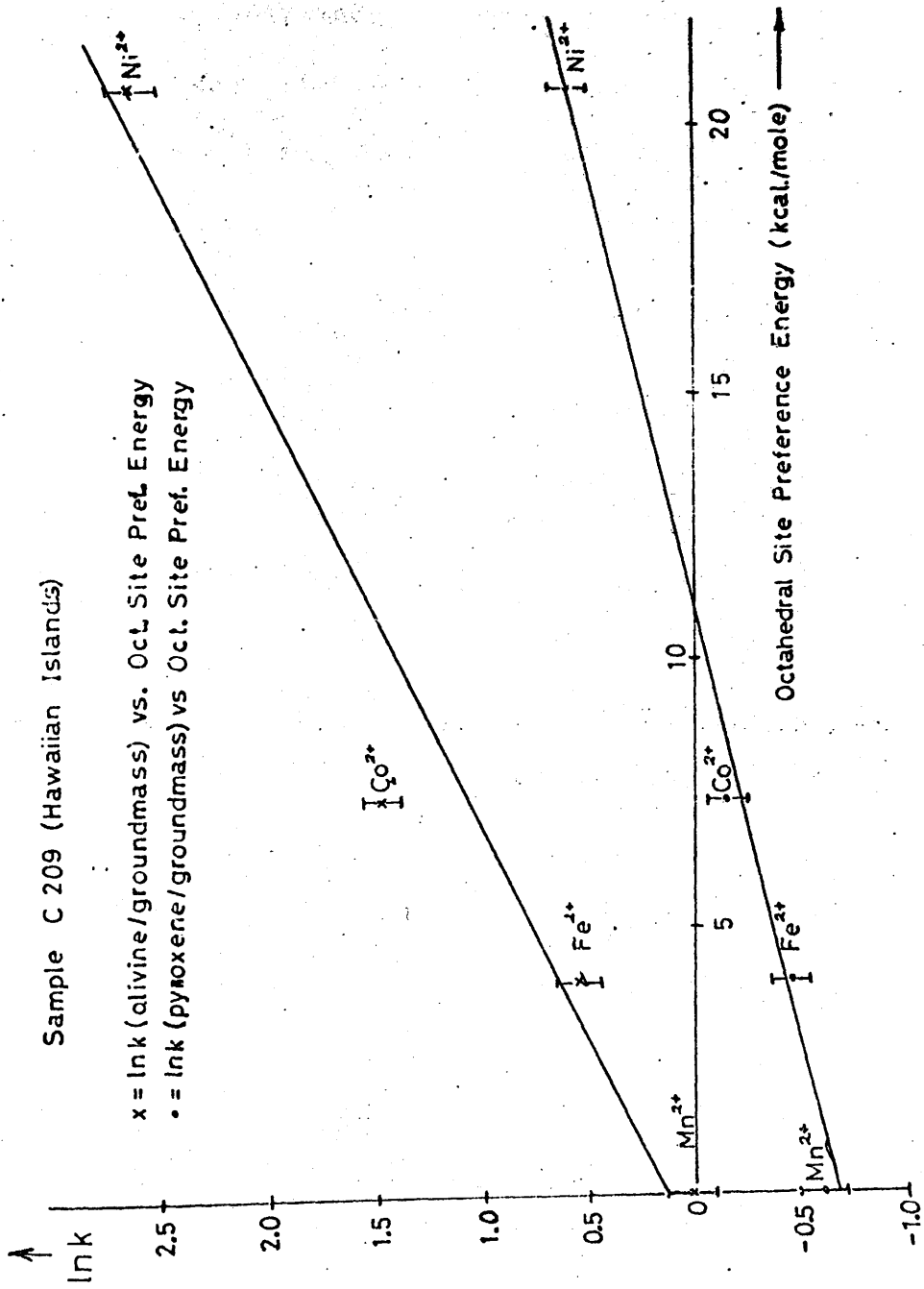


Fig. 12

As will be shown, this effect is evident for the manganese partitioning into pyroxenes in the majority of samples investigated (eight of eleven samples). The cause of this relative enrichment of manganese would merit further detailed study.

The k values found for these samples are slightly lower than the values obtained by Håkli & Wright (1967) in their study of Hawaiian lavas.

Iceland Samples

Results are given in Tables 5 and 5A and Figs. 13-15. Correlation of $\ln k$ and O.S.P.E. is again shown for samples 446 and 448 although Mn^{2+} partition in pyroxenes shows the same deviations from linearity as reported above for the Hawaiian samples.

Specimen 394 (an olivine basalt tuff) does not show good linearity of $\ln k$ Vs O.S.P.E. This sample is an unusual one, quite unlike any of the other samples in this study and should not be considered in any way typical of the results obtained (see Appendix 4, for description of the rock). The ferrous iron analysis for the groundmass is very low (1.04% Fe^{2+}).

The k values for samples 446 and 448 are in general agreement with other results.

Sample 394 (Western Iceland)

x = lnk (olivine/groundmass) vs. Ocl. Site Pref. Energy

• = lnk (pyroxene/groundmass) vs. Ocl. Site Pref. Energy

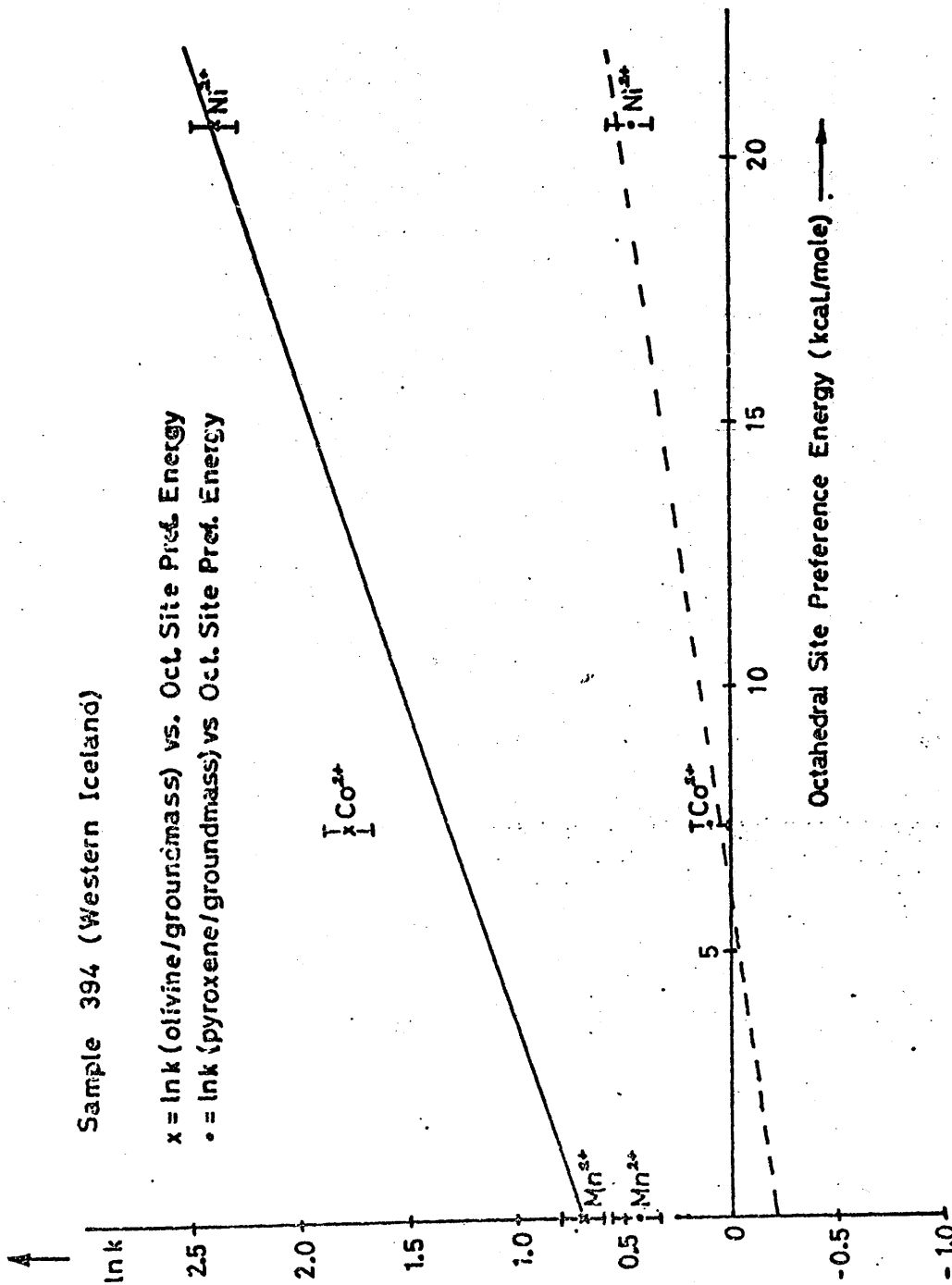


Fig. 13

Sample 446 (Western Iceland)

x = ln k (olivine/groundmass) vs. Oct. Site Pref. Energy
 o = ln k (pyroxene/groundmass) vs. Oct. Site Pref. Energy

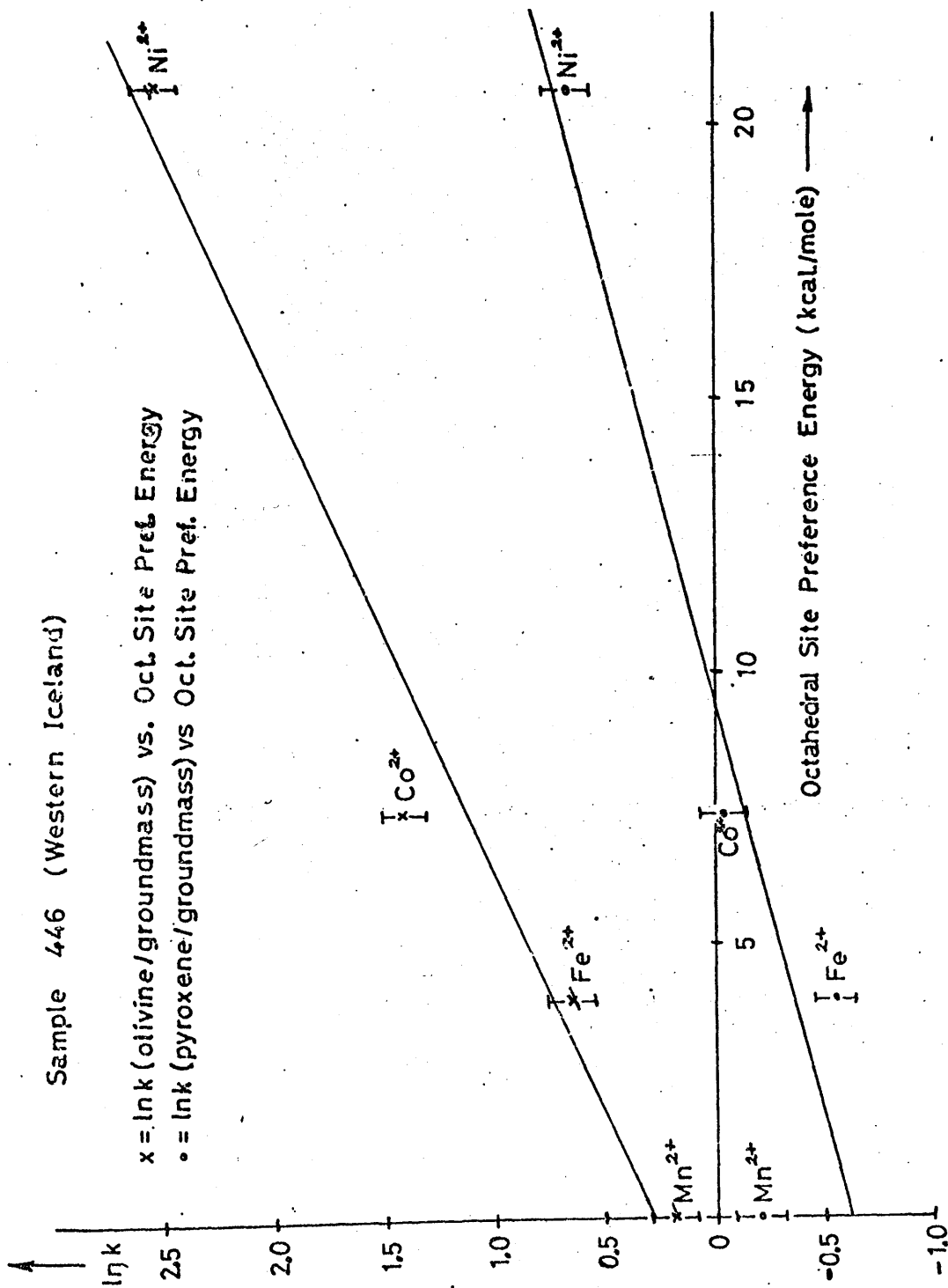


Fig. 14

Sample 448 (Western Iceland)

x = lnk (olivine/groundmass) vs. Oct. Site Pref. Energy
 • = lnk (pyroxene/groundmass) vs Oct. Site Pref. Energy

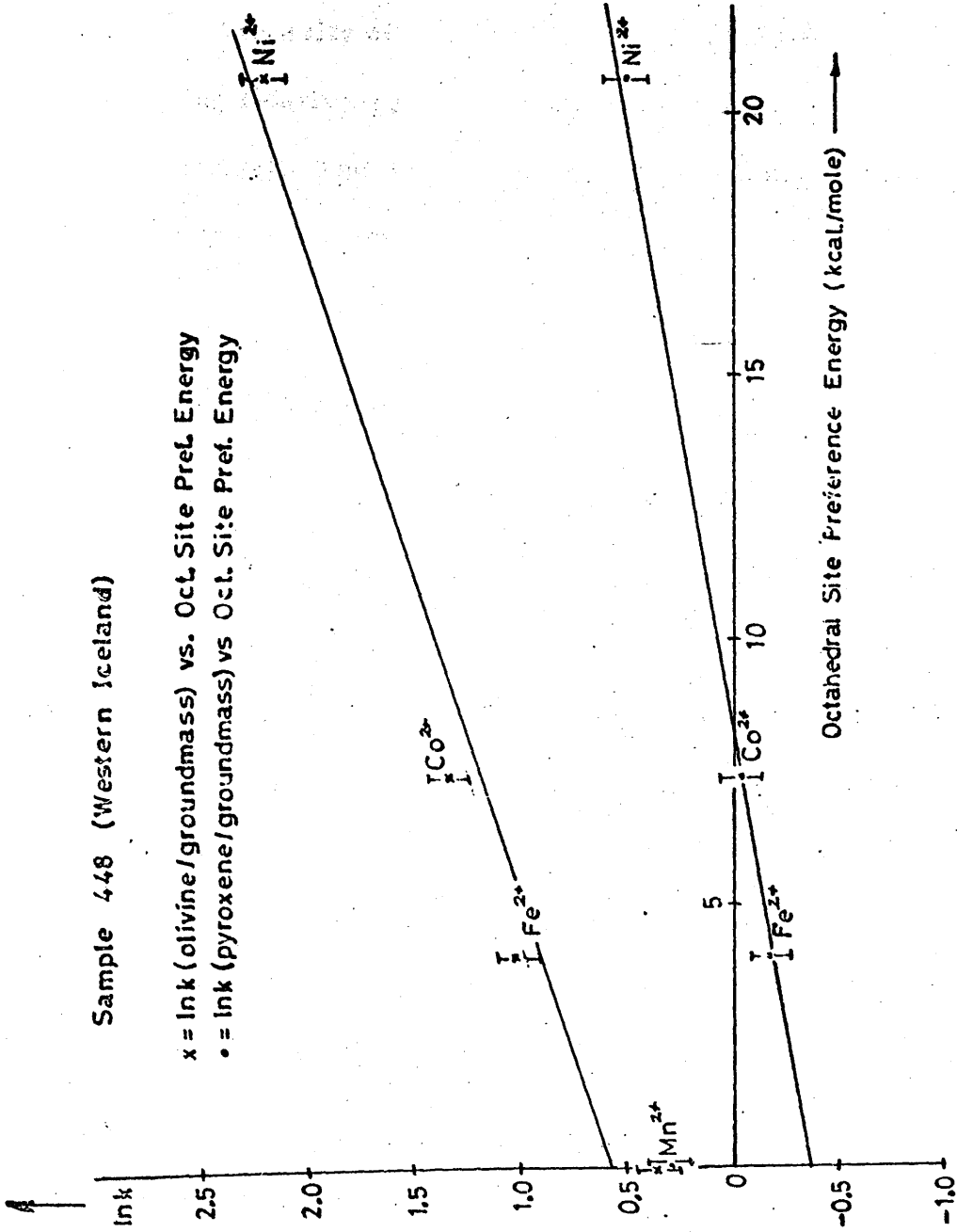


Fig. 15

Red Sea Islands Samples

The results are presented in Tables 6 and 6A and in Figs. 16-18.

Linearity of $\ln k$ Vs O.S.P.E. is again shown with Mn^{2+} again being relatively more concentrated in the pyroxenes (samples Z39A and Z64). The plot of the results for sample Z40 shows good linearity for both olivine to groundmass and pyroxene to groundmass partition.

Greenland Samples

Results are presented in Tables 7 and 7A and Figs. 19-22.

Linearity of $\ln k$ Vs O.S.P.E. is again indicated. The k values are similar to those obtained for other samples, except for L5 where the values are very much lower than expected (Ni^{2+} olivine/groundmass is only 2.68). The correlation of $\ln k$ with O. S. P. E. is not as good as for the other samples from this region which were investigated. In particular, the partitioning of Co^{2+} into olivine is greater ($k = 3.38$) compared with nickel. It is possible that the groundmass separated from the rock was imperfect and small crystals of minerals containing high concentrations of nickel (e.g. olivine)

Sample Z39A (Red Sea Islands)

x = ln k (olivine/groundmass) vs. Oct. Site Pref. Energy
 • = ln k (pyroxene/groundmass) vs Oct. Site Pref. Energy

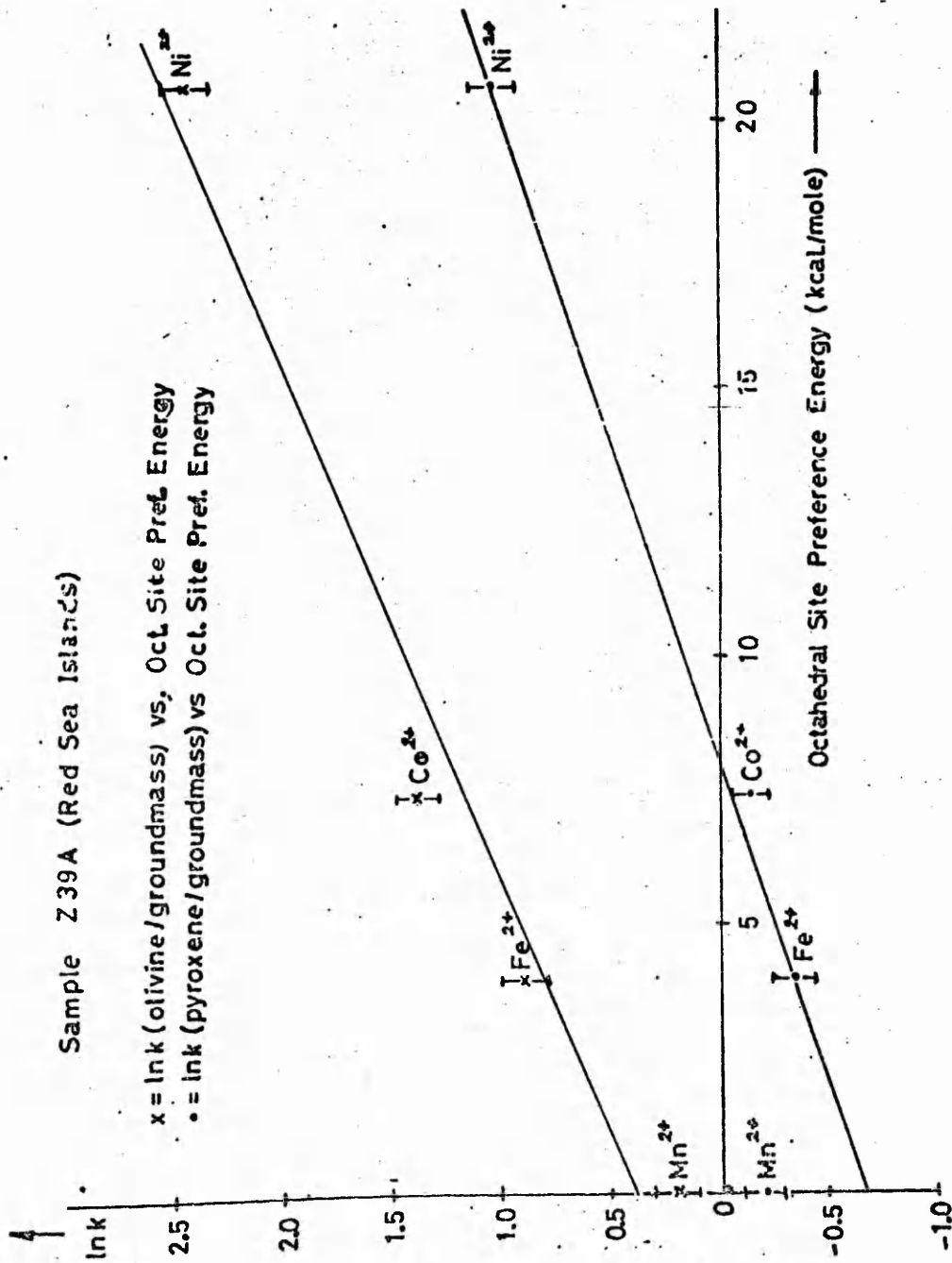


Fig. 16

Sample Z40 (Red Sea Islands)

x = lnk (olivine/groundmass) vs. Oct. Site Pref. Energy
 • = lnk (pyroxene/groundmass) vs Oct. Site Pref. Energy

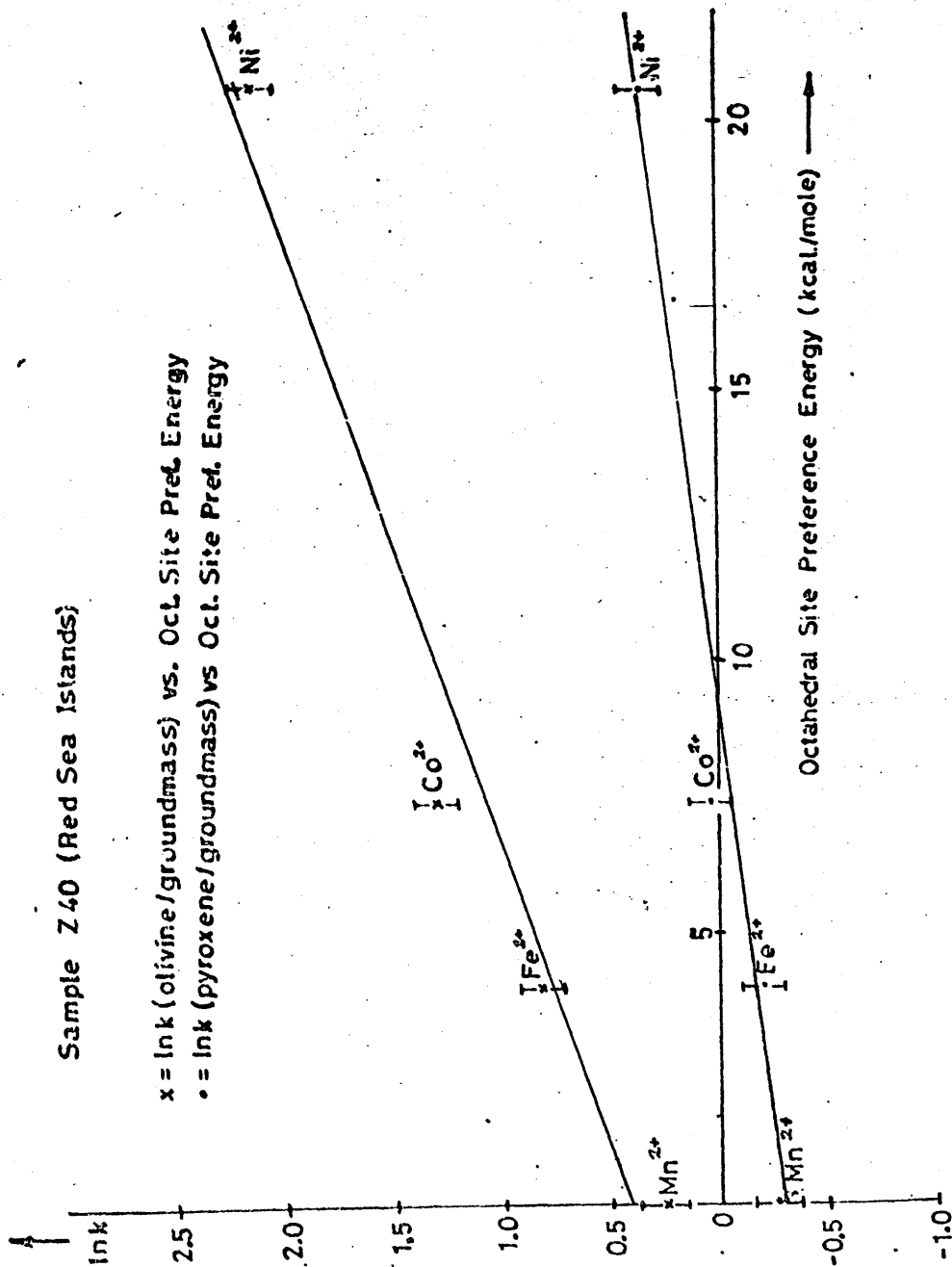


Fig. 17

Sample Z64 (Red Sea Islands)

x = ln k (olivine/groundmass) vs. Oct. Site Pref. Energy
 • = ln k (pyroxene/groundmass) vs. Oct. Site Pref. Energy

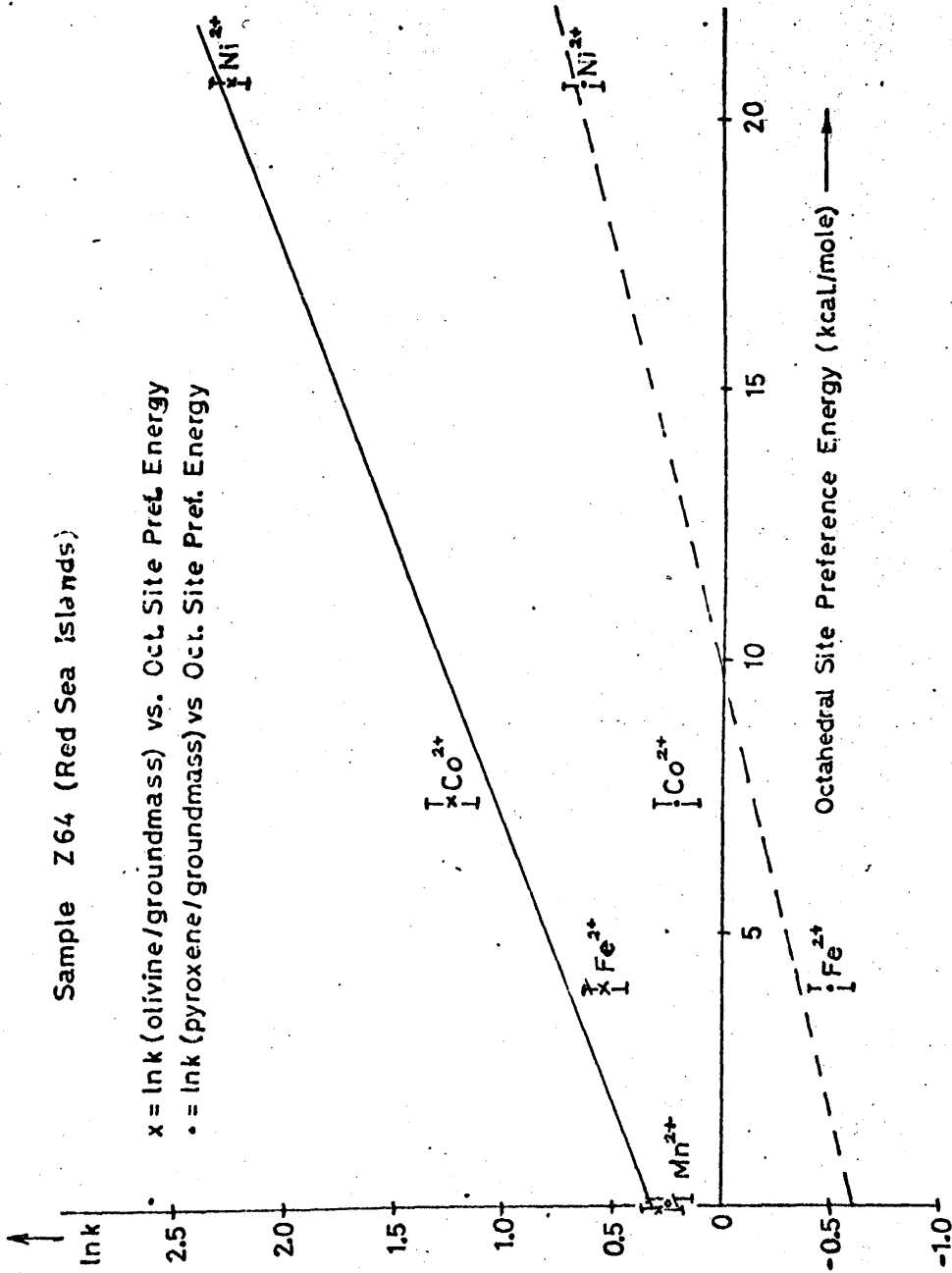


Fig. 18

Sample L5 (West Greenland)

$x = \ln k$ (olivine/groundmass) vs. Oct Site Pref. Energy

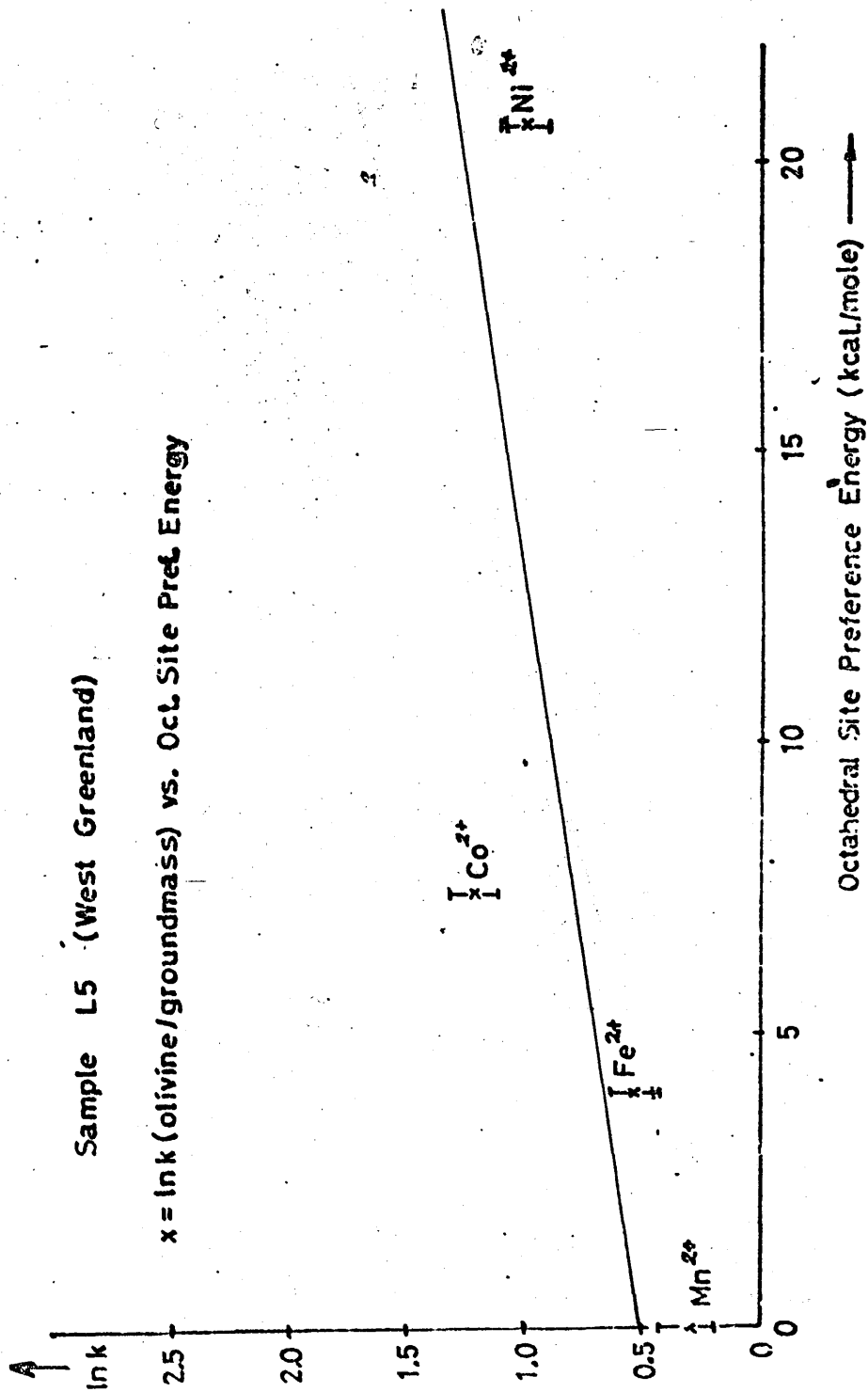


Fig. 19

Sample L7 (West Greenland)

$x = \ln k$ (olivine/groundmass) vs. Oct Site Pref. Energy

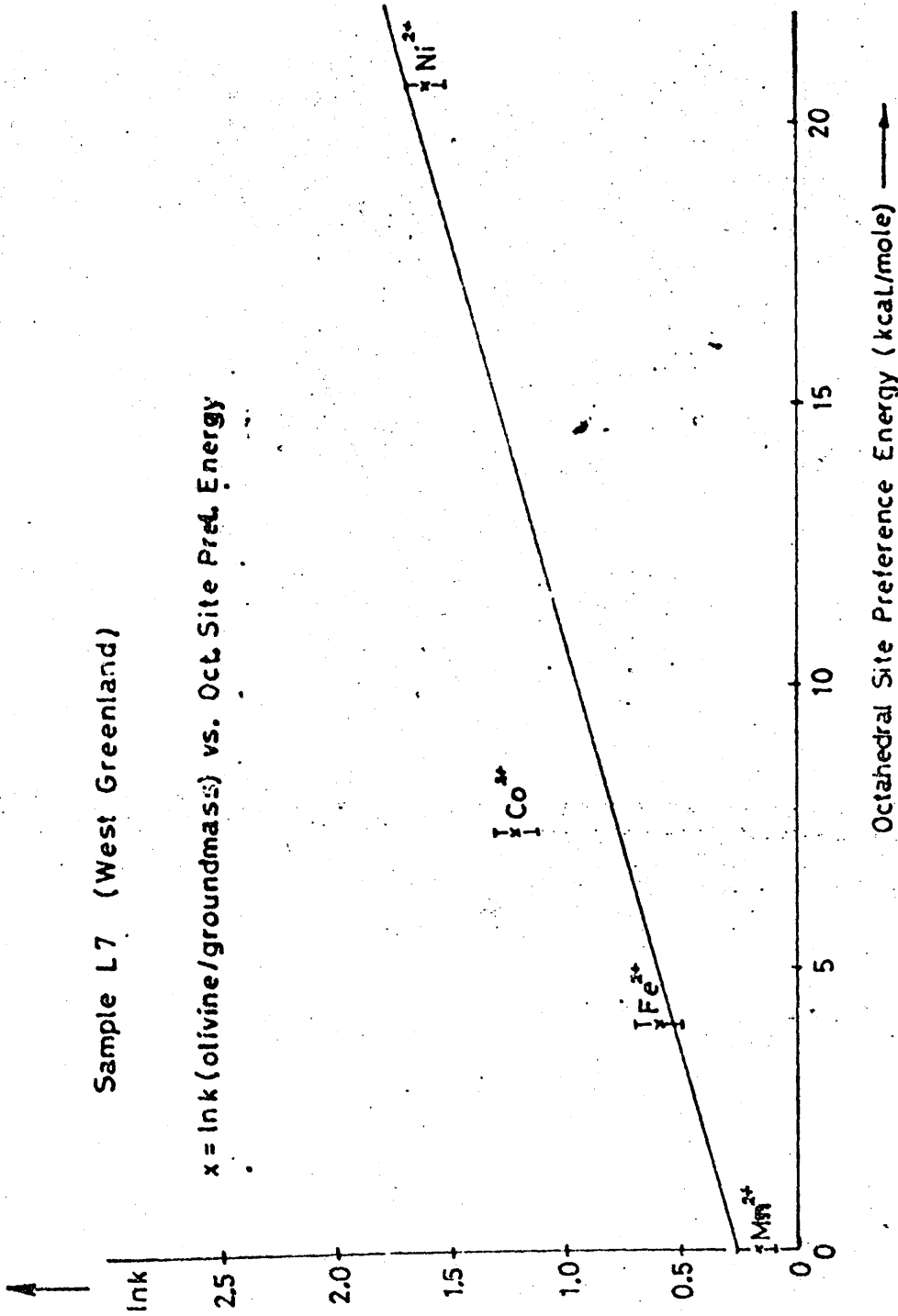


Fig. 20

Sample 120 (West Greenland)

$x = \ln k(\text{olivine/groundmass})$ vs. Oct. Site Pref. Energy

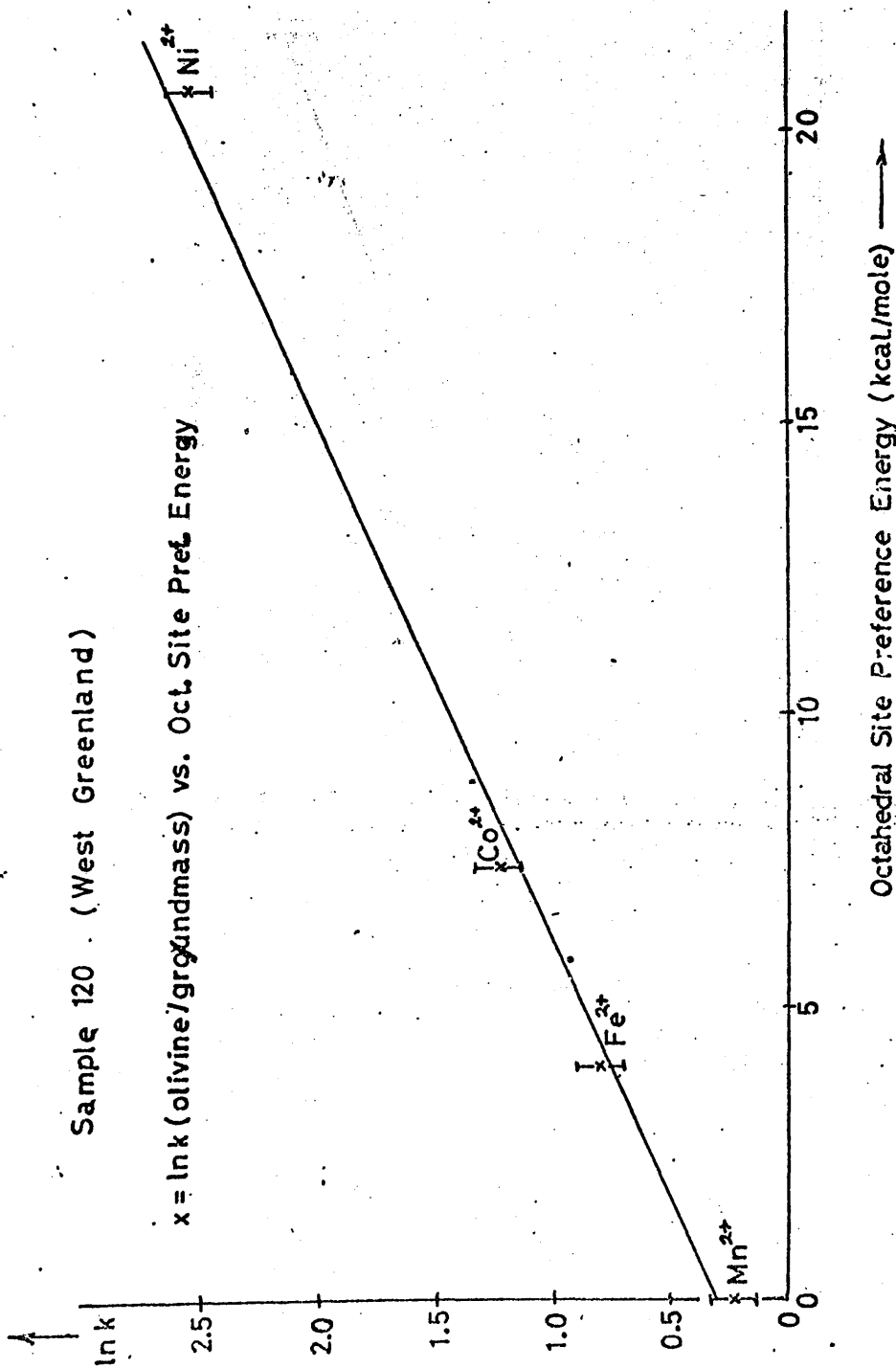


Fig. 21

Sample B5 (West Greenland)

$x = \ln k$ (olivine/groundmass) vs. Oct Site Pref. Energy

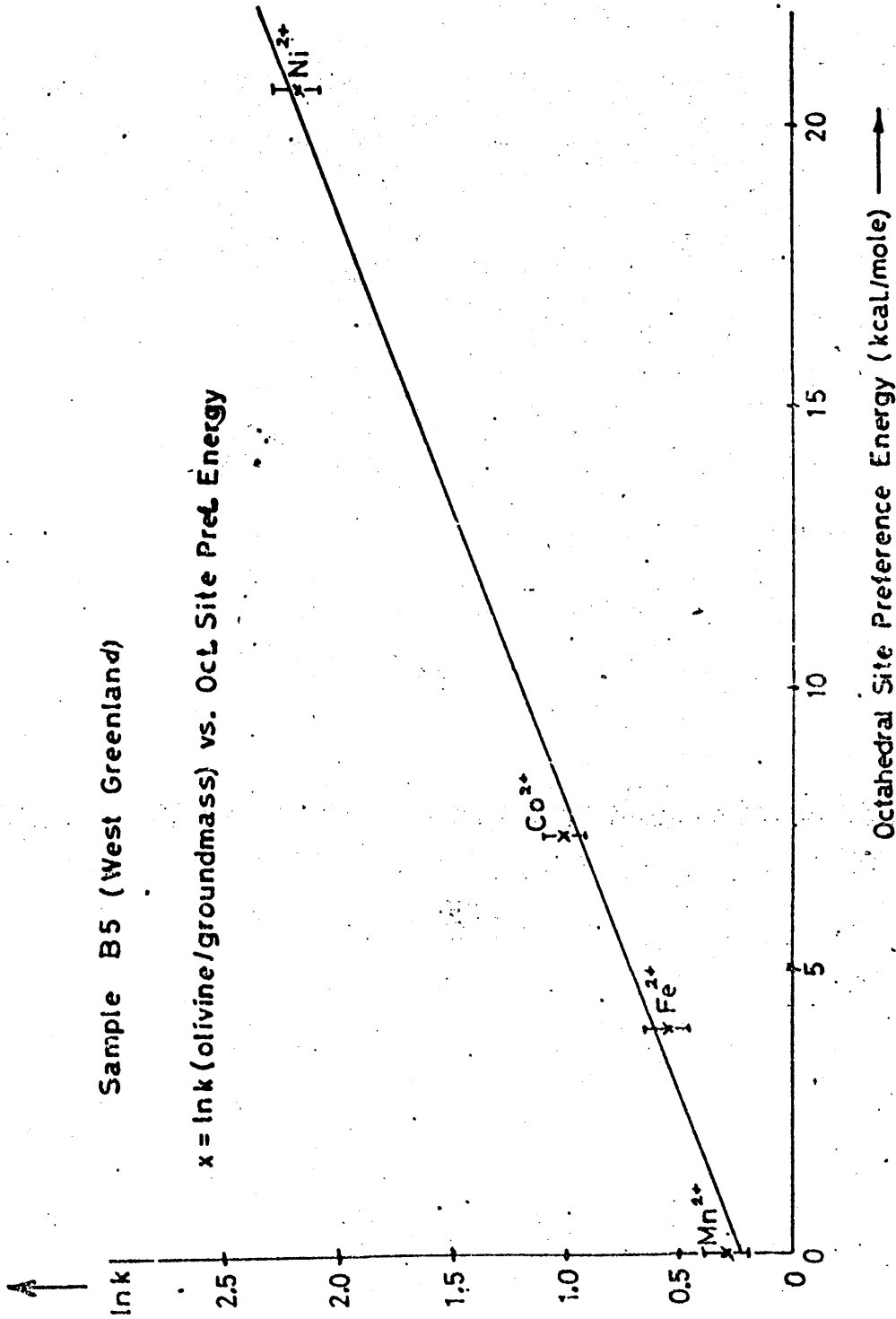


Fig. 22

contaminated the separated materials. A repeat separation and analysis was carried out but the analyses yielded similar results.

The results of the analyses of the separated materials are given in Table 1. The analyses show that the manganese concentration in perthite is about 10% of the groundmass. The linearity of the graphs of D versus C for Mn^{2+} , Fe^{2+} and Ni^{2+} partition between groundmass and perthite help to confirm the data obtained in this study. The distribution between clinopyroxene and groundmass was not made because only total iron content was determined and it was assumed that all the iron in the clinopyroxene was ferrous. The results of Hines (1971) in his study of trace metal behavior in the clinopyroxene of Kilauea Iki, Hawaii, implied the following partition coefficients relative to groundmass:

$$D_{Mn^{2+}} = 0.1; D_{Fe^{2+}} = 1.1; D_{Co^{2+}} = 3; D_{Ni^{2+}} = 10.0.$$

Although these values show the same general

Published Data

There are very few published results with which to compare the values obtained. Hakli & Wright (1967) analysed minerals and glasses from Hawaiian lavas for manganese, iron and nickel, using an electron microprobe. Figs. 23 and 24 show curves based on their results. The plots were made using the assumption that the manganese concentration in pumice is close to that in the groundmass. The linearity of the graphs of $\ln k$ VS O.S.P.E. for Mn^{2+} , Fe^{2+} and Ni^{2+} partition between groundmass and olivine help to confirm the data obtained in this study. Plots of metal ion distribution between clinopyroxene and groundmass could not be made because only total iron content was quoted; it was assumed that all the iron in the olivines was ferrous.

Gunn (1971) in his study of trace metal behaviour in the basaltic lavas of Kilauea Iki, Hawaii, implied the following partition coefficients for olivine to groundmass:

$$Mn^{2+}, 1.0; Fe^{2+}, 1.1; Co^{2+}, 3; Ni^{2+}, 10.0.$$

Although these values show the same general trend as obtained in this work, the actual values are somewhat different. In particular, the iron partition coefficient is much lower than the values

Sample M21-26 (Makapuhi Lava)

Solidified at 1120°C

ln k (olivine / groundmass) vs. Oct. Site Pref. Energy

Data from Häkli and Wright, G.C.A. 31, 877 (1967)

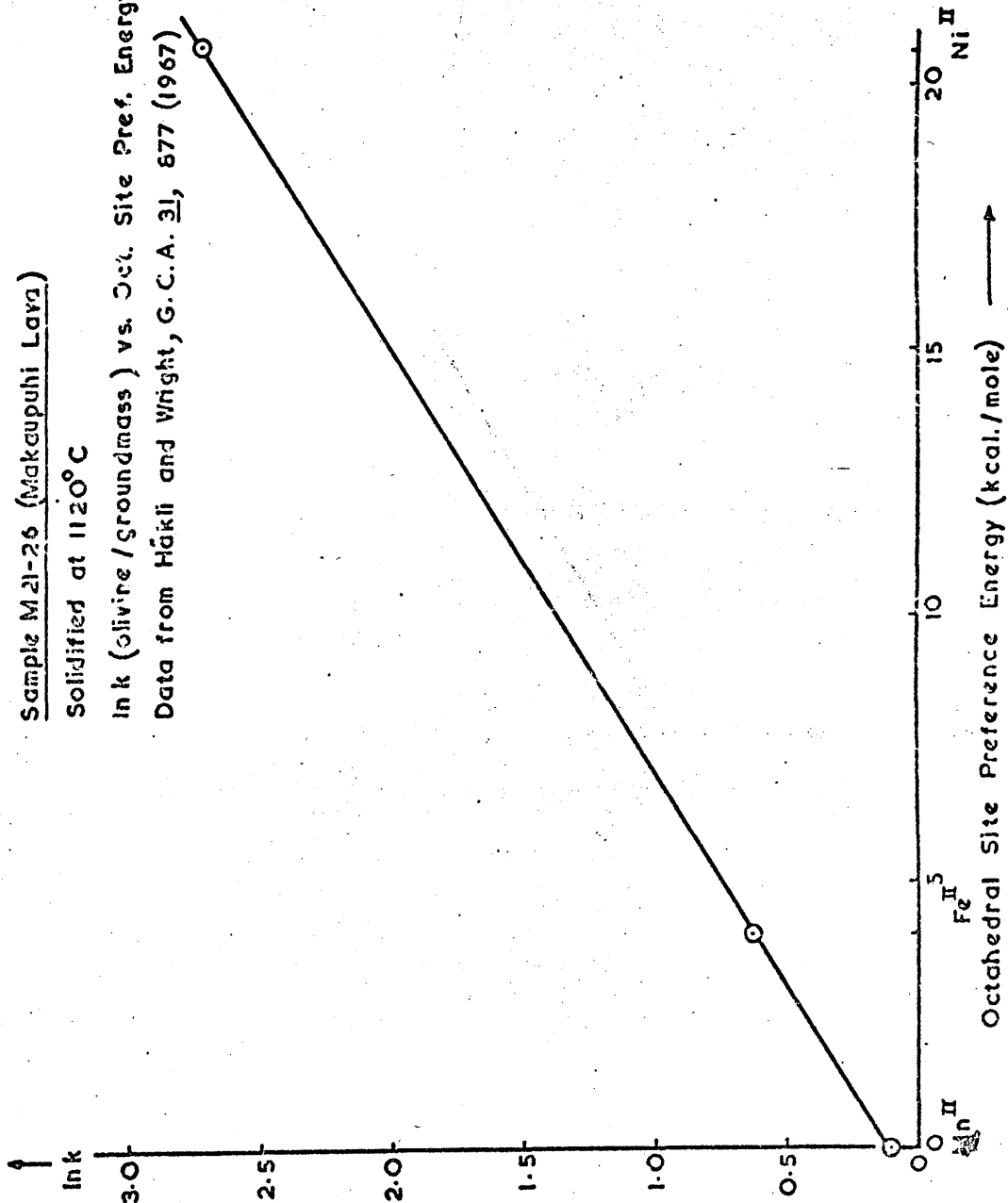


Fig. 23.

Sample M-12 (Makaopuhi Lava)

Solidified at 1160°C

ln k (olivine / groundmass) vs. Oct. Site Pref. Energy

Data from Häkli and Wright G.C.A. 31, 877 (1967)

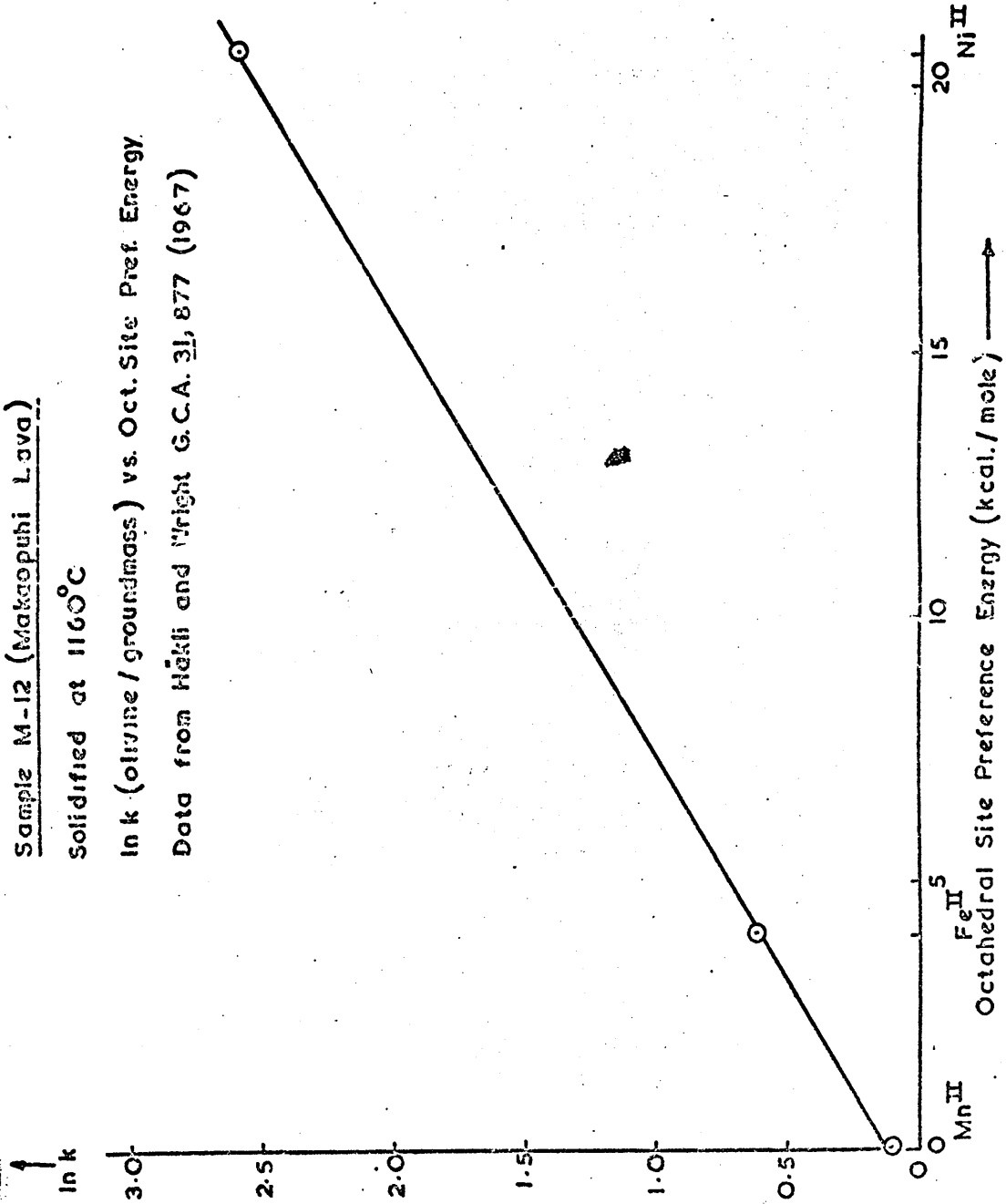


Fig. 24

found in this study. Further investigations into element distribution between minerals and co-existent magma need to be carried out.

... examined show the same general trends with ... basaltic or tholeiitic, (Fig. 25), but with the ... rocks which contain only olivine phenocrysts (17840, 17901, L6 and L7) out of six, ... partition coefficients are considerably lower than other samples. The possibility does exist that a major olivine and pyroxene may have a different ... or has different availabilities for ... This problem merits much further investigation. ... more information on the nature of ...

Partitioning of trivalent ions

Correlation of Partition Coefficients with Magma Types

No correlation of partition coefficient values with alkalic and tholeiitic magma types is evident. Plots of $\ln k$ Vs O.S.P.E. for the partition of the transition metal ions between olivine and groundmass, and clinopyroxene and groundmass for the rocks examined show the same general trends whether the rocks are alkalic or tholeiitic, (Fig. 25), but with the exception of some of the rocks which contain only olivine phenocrysts. In four examples (17840, 17901, L5 and L7) out of six, the values for the partition coefficients are considerably lower than for the other samples. The possibility does exist that a magma which is crystallising olivine and pyroxene may have a different structure in some respects or has different availabilities for the various cation sites. This problem merits much further investigation in order to elucidate more information on the factors involved in element partitioning.

b) Distribution of trivalent ions

Partition data for two trivalent ions were obtained. The clinopyroxene structure can accommodate trivalent ions, unlike olivine, as discussed above. The higher O.S.P.E. of Cr^{3+} (37.7 k cal/mole) is

Composite Graph, Ink vs O.S.P.E.

- = olivine / groundmass
- - = olivine / groundmass, cpx. free samples
- = clinopyroxene / groundmass

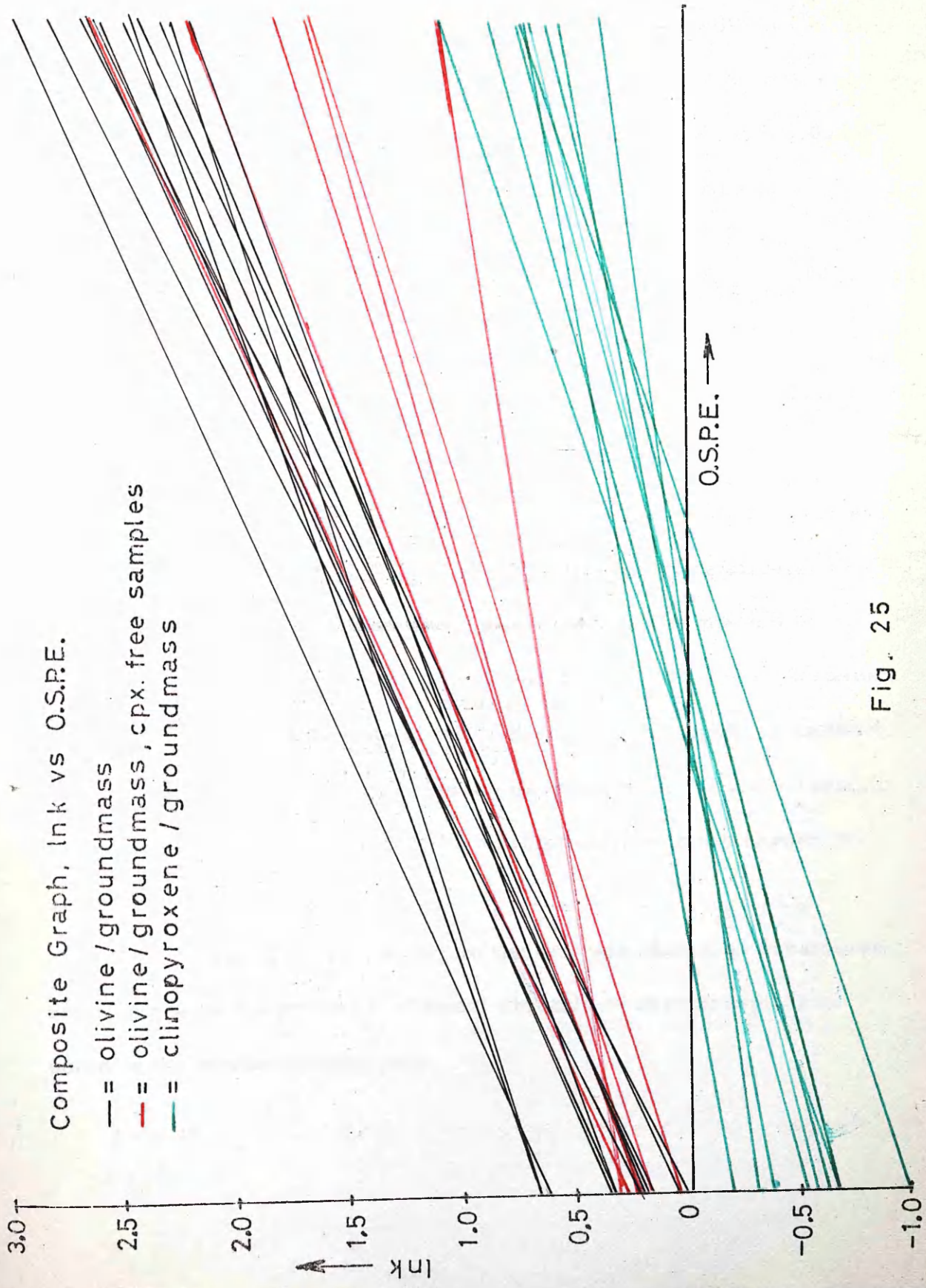


Fig. 25

manifested by its higher partition coefficient compared with Sc^{3+} (O.S.P.E. = 0). k values for Cr^{3+} distribution between pyroxene and groundmass range from 4.72-14.27, with a mean of 7.99 ± 3.00 (the exceptionally low partition coefficient for C129, pyroxene to groundmass, of 2.74 has been excluded from the calculation). k values for Sc^{3+} partition between clinopyroxene and groundmass range from 1.83-3.44, with a mean of 2.47 ± 0.50 .

Gast (1968) estimated a k value for chromium partition between clinopyroxene and liquid as 10.0. The values obtained experimentally in this work are in general agreement with this value.

The partition of Sc^{3+} into the olivines is relatively constant with k values ranging from 0.13-0.22, with a mean of 0.15 ± 0.02 . These values probably reflect a constant level of scandium present in the olivine as impurities, although this impurity is unlikely to be chrome spinel since the scandium content of the olivines remains fairly constant and does not vary sympathetically with the chromium content.

The Cr^{3+} partition into the olivines cannot be considered reliable due to the presence of small crystals of chrome-spinel in some of the olivine phenocrysts.

(c) Distribution of Titanium

Titanium was not detected in any of the olivines investigated. The partition coefficient for titanium (clinopyroxene to groundmass) ranges from 0.33-1.33, with a mean of 0.77 ± 0.29 . While these values are compatible with titanium being present as the Ti^{4+} with an O.S.P.E. of 0, rather than the Ti^{3+} ion with an O.S.P.E. of 6.9 kcal/mole, the partitioning of titanium between clinopyroxene and groundmass and the oxidation state of the ion require much further study before firm conclusions can be drawn.

III. Conclusions

The results from this study may conveniently be summarised in two sections. In the first section accurate analyses have been obtained on the transition metal content of basic volcanic rocks from a variety of geographical locations, thus adding to our knowledge of elemental abundances in rocks. Neutron activation analysis has been shown to be an excellent method for the determination of a range of elements in small samples of rock material. (Dale, Henderson & Walton, 1970). The results obtained for a number of international standard rocks show that neutron activation analysis should be considered one of the most accurate and sensitive techniques available for the analysis of geological samples and accordingly it is surprising that this method has not been employed more widely, on a routine basis, in geochemical laboratories superseding, for example, the D.C. arc spectrograph. It is accepted that although the time involved in processing the sample is about the same for neutron activation and D.C. arc spectroscopy, a time-lag does exist in activation analysis (arranging and carrying out irradiation,

cooling time for the specimen) between receiving the sample and obtaining the results. In spite of this limitation, the higher accuracy, precision and sensitivity, combined with its relative simplicity, once the method has been established, should make neutron activation analysis more attractive for trace metal analysis in geological samples.

The second, and by far the most important section has dealt with transition metal concentrations in the components of basic volcanic rocks. Results were obtained for systems which have hitherto not been investigated. It has been shown that the non-spherical spatial distribution of the d electrons surrounding the transition metal ion exerts a major influence on the partitioning of the ion between olivine and clinopyroxene phenocrysts and the groundmass of basic volcanic rocks. (Henderson & Dale, 1970; Dale & Henderson, in press).

It has been demonstrated, for the first time, that a linear relationship exists between $\ln k$, where k , the partition coefficient, is defined as -

$$\frac{[M]_{\text{crystal}}}{[M]_{\text{groundmass}}}$$

M being a transition metal ion and the octahedral site preference

energy (O.S.P.E.) of the ion, defined as the tetrahedral crystal field stabilisation energy minus the octahedral crystal field stabilisation energy (Dunitz & Orgel, 1957) for the partitioning of the divalent transition metal ions Mn^{2+} , Fe^{2+} , Co^{2+} and Ni^{2+} between olivine and groundmass and clinopyroxene and groundmass of a range of basic volcanic rocks. Zoning of the phenocrysts does not seem to effect the linearity of the plot of $\ln k$ Vs O.S.P.E., e.g. pyroxene, in sample NG367 exhibits zoning under the optical microscope.

No systematic variation of the slope of the line $\ln k$ Vs O.S.P.E. with either alkalic or tholeiitic basalt types is evident. However, those rock samples containing only olivine phenocrysts tend to have lower values for the partition coefficients.

Crystal field effects have also been shown to be significant in the partitioning of the trivalent transition metal ions, Sc^{3+} and Cr^{3+} , between clinopyroxene phenocrysts and the groundmass of a range of basic volcanic rocks.

These results fully support the theories of Williams (1959) and Burns & Fyfe (1964) regarding the importance of crystal field effects in determining the partition of transition metal ions in

igneous rocks.

These results are consistent with and can be explained by the assumption that these transition metal ions occupy tetrahedral and octahedral sites in the magma (Whittaker, 1967) while only octahedral or near octahedral sites are available in the olivine and pyroxene structures. It appears that the conclusion by Boon (1971) concerning the absence of Fe^{2+} ions in tetrahedral sites in the melt is not applicable to melts of basaltic composition investigated in this study.

The fractionation of nickel between olivine, clinopyroxene and glass and its application to the estimation of the temperature of crystallisation of molten rock has been the subject of studies by Håkli & Wright (1967) and Håkli (1968). The wide range of k values for nickel partition found in this study (olivine to groundmass, 2.68-18.5; clinopyroxene to groundmass, 1.42-2.86) fully supports the warning given by Håkli & Wright (1967) regarding the indiscriminate use of partition data for the estimation of crystallisation temperatures of other volcanic rocks. In particular, the effects of oxygen and water pressures and the concentrations of the various chemical components of the rocks on the partition coefficients are at present

unknown. Much valuable research could be carried out in the laboratory into the effects of temperature, pressure and composition on the partition coefficients of metal ions between mineral phases.

The problems of element partition in rocks merit much further investigation. In particular, the effects of chemical and mineral composition of the samples on the partition coefficient should be systematically studied. The occupancy of metal ions in the various available sites within crystals and molten rock is also amenable to investigation by element partitioning. This branch of geochemistry offers exciting and interesting lines of research which would greatly increase our knowledge of the chemistry of rocks and minerals.

APPENDIX 1

Covell's Method for Gamma-Ray Photo-Peak Area Determination

This technique (Covell, 1959) has been very widely used in calculating peak areas in gamma-ray spectrometry.

Fig. 1 shows an idealised gamma ray-peak, with peak position defined as containing a_0 counts, with each channel on the low energy side of the peak containing $a_1, a_2, a_3 \dots a_n$; similarly on the high energy side of the peak $a_1, b_2, b_3 \dots b_n$.

If P is the total area between n channels on either side of a_0 , and a line is drawn connecting the ordinate values of a_n and b_n , the area above this line is N then

$$N = P - Q$$

where Q is the area under the line.

$$P = a_0 + \sum_i^n a_i + \sum_i^n b_i$$

$$Q = \frac{(2n - 1)(a_n + b_n)}{2} + (a_n + b_n)$$

$$= (n + \frac{1}{2})(a_n + b_n)$$

Thus
$$N = a_0 + \sum_i^n a_i + \sum_i^n b_i - (n + \frac{1}{2})(a_n + b_n)$$

The Standard error is given by:-

$$(N) = \sqrt{N + (n - \frac{1}{2})(n + \frac{1}{2})(a_n + b_n)}$$

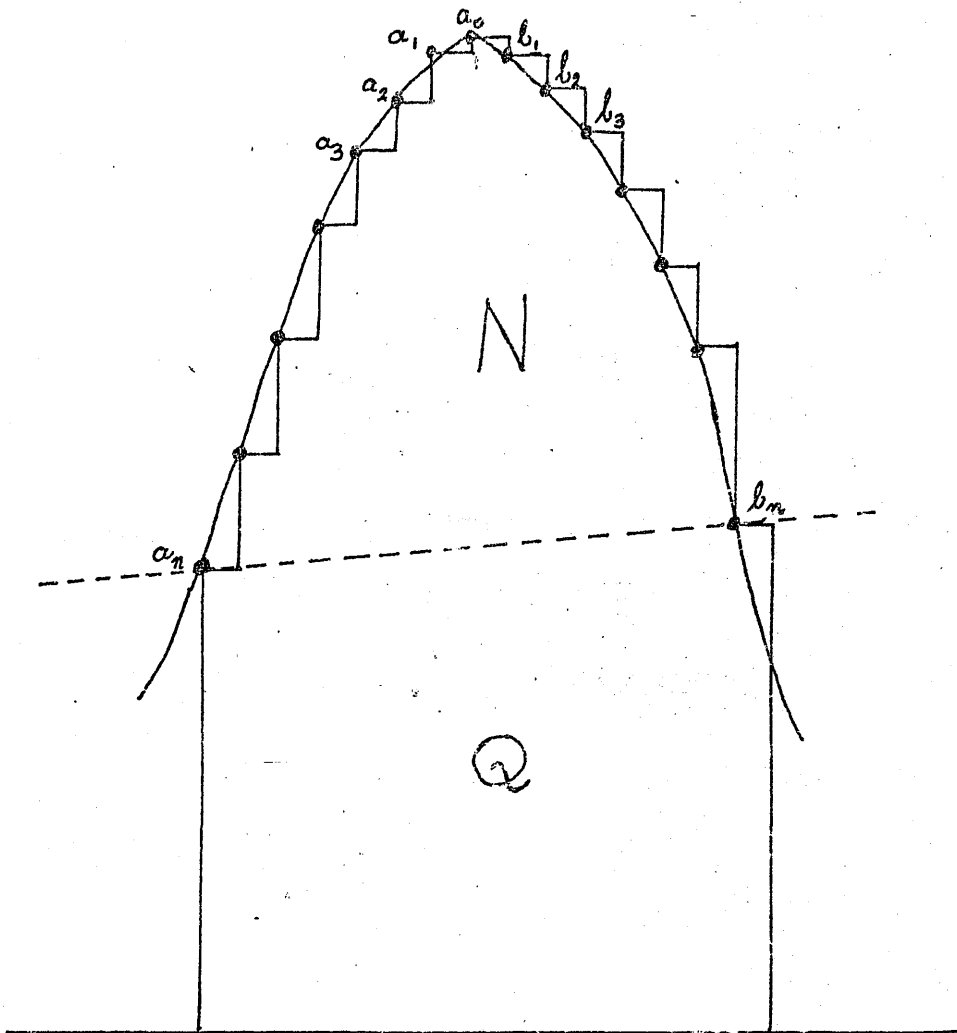


Fig. 1

Idealised Gamma Ray Peak

The expression for N was used throughout this work for determining peak areas.

n was chosen such that a_n and $b_n \approx \frac{1}{2} a_0$

Small changes in n did not affect the analysis to any significant extent.

APPENDIX 2

Description of Sample Preparation

The rock samples were crushed in a pneumatic piston and cylinder device to pea-sized pieces. These pieces were then ground to +100-120 mesh size using a Glen Creston Ball and Mill, the ball and mill being constructed from tungsten carbide. The sieving of the rock powder was carried out using nylon bolting cloth in order to prevent any metallic contamination. The +100-120 mesh fraction was washed with water and particles of dust which had adhered to the rock grains decanted off. This was repeated a number of times; finally the powder was washed with acetone and dried under a heat lamp.

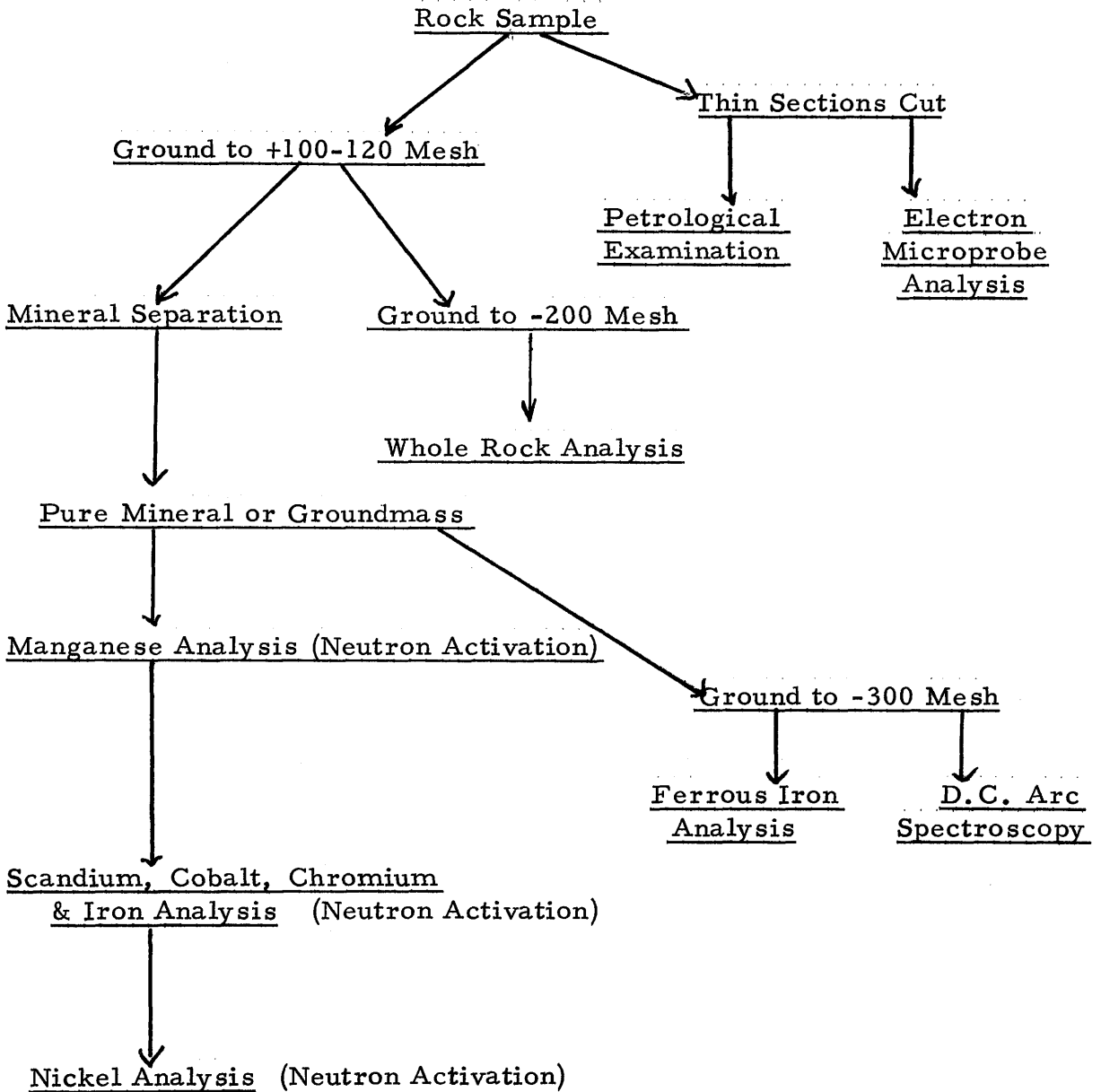
The rock powder at this stage was divided into two portions, one for mineral separation, one for whole rock analysis. The rock powder for whole rock analysis was further ground to -200 mesh.

Mineral Separation

Hand magnetic particles were separated from the sample using a small magnet wrapped in paper. Pure mineral and ground-mass separates were then obtained using a Franz Isodynamic Separator and heavy liquids (mostly diiodo methane). The final purification was

carried out by hand-picking the mineral grains under a X40
binocular microscope.

Scheme of Rock Analysis



Electron Microprobe Analysis

This description of the technique employed for the microprobe analysis of the samples was kindly provided by Mr. G. Taylor, University of Aberdeen.

Rock Sections:-

Chips were cut by diamond saw to approximately 1" x $\frac{3}{4}$ " x 1/8". One face was then ground on a rotating cast-iron lap using coarse grinding powder. The chip was washed, then ground by hand on a glass plate using carborundum powder. Specimens washed, dried and mounted on a glass slide using Araldite epoxy resin. The specimen was then ground to a thickness of 0.12 mm. on a rotating cast-iron lap.

The following procedure was carried out on a specially constructed polishing machine.

	Cast-iron plate - abrasive, Aloxite 95	- to	0.09 mm. thickness
(i)	Paper lap	- "	0.075 "
(ii)	"	- "	0.065 "
(iii)	"	- "	0.06 "
(iv)	"	- "	thickness unchanged
(v)	"	- "	"
(vi)	"	- "	"

(i) ...
 (ii) ...
 (iii) ...
 (iv) ...
 (v) ...
 (vi) ...

The specimen was then photographed and coated with a carbon film in a vacuum unit. The long edges of the glass slide were painted with a solution of colloidal graphite to ensure good electrical contact with the specimen stage in the probe.

Quantitative Analysis

Instrument used was the Cambridge Geoscan.

Pure metal or compound were used as standards.

A minimum of 20 x 10 second counts were recorded over various parts of the mineral under investigation and on the standard.

A monitor, an independently well-analysed compound, was always part of every analysis. The monitor follows the standard in every analysis and if the ratio of monitor counts to standard counts is found to be incorrect, the detector voltages are then rechecked.

The detector voltages were always set-up on the Cu K_{α} peak.

The counting procedure for each element was:-

Standard/Monitor/Sample A/Sample B etc./Standard

The monitor does not in itself form any part of the correction procedure for the unknown sample. It was used basically as a test, a means of checking the alignment of the instrument,

detecting and discriminating systems etc.

Once a full analysis had been carried, a comprehensive set of corrections are applied by computer. These are:-

- a) dead time
- b) background subtractions
- c) mass absorption
- d) atomic number
- and e) fluorescence

Detecting systems:

Gas flow proportional counters are used on both channels of the instrument. The gas is 97.5% argon, 2.5% carbon dioxide.

The counter is 0.0005 inch (0.0013 cm.) diameter nickel chrome.

Extremely thin windows are used, down to 10^3 \AA .

Table 1 is a typical set of counts obtained for iron in C129 olivine and augite.

Specimen No. C129 (Mr. Dob, GLASGOW) Sheet No. 1142 Date 1/9/69
 Kv 25 Beam I 50µA O.V. 1285V Counter - $\frac{\text{Standard}}{\text{Flow}}$ Slits - in / out Coating - Carbon
 Analyser - $\frac{\text{Energy}}{\text{Diff.}}$ E3.7 AEO.40 M.W. - $\frac{\text{Open}}{\text{Closed}}$ Xtal LIF 20 57° 30'
 Specimen I 3.4 x 20 x A Count Time 1085. Analysed Element - IRON T.F.T. 39µm

CHANNEL ONE

Standard	Monitor	Specimen Olivine A	Specimen Augite B	Specimen Augite C	Specimen Augite D	Specimen Olivine E	Standard Fe metal 10029
1 40935	5038	6356 6293	2086 2135	1862 2031	1987 1983	6172 6293	40569
2 40940	5057	6238 6331	2169 2149	1837 2178	1997 1888	6336 6298	40832
3 40916	4961	6420 6376	2061 2087	1781 2246	2154 1948	6361 6493	40749
4 40714	5083	6511 6368	2024 2087	1950 2203	2093 1960	6135 6231	40326
5 40586	5060	6248 6465	1843 2052	2076 2141	2227 1964	6163 6591	40337
6 40529	5285	6021 6483	1965 2227	2070 2169	2224 1983	6091 6406	40479
7 40447	5174	6497 6458	1891 2204	2053 2167	2141 1966	6080 6253	40527
8 40739	5085	6513 6488	1936 2207	2115 2126	2170 1911	6280 6231	40469
9 40767	5316	6610 6502	1933 2257	2115 2159	2193 1743	6141 6293	40749
10 40978	5117	6412 6319	1913 2026	2040 2138	2173 17115	6080 6297	40776
AV 40758.1	5118.6	6392.95	2068.6	2079.35	2009.8	6251.25	40581.3
HP 92 75	19	23	20	14	23	19	16
93 88	21	24	29	23	18	15	26
10 43 57	12	18	11	13	9	8	19
35 38	16	15	21	24	11	9	10
AV 65.125	16.875	24.125	15	15.5	15.5	23.375	40667.2

TABLE I

Counts obtained for Iron in C129 Olivine and Augite using Electron Microprobe

APPENDIX 4

Description of Rock Samples Investigated

All samples investigated were basalts with phenocrysts of olivine and clinopyroxene in a fine-grained groundmass. Some of the phenocrysts were zoned (e.g. NG 367). However, the zoning does not seem to make any difference to the *lnk* - O.S.P.E. linearity.

Reunion Island, Indian Ocean

(Lacrois^x~~e~~, 1912; Upton & Wadsworth, 1966)

Two samples were obtained:-

- RE 331: Oceanite from highest flow in Oceanite Series, 6 km. from mouth of Riviere des Galets, Piton des Neiges. Sample contained olivine (Fo_{85}) and clinopyroxene phenocrysts in a fine-grained groundmass, containing some clinopyroxene.
- RE 512: Differentiated series flow (at base of series) from mouth of Ravine des Colimacons, plagioclase, olivine and clinopyroxene phenocrysts in a fine-grained groundmass.

Rocks from this region have been shown by Upton and Wadsworth (1966) to belong to an intermediate group between tholeiitic and alkali basalts.

Analyses of these samples are presented in Table 1.

New Georgia Group, British Solomon Islands Protectorate

(Stanton & Bell, 1969)

One sample was obtained:-

NG 367: Picrite basalt from Ruhana River, Marovo.

Olivine ($Fo_{87.4}$) and clinopyroxene phenocrysts present in a fine-grained groundmass. Analyses of the rock, groundmass, olivine and clinopyroxene separated from it, are given in Table 1.

Juan Fernandez Islands, Pacific Ocean (Quensel, 1912)

Two samples were obtained:-

17840: Picrite basalt, 1.2 km. south of settlement, Alexander Selkirk. Olivine phenocrysts in a fine-grained groundmass.

17901: Picrite basalt, La Pina, Robinson Crusoe. Olivine phenocrysts in a fine-grained groundmass. Analysis of a picrite basalt (Quensel, 1912) from this region is given in Table 1.

TABLE 1 (cont'd)

	394 Olivine	394 cpx	446	448	Z39A	Z40	Z64	L5
SiO ₂	39.81	50.31	47.9	48.5	48.09	48.54	46.33	44.29
Al ₂ O ₃	0.35	5.65	15.49	15.12	15.17	15.01	14.95	11.57
Fe ₂ O ₃	-	1.86	2.52	4.51	2.33	2.16	1.52	4.44
FeO	11.56	3.72	8.65	6.15	7.97	6.93	7.91	6.82
MgO	48.36	17.08	8.43	8.64	8.36	10.45	10.33	20.80
CaO	0.37	20.67	11.55	11.39	10.50	11.03	12.34	7.70
Na ₂ O	-	0.22	2.49	2.59	4.01	3.50	2.84	1.57
K ₂ O	-	-	0.61	0.71	0.75	0.64	0.62	0.35
H ₂ O	-	-	-	-	-	-	-	-
TiO ₂	0.03	0.58	1.78	1.86	2.64	2.15	2.15	1.28
P ₂ O ₅	-	-	0.34	0.27	0.38	0.33	0.40	0.11
MnO	0.20	0.11	0.22	0.21	0.17	0.15	0.15	0.15
CO ₂	-	-	-	-	-	-	-	-
Total	100.68	100.24	99.98	99.95	100.37	100.89	99.54	100.04

6

7

KEY TO TABLE 1

1. Wadsworth (1971) - personal communication
2. Stanton & Bell (1969) - cpx analysis includes Cr_2O_3 0.59%
3. Quensel (1912)
4. Macdonald & Katsura (1964)
5. Macdonald (1968)
6. Sigurdsson (1971) - personal communication
7. Analyst - I. M. Dale

Analyses are given in Table 1.

Macdonald & Powers, 1968; Macdonald, 1968)

Three samples were obtained:-

- C71: Ankaramite from roadcut on Kamuela-Kona road
3.5 km north of Popoo Gulch, on west slope of
Mauna Kea.
- C129: Basanitoid, transitional to ankaramite; lava flow
extruded about 1790, at the lower road near the east
edge of the flow 0.8 km. northwest of La Perouse Bay.
- C209: Ankaramite; cut on new highway, 3.4 km. east of
junction with the road to Honokaa from Kamuela, Mauna
Kea. Laupahoehoe volcanic series.

Analyses are given in Table 1.

Three samples were obtained:-

394: Ankaramitic olivine basalt tuff, very rich in olivine and clinopyroxene phenocrysts, from Klakkur.

Quaternary sub-glacial eruption. Analyses of olivine (by microprobe) and clinopyroxene (chemically) is given in Table 1.

446: Alkalic basalt lava from Thorgeirsfell. Quaternary eruption. Analysis of the rock (by X-ray fluorescence) is given in Table 1.

448: Olivine basalt from Berserkjahraun recent lava flow. Analysis of the rock (by X-ray fluorescence) is given in Table 1.

Zubair Group of Islands, Red Sea (Gass, Mallick & Cox 1971, in press)

Three samples were obtained, all olivine-phyric basalts

Z39A: Saba Island, west of recent cone

Z40: Saba Island, crater of recent volcanic cone

Z64: Centre Peak Island, scoria cone to N.W. of New Lighthouse.

Analyses are given in Table 1.

Ubekendt Ejland, West Greenland

(Drever, 1956; Drever, 1958; Drever & Johnston, 1957)

Four samples:- L5, L7, B5 and 120 - all picrite lava flows, were obtained from this region.

One analysis is given in Table 1.

Thin Section Descriptions

Microscopic examinations of rock sections were kindly carried out by Dr. P. Henderson. Descriptions are given for samples originally obtained as hand specimens. The other samples are described in the original papers referred to above.

Juan Fernandez Islands

17840 Vesicular olivine-phyric basalt

Rounded olivine phenocrysts up to 50 mm. in diameter, and with slight marginal reaction or alteration. Medium grained groundmass with abundant laths of plagioclase feldspar, some with marked continuous zoning. Altered ferromagnesians and abundant ore. No pyroxene phenocrysts in thin section.

17901

Olivine-phyric basalt

Anhedral to subhedral olivine phenocrysts - some shattered and with reaction rims.

Fine grained groundmass with rounded and lath-shaped iron ore crystals. Rounded olivine and pyroxene but little plagioclase in groundmass.

Hawaiian Samples

C.129

Vesicular basalt

Pyroxene and olivine phenocrysts set in groundmass.

Abundant phenocrysts of subhedral to euhedral clinopyroxene (augite) showing discontinuous zoning. Cores distinct and usually form bulk of each pyroxene grain. One grain has rounded core with euhedral overgrowth. Minor amounts of subhedral to anhedral olivine. Ore and small laths of plagioclase feldspar present in groundmass.

Iceland Samples

394

Basic tuff

Phenocrysts of olivine, clinopyroxene and plagioclase feldspars up to 5 mm. diameter set in very fine-grained groundmass. Phenocrysts show brecciated and rounded

texture, as well as stress zoning. Groundmass partially glassy and devitrified and variable in colour.

446 Olivine basalt

Phenocrysts of olivine and minor amounts of clinopyroxene. Rare large (0.5 mm.) crystals of semi-translucent, subhedral, (chrome ?) spinel. Medium grained groundmass containing abundant plagioclase laths, olivine and iron-ore.

448 Olivine basalt

Anhedral phenocrysts of olivine and clinopyroxene set in fine grained groundmass which contains zoned plagioclase laths, olivine, pyroxene and ore.

Red Sea Islands Samples

Z39A Olivine-phyric basalt

Phenocrysts subhedral to euhedral of variable size. Crystalline groundmass of plagioclase laths, olivine and opaques. No pyroxene or feldspar phenocrysts in section.

Z40

Ba salt

Olivine, feldspar and clinopyroxene phenocrysts in finely crystalline groundmass. Large subhedral plagioclase phenocrysts (up to 3 x 2 mm.) with Carlsbad and albite twinning, and also patchy and oscillatory zoning in some cases. Olivine phenocrysts (up to 3 mm. diameter) generally anhedral to subhedral, some with chromite (?) inclusions. Slight zoning is present. Clinopyroxene - generally a few rounded phenocrysts up to 2 mm. diameter. Normal zoning is present.

Crystalline groundmass with abundant zoned plagioclase laths, anhedral olivine, pyroxene and opaques.

Z64

Olivine-phyric basalt

Anhedral to subhedral olivine phenocrysts (up to 5 mm. diameter) set in fine grained groundmass. Groundmass with abundant laths (of maximum length 1 mm.) of strongly zoned plagioclase and some subhedral olivine crystals. Plagioclases show trachytic texture around olivine phenocrysts. Little ore present in groundmass.

Greenland Samples

L5

Olivine basalt

Olivine phenocrysts set in fine grained groundmass.

Subhedral olivine grains vary in size up to 4 mm.

diameter. Some show slight alteration to a light brown,

pleochroic alteration product. Occasional small

subhedral grains of chromite (?) included in olivine but

no reaction rims are seen.

Opaques and plagioclase are the only identifiable minerals

in the fine grained groundmass. The opaques occur as

anhedral grains with irregular "rough" boundaries,

distributed randomly throughout groundmass.

Two rounded inclusions (zeolites ?) of 4 mm. diameter

observed in section.

No pyroxene present in section.

L7

Olivine-phyric basalt

Abundant rounded and zoned phenocrysts (up to 3.5 mm

diameter) of olivine set in a finely crystalline groundmass

of plagioclase, mafic minerals, opaques and alteration

products. Some olivine phenocrysts contain small amounts

of opaque anhedral inclusions and there are olivine

alteration products (including chlorite). No phenocrysts of pyroxene or feldspar in section.

120

Ba salt

Rounded olivine phenocrysts with marked cleavage, set in fine grained groundmass containing some laths of feldspar, olivine crystals, and clusters of iron-ore.

BRIDGMAN, D. C. (1962) The crystal structure of olivine. *Am. Mineralogist*, 47, 100-110.

BRIDGMAN, D. C. (1963) Olivine. *Am. Mineralogist*, 48, 100-110.

BRIDGMAN, D. C. (1964) Olivine. *Am. Mineralogist*, 49, 100-110.

BRIDGMAN, D. C. (1965) Olivine. *Am. Mineralogist*, 50, 100-110.

BRIDGMAN, D. C. (1966) Olivine. *Am. Mineralogist*, 51, 100-110.

BRIDGMAN, D. C. (1967) Olivine. *Am. Mineralogist*, 52, 100-110.

BRIDGMAN, D. C. (1968) Olivine. *Am. Mineralogist*, 53, 100-110.

BRIDGMAN, D. C. (1969) Olivine. *Am. Mineralogist*, 54, 100-110.

BRIDGMAN, D. C. (1970) Olivine. *Am. Mineralogist*, 55, 100-110.

BRIDGMAN, D. C. (1971) Olivine. *Am. Mineralogist*, 56, 100-110.

BRIDGMAN, D. C. (1972) Olivine. *Am. Mineralogist*, 57, 100-110.

BRIDGMAN, D. C. (1973) Olivine. *Am. Mineralogist*, 58, 100-110.

BRIDGMAN, D. C. (1974) Olivine. *Am. Mineralogist*, 59, 100-110.

BRIDGMAN, D. C. (1975) Olivine. *Am. Mineralogist*, 60, 100-110.

BRIDGMAN, D. C. (1976) Olivine. *Am. Mineralogist*, 61, 100-110.

BRIDGMAN, D. C. (1977) Olivine. *Am. Mineralogist*, 62, 100-110.

BRIDGMAN, D. C. (1978) Olivine. *Am. Mineralogist*, 63, 100-110.

BRIDGMAN, D. C. (1979) Olivine. *Am. Mineralogist*, 64, 100-110.

BRIDGMAN, D. C. (1980) Olivine. *Am. Mineralogist*, 65, 100-110.

BRIDGMAN, D. C. (1981) Olivine. *Am. Mineralogist*, 66, 100-110.

BRIDGMAN, D. C. (1982) Olivine. *Am. Mineralogist*, 67, 100-110.

BRIDGMAN, D. C. (1983) Olivine. *Am. Mineralogist*, 68, 100-110.

BRIDGMAN, D. C. (1984) Olivine. *Am. Mineralogist*, 69, 100-110.

BRIDGMAN, D. C. (1985) Olivine. *Am. Mineralogist*, 70, 100-110.

BRIDGMAN, D. C. (1986) Olivine. *Am. Mineralogist*, 71, 100-110.

BRIDGMAN, D. C. (1987) Olivine. *Am. Mineralogist*, 72, 100-110.

BRIDGMAN, D. C. (1988) Olivine. *Am. Mineralogist*, 73, 100-110.

BRIDGMAN, D. C. (1989) Olivine. *Am. Mineralogist*, 74, 100-110.

BRIDGMAN, D. C. (1990) Olivine. *Am. Mineralogist*, 75, 100-110.

BRIDGMAN, D. C. (1991) Olivine. *Am. Mineralogist*, 76, 100-110.

BRIDGMAN, D. C. (1992) Olivine. *Am. Mineralogist*, 77, 100-110.

BRIDGMAN, D. C. (1993) Olivine. *Am. Mineralogist*, 78, 100-110.

BRIDGMAN, D. C. (1994) Olivine. *Am. Mineralogist*, 79, 100-110.

BRIDGMAN, D. C. (1995) Olivine. *Am. Mineralogist*, 80, 100-110.

BRIDGMAN, D. C. (1996) Olivine. *Am. Mineralogist*, 81, 100-110.

BRIDGMAN, D. C. (1997) Olivine. *Am. Mineralogist*, 82, 100-110.

BRIDGMAN, D. C. (1998) Olivine. *Am. Mineralogist*, 83, 100-110.

BRIDGMAN, D. C. (1999) Olivine. *Am. Mineralogist*, 84, 100-110.

BRIDGMAN, D. C. (2000) Olivine. *Am. Mineralogist*, 85, 100-110.

BRIDGMAN, D. C. (2001) Olivine. *Am. Mineralogist*, 86, 100-110.

BRIDGMAN, D. C. (2002) Olivine. *Am. Mineralogist*, 87, 100-110.

BRIDGMAN, D. C. (2003) Olivine. *Am. Mineralogist*, 88, 100-110.

BRIDGMAN, D. C. (2004) Olivine. *Am. Mineralogist*, 89, 100-110.

BRIDGMAN, D. C. (2005) Olivine. *Am. Mineralogist*, 90, 100-110.

BRIDGMAN, D. C. (2006) Olivine. *Am. Mineralogist*, 91, 100-110.

BRIDGMAN, D. C. (2007) Olivine. *Am. Mineralogist*, 92, 100-110.

BRIDGMAN, D. C. (2008) Olivine. *Am. Mineralogist*, 93, 100-110.

BRIDGMAN, D. C. (2009) Olivine. *Am. Mineralogist*, 94, 100-110.

BRIDGMAN, D. C. (2010) Olivine. *Am. Mineralogist*, 95, 100-110.

BRIDGMAN, D. C. (2011) Olivine. *Am. Mineralogist*, 96, 100-110.

BRIDGMAN, D. C. (2012) Olivine. *Am. Mineralogist*, 97, 100-110.

BRIDGMAN, D. C. (2013) Olivine. *Am. Mineralogist*, 98, 100-110.

BRIDGMAN, D. C. (2014) Olivine. *Am. Mineralogist*, 99, 100-110.

BRIDGMAN, D. C. (2015) Olivine. *Am. Mineralogist*, 100, 100-110.

BIBLIOGRAPHY

- AGRELL, S.O., SCOON, J.H., MUIR, I.D., LONG, J.V.P.,
McCONNELL, J.D.C. & PECKETT, A. (1970) Observations on
the chemistry, mineralogy and petrology of some Apollo 11 lunar
samples. Proc. Apollo 11 Lunar Sci. Conf. 1, 93-128.
- AHRENS, L.H. (1953) The use of ionisation potentials - II. Anion
affinity and geochemistry. Geochim. et Cosmochim. Acta 3, 1-29
- AHRENS, L.H. & TAYLOR, S.R. (1961) Spectrochemical Analysis,
2nd ed., Addison-Wesley Publishing Co. Ltd., London, 1961.
- ALIAN, A. & SHABANA, R. (1967) Neutron Activation Analysis by
standard addition and solvent extraction. Determination of some
trace elements in granite and diabase rocks. Microchem. J. 12,
427-33.
- ALKEMADE, C.T.J. & MILATZ, J.M.W. (1955) Double-beam method
of spectral selection with flames. Appl. Scient. Res. 48, 288-99.
- ANTHMANN, S.O.W., LANDIS, D.A., PEHL, R.H. (1966)
Measurements of the Fano factor and the energy per hole - electron
pair in germanium. Nucl. Instr. Methods 40, 272-6.
- BANCROFT, G.M., BURNS, R.G. & HOWIE, R.A. (1967) Determination
of cation distribution in the orthopyroxene series by the Mössbauer
effect. Nature, London 213, 1221-1223.
- BANCROFT, G.M., BURNS, R.G., MADDOCK, A.G. (1967)
Applications of the Mössbauer effect to silicate mineralogy. Part 1.
Iron silicates of known crystal structure. Geochim. et Cosmochim.
Acta 31, 2219-2246.
- BARTH, T.W.F. & ROSENQUIST, T. (1949) Thermodynamic relations
of immiscibility and crystallisation of molten silicates. Am. J. Sci.
247, 316-323.
- BERNAL, J.D. (1964) The structure of liquids. Proc. Roy. Soc.
(London) A280, 299-322.
- BETHE, H. (1929) Term-aufspaltung in Kristallen (Splitting of Terms
in Crystals) Ann. Phys. 3, 133-206.
- BILGER, H.R. (1967) Fano factor in germanium at 77° K. Phys. Rev.
163, 238-53.
- BLANDER, M. (1970) The partitioning of cations between coexisting one
site-two site phases. Geochim. et Cosmochim. Acta 34, 515-518.
- BOON, J.A. (1971) Mössbauer investigations in the system Na₂O - FeO -
SiO₂. Chem. Geol. 7, 153-169.

- BROWN, G.M., EMELEUS, C.H., HOLLAND, J.G. & PHILIPS, R. (1970) Mineralogical, chemical and petrological features of Apollo 11 rocks and their relationship to igneous processes. Proc. Apollo 11 Lunar Sci. Conf. 1, 195-219.
- BRUNFELT, A.O. & STEINNES, E. (1966) Instrumental neutron-activation analysis of "standard rocks". Geochim. et Cosmochim. Acta 30, 921-928
- BURNS, R.G. (1968) Enrichments of transition metal ions in silicate crystal structures. Origin & Distribution of the Elements ed. by L. H. Ahrens - Pergamon Press, Oxford & New York, 1968 pp. 1151-1164.
- BURNS, R.G. (1969) Site Preference of transition metal ions in silicate crystal structures. Chem. Geol. 5, 275-283
- BURNS, R.G. (1970) Mineralogical Applications of Crystal Field Theory. Cambridge University Press
- BURNS, R.G. & FYFE, W.S. (1964) Site preference energy and selective uptake of transition metal ions from a magma. Science 144, 1001-1003
- BURNS, R.G. & FYFE, W.S. (1966) Distribution of elements in geological processes. Chem. Geol. 1, 49-56.
- BURNS, R.G. & FYFE, W.S. (1967) Trace element distribution rules and their significance. Chem. Geol. 2, 89-104
- CARR, M.H. & TUREKIAN, K.K. (1961) The geochemistry of cobalt. Geochim. et Cosmochim. Acta 23, 9-60
- CHASE, R.L. (1961) Nuclear Pulse Spectrometry. McGraw-Hill Book Co. Inc. New York, pp. 221
- CLARKE, F.W. (1924) The data of geochemistry. U.S. Geol. Survey Bull. 770.
- COBB, J.C. (1967) Determination of Lanthanide distribution in rocks by neutron activation and direct gamma counting. Anal. Chem. 39, 127-131
- CORNWALL, H.R. & ROSE, H.J. (1957) Minor elements in Keweenawan lavas, Michigan. Geochim. et Cosmochim. Acta 12, 209-224
- COTTON, F.A. & WILKINSON, G. (1966) Advanced Inorganic Chemistry, 2nd ed. Interscience, New York.
- COVELL, D.F. (1959) Determination of gamma-ray abundance directly from the total absorption peak. Anal. Chem. 31, 1785-1790
- CROUTHAMEL, C.E. (1960) Applied Gamma-Ray Spectrometry Pergamon Press, New York.

- CURTIS, C.D. (1963) Applications of the Crystal Field Theory to the Inclusion of Trace Transition Elements in Minerals during Magmatic Differentiation. *Geochim. et Cosmochim. Acta* 28, 389-403
- DALE, I.M., HENDERSON, P., WALTON, A. (1970) Non-destructive neutron activation analysis for some transition elements in rocks *Radiochem. Radioanal. Letters* 5, 91-101
- DALE, I.M., & HENDERSON, P. (In Press) The partition of transition elements in phenocryst-bearing basalts and the implications about melt structure. 24th International Geological Congress, Montreal, Canada, 1972.
- DEER, W.A., HOWIE, R.A., ZUSSMANN, J. (1966) An Introduction to the Rock-Forming Minerals. Longmans, London.
- DREVER, H.I. (1956) The Geology of Ubekendt Ejland, West Greenland Part 11. The picritic Sheets & Dykes of the East Coast. *Medd. Grønland*, 137, No. 4, 1-39,
- DREVER, H.I. (1958) Geological Results of Four Expeditions to Ubekendt Ejland, West Greenland. *Arctic* 11, 199-210
- DREVER, H.I. & JOHNSTON, R. (1957) Crystal growth of forsteritic olivines in magmas and melts. *Trans. Roy. Soc. Edin.*, 63, 289-315
- DUNITZ, J.D. & ORGEL, L.E. (1957) Electronic properties of transition metal oxides - 11. Cation distribution amongst octahedral and tetrahedral sites. *J. Phys. Chem. Solids*, 3, 318-323
- ECKSEHLAGER, K. (1969) Errors, Measurement and Results in Chemical Analysis, translated by C. Sofr, edited by R. A. Chalmers. Van Nostrand Reinhold Co., London
- FERMI, E., AMALDI, E., D'ANGOSTINO, O., RASETTI, F. & SEGRE, E. (1934) Artificial radioactivity produced by neutron bombardment *Proc. Roy. Soc. (London)*, A146, 483
- FLANAGAN, F.J. (1969) U.S. Geological Survey standards - 11. First compilation of data for the new U.S.G.S. rocks. *Geochim. et Cosmochim. Acta* 33, 81-120
- FLEISCHER, M. (1969) U.S. Geological Survey standards - 1. Additional data on rocks G-1 and W-1, 1965-1967. *Geochim. et Cosmochim. Acta* 33, 65-79
- FRIEDLANDER, G., KENNEDY, J.W., MILLER, J.M. (1964) Nuclear & Radiochemistry, 2nd ed. John Wiley & Sons Inc., New York
- GASS, I.G., MALLICK, D.I.J. & COX, K.G. (1971) Volcanic Rocks of the Red Sea. Submitted to Quarterly Journal of Geol. Society.

- GAST, P.W. (1968) Trace element fractionation and the origin of tholeiitic and alkaline magma types. *Geochim. et Cosmochim. Acta* 32, 1057-1086
- GEORGE, P. & McCLURE, D.S. (1959) The Effect of Inner Orbital Splitting on the Thermodynamic Properties of Transition Metal Compounds and Co-ordination Complexes in *Progress in Organic Chemistry* 1, 381-463; Interscience Publishers Inc., New York.
- GERLACH, W. (1925) Zur Frage der richtigen Ausführung und Deutung der "quantitativen Spektralanalyse". *Z. Anorg. Chem.* 142, 383
- GERLACH, W. & SCHWEITZER, E. (1929) *Foundations and Methods of Chemical Analysis by the Emission Spectrum*. Adam Hilger Ltd., London.
- GIBB, F.G.F. & ZUSSMAN, J. (1971) Zoned olivines in four Apollo 12 Samples. *Earth & Plan. Sci. Letters* 11, 161-167
- GIRARDI, F., GUZZI, G. & PAULY, J. (1967) The use of Ge(Li) detectors in activation analysis. *Radiochim. Acta* 7, 202
- GIRARDI, F. & GUZZI, G. (1969) in *Advances in Activation Analysis* ed. by J. M. A. Lenihan & S. J. Thomson, Academic Press, London.
- GOLDSCHMIDT, V.M. (1937) The principles of distribution of chemical elements in minerals and rocks. *J. Chem. Soc.* 655-672
- GOLDSCHMIDT, V.M. (1954) *Geochemistry*. Oxford University Press, Oxford.
- GORDON, G.E., RANDLE, K., GOLES, G.G., CARLISS, J.B., BEESON, M.H., OXLEY, S.S. (1968) Instrumental activation analysis of standard rocks with high resolution γ -ray detectors. *Geochim. et Cosmochim. Acta* 32, 369-396
- GREENLAND, L.P. (1970) An equation for trace element distribution during magmatic crystallisation. *Amer. Mineral.* 55, 455-465
- GROVER, J.E. & ORVILLE, P.M. (1969) The partitioning of cations between coexisting single and multi-site phases with application to the assemblages orthopyroxene-clinopyroxene and orthopyroxene-olivine. *Geochim. et Cosmochim. Acta* 33, 205-226
- GUNN, B.M. (1971) Trace element partition during olivine fractionation of Hawaiian basalts. *Chem. Geol.* 8, 1-13
- HAKLI, T.A. (1968) An attempt to apply the Makaopuhi nickel fractionation data to the temperature determination of a basic intrusive. *Geochim. et Cosmochim. Acta* 32, 449-460
- HAKLI, T. & WRIGHT, T.L. (1967) The fractionation of nickel between olivine and augite as a geothermometer. *Geochim. et Cosmochim. Acta* 31, 877-884.

- HANKE, K. (1965) Beiträge zur Kristallstrukturen von Olivin-Typ. Beitr. Mineral. Petrog. 11, 535-558
- HEATH, R.L. (1969) In Handbook of Chemistry & Physics ed. by R.C. Weast, The Chemical Rubber Co., Ohio.
- HENDERSON, P. & DALE, I.M. (1969) The partitioning of selected transition element ions between olivine and groundmass of oceanic basalts. Chem. Geol. 5, 267-274
- HEVESY, G. & LEVI, H. (1936) The action of neutrons on the rare earth elements. K. dansk. vidensk. Selsk. Math.-fys. Medd. 14, No. 5.
- HIRST, D.M. (1962) Geochemistry of modern sediments from the Gulf of Paria 11. The location and distribution of trace elements. Geochim. et Cosmochim. Acta 26, 1147-87.
- JEFFREY, P.G. (1970) Chemical Methods of Rock Analysis. Pergamon Press, Oxford, 1970.
- JOHANSEN, O. & STEINNES, E. (1968) Precision analyses of manganese in rocks by neutron activation analysis. Anal. Chim. Acta 40, 201-205.
- LACROIX, A. (1912) Les laves du volcan actif de la Reunion. Compt. Rend. de l'Academie des Sciences, 154, 251-257
- LAUL, J.C., CASE, D.R., WECHTER, M. SCHMIDT-BLEEK, F., LIPSCHULTZ, M.E. (1970) Activation analysis technique for determining groups of trace elements in rocks and chondrites. J. Radioanal. Chem. 4, 241-64.
- LENIHAN, J.M.A. & THOMSON, S.J. (1965) Activation Analysis. Academic Press, London.
- LIEBHAFSKY, H.A., PFEIFFER, H.G. & WINSLOW, E.H. (1964) in Treatise on Analytical Chemistry Part I. Vol. 5. edited by I. M. Kolthoff & P. J. Elving, Interscience, New York, 1964.
- LONG, J.V.P. (1967) in Physical Methods in Determinative Mineralogy ed. by J. Zussman, Academic Press, London and New York, 1967.
- LOW, W. (1968) Electron Spin Resonance - A Tool in Mineralogy & Geology. in Adv. in Electronics & Electron Physics, Vol.24. Academic Press Inc., New York.
- McCLURE, D.S. (1957) The distribution of transition metal cations in spinels. J. Phys. Chem. Solids, 3, 311-317.
- MACDONALD, G.A. (1968) Composition and origin of Hawaiian lavas. Geol. Soc. Amer. Memoir 116 - Studies in Volcanology ed. by Coats, Hays & Anderson.

- MACDONALD, G.A. & KATSURAT, T. (1964) Chemical composition of Hawaiian lavas. *J. Petrol.* 5, 82-133.
- MACDONALD, G.A. & POWERS, H.A. (1968) A further contribution to the petrology of Haleakala Volcano, Hawaii. *Geol. Soc. Amer. Bull.* 79, 877-888.
- McINTYRE, W.L. (1963) Trace element partition coefficients - a review of theory and applications to geology. *Geochim. et Cosmochim. Acta* 27, 1209-1264.
- MANSON, V. (1967) *Geochemistry of Basaltic Rocks: Major Elements in Basalts - The Poldervaart Treatise on Rocks of Basaltic Compositions.* ed. by H.H. Hess & A. Poldervaart. J. Wiley & Sons., New York.
- MAPPER, D. (1960) in *Methods in Geochemistry.* ed. by A.A. Smales and L. R. Wager. Interscience Publishers Inc., New York & London.
- MAXWELL, J.A. (1968) *Rock & Mineral Analysis.* Interscience Publishers, New York.
- MELSOM, S. (1970) Precision and accuracy of rare earth determinations in rock samples using instrumental neutron activation analysis and a Ge(Li) detector. *J. Radioanal. Chem.* 4, 355-363.
- MITCHELL, R.L. (1964) *The Spectrochemical Analysis of Soils, Plants and Related Material, Commonwealth Bureau of Soils, Technical Communication 44A.*
- MOORE, J.G. & EVANS, B.W. (1967) The role of olivine in the crystallisation of the prehistoric Makaopuhi tholeiitic lava lake, Hawaii. *Centr. Mineral. Petrol.* 15, 202-223.
- MORRISON, G.H., GERRARD, J.T., TRAVESI, A., CURRIE, R.L., PETERSON, S.F., POTTER, N.M. (1969) Multielement neutron activation analysis of rock using chemical group separations and high resolution gamma spectrometry. *Anal. Chem.* 41, 1633-1637.
- MUIR, I.D. & TILLEY, C.E. (1964) Basalts from the Northern part of the rift zone of the Mid-Atlantic Ridge. *J. Petrol.* 5, 409-434.
- NEUMANN, H., MEAD, J., VITALIANO, C.J. (1954) Trace element variation during fractional crystallisation as calculated from the distribution law. *Geochim. et Cosmochim. Acta* 6, 90-99.
- NOCKOLDS, S.R. (1966) The behaviour of some elements during fractional crystallisation of magma. *Geochim. et Cosmochim. Acta* 30, 267-278.

- NORRISH, K. & HUTTON, J.T. (1964) Preparation of samples for analysis by X-ray fluorescence spectrography. Divl. Rep. Div. Soils.C.S.I.R.O. 3/64.
- NORRISH, K. & CHAPPELL, B.W., (1967) in Physical Methods in Determinative Mineralogy ed. by J. Zussman, Academic Press, London & New York.
- ONUMA, N., HIGUCHI, H., WAKITA, H. & NAGASAWA, H. (1968) Trace element partition between two pyroxenes and the host lava. Earth and Pl. Sci. Letters 5, 47-518.
- ORGEL, L.E. (1952) The Effects of Crystal Fields on the Properties of Transition Metal Ions. Journ. Chem. Soc. 4756-61.
- ORGEL, L.E. (1966) An Introduction to Transition Metal Chemistry; Ligand Field Theory. Methuen, London.
- PAULING, L. (1948) The Nature of the Chemical Bond. Cornell Univ. Press, New York.
- PRINZ, M. (1967) Geochemistry of Basaltic Rocks: Trace Elements in Basalts - The Poldervaart Treatise on Rocks of Basaltic Composition ed. by H.H. Hess & A. Poldervaart, John Wiley & Sons, New York.
- QUENSEL, P.D. (1912) Die Geologie der Juan Fernandezinseln Bull. Geol. Inst. Upsala 11, 253-290.
- RAMBERG, H. (1952) Chemical bonds and distribution of cations in silicates. J. Geol. 60, 331-355.
- RAMBERG, H. & DEVORE, G. (1951) The distribution of iron and magnesium in coexisting olivines and pyroxenes. J. Geol. 59, 193-210.
- RAMIREZ-MUNOZ, J. (1968) Atomic-Absorption Spectroscopy Elsevier Publishing Co., Amsterdam-London-New York, (1968).
- RIGG, T. & WAGENBAUER, H.A. (1961) Spectrophotometric determination of titanium in silicate rocks. Anal. Chem. 33, 1347-1349.
- RINGWOOD, A.E. (1955) The principle governing trace element distribution during magmatic crystallisation - 1. The influence of electronegativity. Geochim. et Cosmochim. Acta 10, 297-303.
- DE LA ROCHE, H., GOVINDARAJU, K. (1969) Rapport sur deux roches, diorite DR-N et serpentine UB-N. Bull. de la Societe Francaise de Ceramique 85, 35-50.
- DE LA ROCHE, H., GOVINDARAJU, K. (1970) Rapport sur un minerai d'aluminium bauxite Bx-N et sur un refractaire silico-alumineux disthene DT-N proposes comme etalons analytiques. Commission: "Matières premières minérales" de l'Association Nationale de la Recherche Technique, Circulaire 721.

- RODGERS, K.A. & BROTHERS, R.N. (1969) Olivine, pyroxene, feldspar and spinel in ultramafic nodules from Auckland, New Zealand. *Min. Mag.* 37, 375-390.
- ROUBAULT, M. DE LA ROCHE, H., GOVINDARAJU, K. (1968) Report (1966-1968) on geochemical standards; Granites GR, GA & GH, Basalt BR. *Sciences de la Terre*, 13, 379-404.
- SCHULZE, W. (1969) in *Advances in Activation Analysis* ed. by J. M. A. Lenihan & S. J. Thomson, Academic Press, London.
- SCHWARCZ, H.P. (1966) The effect of crystal field stabilisation on the distribution of transition metals between metamorphic minerals. *Geochim. et Cosmochim. Acta* 31, 503-517
- SCRIBNER, B.F. & MARGOSHES, M. (1965) in *Treatise on Analytical Chemistry*, Part 1, Vol. 6, ed. by I. M. Kolthoff & P. J. Elving, Interscience, New York, 1965.
- SEWARD, T.M. (1971) The distribution of transition elements in the system $\text{Ca Mg Si}_2\text{O}_6$ - $\text{Na}_2\text{Si}_2\text{O}_5$ - H_2O . *Chem. Geol.* 7, 73-95.
- SHAPIRO, L. & BRÄNNOCK, W.W. (1962) Rapid analysis of silicate, carbonate & phosphate rocks. *U.S. Geol. Surv. Bull.* 1144-A.
- SHAW, D.M. (1953) The camouflage principle and trace element distribution in magmatic minerals. *J. Geol.* 61, 142-151.
- SIGURDSSON, H. (1966) *Geology of the Setberg Area, Snaefellsnes, Western Iceland*. *Soc. Sci. Islandica* 4, 53-125.
- SIGURDSSON, H. (1971) Personal communication.
- SIMKIN, T. & SMITH, J.V. (1970) Minor-element distribution in olivine. *J. Geol.* 78, 304-325.
- SLAVIN, W. (1968) *Atomic Absorption Spectroscopy*. Interscience Publishers, New York-London-Sydney, 1968.
- SMALES, A.A., MAPPER, D. & WOOD, A.J. (1957) The determination, by radioactivation, of small quantities of nickel, cobalt & copper in rocks, marine sediments and meteorites. *Analyst*, 82, 75-88.
- SMITH, J.V. (1966) X-ray emission analysis of rock-forming minerals, 11: olivines. *J. Geol.* 74, 1-16.
- SPECTROSCOPY SOCIETY of CANADA, (1968) Ottawa, Canada.
- STANTON, R.L. & BELL, J.D. (1969) Volcanic & associated rocks of the New Georgia Group, British Solomon Islands Protectorate. *Overseas Geology & Mineral Resources*, 10, 113-145.
- STUEBER, A.M. & GOLES, G.G. (1967) Abundances of Na, Mn, Cr, Sc & Co. in ultramafic rocks. *Geochim. et Cosmochim. Acta* 31, 75-93.

- STROUTS, C.R.N., WILSON, H.N. & PARRY-JONES, R.T. (1962) Chemical Analysis, Vol. 1, Oxford University Press, Oxford.
- SWEATMAN, T.R. & LONG, J.V.P. (1969) Quantitative electron-probe microanalysis of rock-forming minerals. *J. Petrology* 10, 332-79.
- TANZANIAN GEOLOGICAL SURVEY, (1963) Standard Geochemical Standard T-1, Tanzanian Geological Survey, Dar Es-Salaam, Tanzania.
- TAYLOR, S.R. & KOLBE, P. (1964) Geochemical Standards. *Geochim. et Cosmochim. Acta* 28, 447-54.
- THIESEN, R. (1965) Quantitative Electron Microprobe Analysis. Springer Verlag, Berlin-Heidelberg-New York.
- TUREKIAN, K. K. (1963) The chromium & nickel distribution in basaltic rocks and eclogites. *Geochim. et Cosmochim. Acta* 27, 835-846.
- UPTON, B.G.J. & WADSWORTH, W.J. (1966) The basalts of Reunion Island, Indian Ocean. *Bulletin Volcanologique* 19, 7-24.
- WADSWORTH, W.J. (1971) Personal communication.
- WAGER, L. R., MITCHELL, R.L. (1951) The distribution of trace elements during strong fractionation of basic magma. *Geochim. et Cosmochim. Acta* 1, 129-208.
- WALSH, A.A. (1955) The application of atomic absorption spectra to chemical analysis. *Spectrochim. Acta* 7, 108-117.
- WARREN, B. & BRAGG, W.L. (1928) The structure of diopside, $\text{CaMg}(\text{SiO}_3)_2$. *Zeit. Krist.*, 69, 168-193.
- WASSERBURG, G.J. (1957) The effects of H_2O in silicate melts. *J. Geol.* 65, 15-23.
- WHITE, R. W. (1966) Ultramafic Inclusions in basaltic rocks from Hawaii. *Contr. Minerl. & Petrol.* 12, 245-314.
- WHITTAKER, E.J.W. (1967) Factors Affecting Element Ratios in Crystallisation of Minerals. *Geochim. et Cosmochim. Acta* 31, 2275-2288.
- WHITTAKER, E.J.W. & MUNTUS, R (1970) Ionic radii for use in geochemistry. *Geochim. et Cosmochim. Acta* 34, 945-956.
- WILLIAMS, R.J.P. (1959) Deposition of Trace Elements in Basic Magma, *Nature*, 184, 44.
- WILSON, A.D. (1955) A new method for the determination of ferrous iron in rocks and minerals. *Bull. Geol. Surv. G.B.* 9, 56-58.

- WILSON, A.D. (1960) The microdetermination of ferrous iron in silicate minerals by a volumetric and a colorimetric method. *Analyst* 85, 823-827.
- WINCHESTER, J.W. (1961) Radioactivation Analysis in Inorganic Geochemistry, in *Progress in Inorganic Chemistry* Vol. 2 ed. by F.A. Cotton, Interscience Publishers, New York.
- WITTRY, D.B. (1964) Methods of quantitative electron-probe analysis, in "Advances in X-Ray Analysis" Vol. 7. Plenum Press, New York, 1964.
- WYTTENBACH, A. (1969) Rapid Instrumental Nuclear Activation Analysis of rocks, cements and meteorites. *Helv. Chim. Acta* 52, 2458-2465.

NON-DESTRUCTIVE NEUTRON ACTIVATION ANALYSIS FOR SOME
TRANSITION ELEMENTS IN ROCKS

I.M.Dale, P.Henderson^{*}, A.Walton

Department of Chemistry, the University,
Glasgow W.2, U.K.

Received 4 September 1970

Accepted 15 September 1970

The Sc, Cr, Mn, Fe and Co contents of ten standard rock samples have been determined by instrumental neutron activation analysis. A comparison between these new results with those obtained by similar techniques and other methods has been made.

INTRODUCTION

Accurate determinations of transition elements at ppm concentrations in small quantities of rock samples or separated minerals can be performed using various techniques. Non-destructive neutron activation analysis is particularly useful for several elements. In this paper new results obtained with this technique for a number of recently prepared, as well as established, standard rock samples are presented. The elements investigated were Sc, Cr, Mn, Fe and Co.

EXPERIMENTAL

Table 1 presents the relevant nuclear data for the elements studied.

^{*}Present address: Department of Geology, Chelsea College of Science and Technology, London, S.W.3.

TABLE 1
Nuclear data for elements investigated

Element	Target isotope	Isotopic abundance, %	Product nuclide	Half-life	Thermal neutron absorption cross-section, barn	Energies of γ -rays, Mev
Sc	^{45}Sc	100	^{45}Sc	83.9 d	23	0.889, 1.120, 2.009 /sum/
Cr	^{50}Cr	4.31	^{51}Cr	27.8 d	17	0.320
Mn	^{55}Mn	100	^{56}Mn	2.58 h	13.3	0.847
Fe	^{58}Fe	0.31	^{59}Fe	45 d	1.1	1.100, 1.291
Co	^{59}Co	100	^{60}Co	5.26 y	37	1.173, 1.322 2.495 /sum/

Two irradiations of the samples were required, the first of two minutes at a thermal neutron flux of $10^{12} \text{ ncm}^{-2} \text{ sec}^{-1}$ in the Scottish Research Reactor, East Kilbride, for the analysis of ^{56}Mn ; the second of four days at a thermal neutron flux of $2 \times 10^{12} \text{ ncm}^{-2} \text{ sec}^{-1}$ in the DIDO Reactor, A.E.R.E., Harwell, for ^{46}Sc , ^{51}Cr , ^{59}Fe and ^{60}Co .

Sample preparation was the same in each case. 50-100 mg of the rock powder were heat-sealed in 3 cm lengths of polythene tubing and then wrapped in aluminium foil. Standards were prepared by dissolution of spectroscopically pure metal /Mn, Cr, Fe and Co/ or metal oxide / Sc_2O_3 / and 10 μl aliquots of these solutions were placed on 1 cm diameter circles of glass-fibre filter paper with a calibrated syringe. Each metal standard was prepared in triplicate and the weights of metal placed on the filter papers were Sc 2 μg ; Cr 250 μg ; Mn 60 μg ; Fe 2 mg; Co 100 μg , respectively. The samples and standards were then packed in containers for irradiation.

After irradiation the rock powders were accurately weighed into clean 2.5 ml polythene containers, the filter papers being placed in similar containers. Counting was delayed for some time after irradiation to allow any short lived interfering isotopes to decay e.g. ^{28}Al and ^{24}Na , /i.e. 3-4 weeks for Sc, Cr, Fe and Co; 2-3 hrs for Mn/.

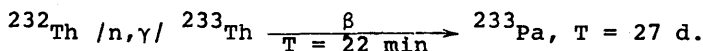
Samples and standards were counted with the following systems:

- /i/ a 4.5" x 4.5" NaI/Tl/ flat topped crystal and an Inter-technique 400-channel analyser. /Sc and Co determination/.

/ii/ a 40 cm³ Ge/Li/ detector and a Technical Measurement Corporation 400-channel analyser. /Mn, Cr and Fe determination/.

Counting times chosen to give good counting statistics were typically 1 to 3 min for the NaI/Tl/ detector and 10 min for the Ge/Li/ detector.

For ⁴⁶Sc and ⁶⁰Co, the sum peaks were measured as suggested by Gordon et al.¹ while for the remaining nuclides the γ -ray peaks employed are shown in Table 1. /Rocks with appreciable quantities of Th cannot be analysed for Cr by this method because of strong interference from the 0.312 MeV peak of ²³³Pa, formed as follows:



Peak areas were determined by the method described by Coveil.²

RESULTS

In Tables 2-6 our results are presented for ten standard rocks. Seven standards were supplied by the United States Geological Survey /W-1, G-2, GSP-1, AGV-1, PCC-1, DTS-1, BCR-1/, one by the Tanzanian Geological Survey /T-1/ and two by the Spectroscopy Society of Canada /SY2 and SY3/. Average or recommended concentrations³⁻⁵ of the various elements are quoted except for SY2 and SY3, where the single provisional analysis is given.⁶ Means and standard deviations were calculated from the results obtained by neutron activation⁷⁻¹⁸ and other methods³⁻⁵ of analysis.

TABLE 2
Concentration /ppm/ of scandium in rock standards

Rock	Split and position, No	This work	Other N.A.A. results /Mean \pm S.D./	Other methods /Mean \pm S.D./	Recommended or average
W-1		33.7	34.8 \pm 1.3	42.0 \pm 5.7	34.0 3
G-2	92-19	3.6	3.3 \pm 0.2	5.3 \pm 1.9	3.9 4
GSP-1	9-12	5.8	5.9 \pm 0.2	10.2 \pm 4.5	9.2 4
AGV-1	17-17	12.2	11.6 \pm 0.4	12.8 \pm 3.2	13.3 4
PCC-1	35-7	9.2	8.3 \pm 0.9	8.3 \pm 1.8	8.7 4
DTS-1	58-24	3.8	3.4 \pm 0.4	4.0 \pm 0.9	3.8 4
BCR-1	44-8	34.9	32.5 \pm 1.5	37.0 \pm 6.5	36.5 4
T-1		11.0			10-20 5
SY2		6.3			10 6
SY3		5.6			10 6

- 3 Fleischer /1969/
 4 Flanagan /1969/
 5 Tanzanian Geological Survey /1963/
 6 Spectroscopy Society of Canada /1968/

TABLE 3
Concentrations /ppm/ of chromium in rock standards

Rock	Split and position, NO	This work	N.A.A. results /Mean \pm S.D./	Other methods /Mean \pm S.D./	Recommended or average
W-1		89	108 \pm 15.5	121 \pm 18	120 ³
PCC-1	35-7	2660	2715 \pm 55	2923 \pm 725	3090 ⁴
DTS-1	58-24	4210	4200 \pm 10	4019 \pm 736	4230 ⁴

³Fleischer /1969/

⁴Flanagan /1969/

TABLE 4
Concentrations /ppm/ of manganese in rock standards

Rock	Split and position, No	This work	N.A.A. results /Mean \pm S.D./	Other methods /Mean \pm S.D./	Recommended or average
W-1		1130	1277 \pm 78	1347 \pm 134	1316 3
G-2	92-19	253	253 \pm 20	262 \pm 59	265 4
GSP-1	9-12	307	296 \pm 19	320 \pm 56	326 4
AGV-1	17-17	773	700 \pm 41	719 \pm 154	728 4
PCC-1	35-7	895	888 \pm 8	929 \pm 240	889 4
DTS-1	58-24	988	949 \pm 39	971 \pm 221	963 4
BCR-1	44-8	1330	1360 \pm 56	1357 \pm 294	1350 4
T-1		840			850 5
SY2		2610			2650 6
SY3		2420			2480 6

3 Fleischer /1969/

4 Flanagan /1969/

5 Tanzanian Geological Survey /1963/

6 Spectroscopy Society of Canada /1968/

TABLE 5
Concentrations /As Fe₂O₃%/ of iron in rock standards

Rock	Split and position, No	This work	N.A.A. results /Mean ± S.D./	Other methods /Mean ± S.D./	Recommended or average
G-2	92-19	2.39	2.51 ± 0.13	2.72 ± 0.27	2.69 4
GSP-1	9-12	4.00	4.05 ± 0.08	4.32 ± 0.23	4.35 4
AGV-1	17-17	6.61	6.67 ± 0.35	6.81 ± 0.24	6.79 4
PCC-1	35-7	7.68		8.58 ± 0.68	8.41 4
DTS-1	58-24	8.14		8.92 ± 0.64	8.75 4
T-1		5.82		6.01 ± 0.17	6.02 5
SY2		6.36			7.15 6
SY3		5.86			7.01 6

4 Flanagan /1969/
5 Tanzanian Geological Survey /1963/
6 Spectroscopy Society of Canada /1968/

TABLE 6
Concentrations /ppm/ of cobalt in rock standards

Rock	Split and position, No	This work	N.A.A. results /Mean \pm S.D./	Other methods /Mean \pm S.D./	Recommended or average
W-1		49.4	48.2 \pm 3.9	42.7 \pm 5.8	50 ³
G-2	92-19	5.5	4.7 \pm 0.8	6.1 \pm 4.1	4.9 ⁴
GSP-1	9-12	7.6	7.3 \pm 1.2	8.4 \pm 4.8	7.5 ⁴
AGV-1	17-17	15.3	15.4 \pm 1.5	16.8 \pm 4.6	15.5 ⁴
PCC-1	35-7	121	124 \pm 10	115 \pm 46	112 ⁴
DTS-1	58-24	145	144 \pm 2.5	134 \pm 27	132 ⁴
BCR-1	44-8	41.2	39.3 \pm 3.2	36.5 \pm 4.9	35.5 ⁴
T-1		12.8			13 ⁵
SY2		10.8			20 ⁶
SY3		11.6			N.D.

³ Fleischer /1969/

⁴ Flanagan /1969/

⁵ Tanzanian Geological Survey /1963/

⁶ Spectroscopy Society of Canada /1968/

N.D. = Not detected

The errors associated with our results, based on replicate analyses, are less than 5%.

DISCUSSION

Agreement between analysts using neutron activation, both destructive and non-destructive, is in every case but one /Fe in AGV-1/ much better than for other methods. It is clear from these tables that there is very poor agreement between laboratories using different methods for trace element analysis especially for Sc and Co where the percentage standard deviations in some cases exceed 60%.

In 24 cases out of 29 the means of the activation results lower than the overall averages. This suggests that interferences from other radioactive nuclides do not appear to be of significance for Sc, Cr, Mn, Fe and Co.

The one major difference between activation analysis and other results is Sc in GSP-1. The mean of the activation results is 5.9 ± 0.2 ppm whereas the average quoted value is 9.2 ppm.⁴ This discrepancy is in part due to three higher values obtained by optical spectrography /11.0, 11.3 and 22/, thus weighting the mean and giving rise to a large standard deviation 9.1 ± 4.3 ; without these values the mean is 7.3 ± 1.3 .

*

We wish to thank Professor H.W.Wilson and the staff of the Scottish Research Reactor Centre for irradiation and counting facilities, also Professor G.Forbes of the Department of Forensic Medicine, Glasgow University, for use of counting equipment. One of us /I.M.D./ acknowledges a Natural Environmental Research Council Grant.

REFERENCES

1. G.E.Gordon, K.Randle, G.G.Goles, J.B.Carliss, M.H.Beeson, S.S.Oxley, Geochim.Cosmochim.Acta, 32 /1968/ 369.
2. D.F.Covell, Anal.Chem., 31 /1959/ 1785.
3. M.Fleischer, Geochim.Cosmochim.Acta, 33 /1969/ 65.
4. F.J.Flanagan, Geochim.Cosmochim.Acta, 33 /1969/ 81.
5. Tanzanian Geological Survey, Dar Es Salaam, Tanzania, 1963.
6. Spectroscopy Society of Canada, Ottawa, Canada, 1968.
7. A.O.Brunfelt, E.Steinnes, Geochim.Cosmochim.Acta, 30 /1966/ 921.
8. W.S.Sijperda, quoted by Flanagan.⁴
9. H.A.Das, quoted by Flanagan.⁴
10. J.C.Cobb, Anal.Chem., 39 /1967/ 127.
11. S.Melsom, J.Radioanal.Chem., 4 /1970/ 355.
12. G.H.Morrison, J.T.Gerard, A.Travesi, R.L.Currie, S.F.Peterson, N.M.Potter, Anal.Chem., 41 /1969/ 1633.
13. A.Alian, R.Shabana, Microchem.J., 12 /1967/ 427.
14. A.M.Steuber, G.G.Goles, Geochim.Cosmochim.Acta, 31 /1967/ 75.
15. O.Johansen, E.Steinnes, Anal.Chim.Acta, 40 /1968/ 201.
16. A.Wyittenbach, Helv.Chim.Acta, 52 /1969/ 2458.
17. G.P.Bender, quoted by Flanagan.⁴
18. L.P.Greenland, quoted by Flanagan.⁴